DOKUZ EYLÜL UNIVERSITY

GRADUATE SCHOOL OF NATURAL AND APPLIED SCIENCES

NUMERICAL STUDY OF HEAT TRANSFER PERFORMANCE ON THE AIR SIDE OF EVAPORATOR FOR SPLIT AIR CONDITIONING SYSTEMS

by

Funda KURU

November, 2010

İZMİR

NUMERICAL STUDY OF HEAT TRANSFER PERFORMANCE ON THE AIR SIDE OF EVAPORATOR FOR SPLIT AIR CONDITIONING SYSTEMS

A Thesis Submitted to the

Graduate School of Natural and Applied Sciences of

Dokuz Eylül University

In Partial Fulfillment of the Requirements for the Degree of Master of Science in Mechanical Engineering, Energy Program

by

Funda KURU

November, 2010

İZMİR

M.Sc THESIS EXAMINATION RESULT FORM

We have read the thesis entitled **"NUMERICAL STUDY OF HEAT TRANSFER PERFORMANCE ON THE AIR SIDE OF EVAPORATOR FOR SPLIT AIR CONDITIONING SYSTEMS"** completed by **FUNDA KURU** under supervision of **ASSOC. PROF. DR. DİLEK KUMLUTAŞ** and we certify that in our opinion it is fully adequate, in scope and in quality, as a thesis for the degree of Master of Science.

.....

Assoc. Prof. Dr. Dilek KUMLUTAŞ

Supervisor

.....

(Jury Member)

.....

(Jury Member)

Dire Prof. Dr. Mustafa SABUNCU

Director

Graduate School of Natural and Applied Sciences

ACKNOWLEDGEMENTS

First of all, I would like to thank my supervisor, Assoc. Prof. Dr. Dilek KUMLUTAŞ, for her incomparable knowledge and moral support, valuable advises and guidance throughout this thesis study.

This study is supported by the Ministry of Industry and Commerce, with the 00343.STZ.2008-2 encoded SANTEZ project and Vestel Air-Conditioner Product Company. I would like to express my gratitude about being in this project.

I also wish to express my gratitude to Assist. Ziya Haktan KARADENİZ and my friends at Department of Mechanical Engineering Energy program for their patience and help.

Finally, I would like to gratefully thanks to my mother and brother for their endless encouragement, patience and valuable support in every part of my life. Special thanks to my father who watching me from heaven and be with me every time and everywhere.

Funda KURU

NUMERICAL STUDY OF HEAT TRANSFER PERFORMANCE ON THE AIR SIDE OF EVAPORATOR FOR SPLIT AIR CONDITIONING SYSTEMS

ABSTRACT

The aim of this study is to investigate the evaporator’s heat transfer performance with air flow characteristics in split air conditioners' indoor unit, which have an increasing number of usage in houses and workplaces due to climatic changes, numerically. Thus, indoor unit is modeled using Computational Fluid Dynamics and Heat Transfer (CFDHT) method and analyses were made. Results of the numerical study are compared with the measurements made by the producer company. So, it was possible to determine the temperature and velocity distributions and heat transfer performance without experimental tests which are expensive and take long time. The success of this study is to develop a numerical method to analyze split air conditioner indoor unit heat exchanger performance with heat transfer and air flow together.

Keywords: Split air conditioners, evaporator, computational fluids dynamics.

SPLİT İKLİMLENDİRME SİSTEMLERİNDEKİ ISI DEĞİŞTİRGECİNİN HAVA TARAFINDAKİ ISI TRANSFERİ PERFORMANSININ SAYISAL İNCELEMESİ

ÖZ

Bu çalışmanın amacı, değişen iklim şartları ile birlikte her geçen gün işyerleri ve evlerde kullanımı artan split klimaların iç ünitesi içindeki evaporatorün ısı transferi performansının, akış karakteristiğinin etkisi de dahil edilerek nümerik olarak araştırılmasıdır. Bu amaçla iç ünite, Hesaplamalı Akışkanlar Dinamiği ve Isı Transferi (HADIT) yöntemi kullanılarak modellenmiş ve analizler gerçekleştirilmiştir. Sayısal çalışmanın sonuçları, üretici firma tarafından yapılan deneysel ölçümler ile karşılaştırılmıştır. Böylece, pahalı ve uzun zaman alan deneysel testler olmaksızın sıcaklık, hız dağılımları ve ısı transferi performansını belirlemek mümkün kılınmıştır. Bu çalışmanın başarısı, split klima iç ünitesi içerisindeki ısı değiştirgeci performansını, ısı transferi ve akışı birarada çözümleyerek hesaplamamıza olanak sağlayan nümerik yöntemi geliştirmiş olmaktır.

Anahtar sözcükler: Split klima, evaporator, hesaplamalı akışkanlar dinamiği.

CONTENTS

Page

M. Sc THESIS EXAMINATION RESULTS FORM i
ACKNOWLEDGEMENTS iii
ABSTRACT iv
ÖZ..... v

CHAPTER ONE - LITERATURE SURVEY 1

1.1 Literature 1

CHAPTER TWO - SPLIT AIR CONDITIONERS 7

2.1 History of Air Conditioners Development 7
2.2 Split Air Conditioners 9
2.2.1 Air Conditioner Evaporator 10
2.2.2 Air Conditioner Compressors 13
2.2.3 Air Conditioner Condenser 13
2.2.4 Thermostatic Expansion Valve (TEV) 14
2.3 Air Conditioning System Basics and Theories 15
2.3.1 Refrigeration Cycle 15
2.3.2 The P-h Diagram 18
2.4 Refrigerants 21
2.4.1 CFC Refrigerants 22
2.4.2 HCFC Refrigerants 22
2.4.3 HFC Refrigerants 23
2.4.4 Refrigerant Blends 23

CHAPTER THREE - HEAT EXCHANGERS 24

3.1 Classification Of Heat Exchangers 24

3.1.1 Recuperation and Regeneration 25
3.1.2 Transfer Processes 27
3.1.3 Geometry of Construction 28
3.1.3.1 Tubular Heat Exchangers 28
3.1.3.1.1 Double-Pipe Heat Exchangers 29
3.1.3.1.2 Shell and Tube Heat Exchangers 29
3.1.3.1.3 Spiral-Tube Heat Exchangers 30
3.1.3.2 Plate Heat Exchangers 31
3.1.3.2.1 Gasketed-Plate Heat Exchangers 31
3.1.3.2.2 Welded and Other Plate Heat Exchangers 32
3.1.3.2.3 Spiral Plate Heat Exchangers 33
3.1.3.2.4 Lamella Heat Exchangers 34
3.1.3.3 Extended Surface Heat Exchangers 35
3.1.3.3.1 Plate-Fin Heat Exchangers 35
3.1.3.3.2 Tube-Fin Heat Exchangers 36
3.1.4 Heat Transfer Mechanism 38
3.1.5 Flow Arrangement 39
3.2 Evaporators 40

CHAPTER FOUR- NUMERICAL METHODS 43

4.1 Computational Fluid Dynamics (CFD) 43
4.1.1 The History of CFD 44
4.1.2 The Mathematics of CFD 45
4.1.2.1 Finite Control Volume 46
4.1.2.2 Infinitesimal Fluid Element 47
4.2 Conservation Laws 48
4.2.1 The Continuity Equation 48
4.2.2 The Momentum Equation 49
4.2.3 The Energy Equation 51
4.3 Conservative Form of the Governing Equations of Fluid Flow 53
4.4 The Control Volume 54

4.5 General Solution Procedure of CFD 54
4.5.1 Solution Strategy of ANSYS CFD - The Coupled Solver..... 55
4.6 CFD with Heat Transfer 59

CHAPTER FIVE-THEORETICAL STUDY 60

6.1 Air Side Heat Transfer Coefficient 60
6.1.1 Colburn-j Factor..... 64
6.2 Pressure Drop 64
6.2.1 f-Friction Factor..... 65

CHAPTER SIX-NUMERICAL STUDY 67

6.1 Preparing Cad Model for Numerical Study..... 67
6.2 Meshing..... 72
6.3 Boundary Conditions..... 76
6.4 Solver..... 77

CHAPTER SEVEN- RESULTS AND DISCUSSIONS..... 80

7.1 Results and Discussions 80
7.1.1 Flow Characteristics (Streamlines) Results..... 83
7.1.2 Pressure Drop Results..... 84
7.1.3 Velocity Distribution Results 86
7.1.4 Temperature Distribution Results..... 90

CHAPTER EIGHT- CONCLUSIONS 95

REFERENCES..... 97

CHAPTER ONE
LITERATURE SURVEY

1.1 Literature

The aim of this study is to investigate the heat transfer and flow characteristics in split air conditioners' indoor unit, which have an increasing number of usage in houses and workplaces due to climatic changes, numerically and compare this results with the experimental data to obtain the numerical method’s ability.

Thus, experimental and numerical studies have been investigated for understanding the heat transfer effects of fin and tube heat exchangers. In order to improve the performance of fin and tube heat exchangers, requirement of increasing the air-side heat transfer coefficient was projected from the study of Wang (2000). The air side has higher thermal resistance; therefore, mainly in the literature the air-side studies were founded. In the other researchers studies such as Wang, Lee & Sheu (2001), Yun & Lee (1999), Yan, Li, Wu, Lin & Chang (2003), Mendez, Sen, Yang & McClain (2003), for fin and tube heat-exchanger, the minimum part of it was modeled and the impact of material properties, the distance between fin and pipes, blasting agents, the shape of fins to heat transfer and flow conditions were reviewed.

Another similar study was examined the thermal behavior and pressure drop for fin and tube heat-exchangers with variable inclined fin angles, using the Computational Fluid Dynamics (CFD) method by Şahin, Dal & Baysal (2007) . The two dimensional (2D) and three dimensional (3D) CFD analyses for louvered and wavy finned heat exchangers were made and with the investigations of flow separations, pressure drop and heat transfer performance, the alternative fin structure ideas were obtained from the studies of Jang & Chen (1997), Perrotin & Clodic (2004) and Tao, He, Huang, Wu & Tao (2007).

In the study of Yun & Lee (1999), the effects of the shapes of interrupted surfaces on the performance of fin and tube heat exchanger in wind tunnel was experimentally investigated. It was shown that for estimating the heat transfer characteristics of a heat exchanger the scale-up model (various kinds of fin shapes) experiments are very useful. To analyze the characteristics of heat transfer coefficient and pressure drop for each fin the scale-up and prototype experiments have been performed and an optimal fin shape for home air conditioners was selected from their existing and newly designed models.

At similar technique, to have a database about the heat exchangers having different geometry and to build an experimental setup on which the performance test of heat exchangers in wind tunnel are performed by the study of Tuztas & Egrican (2002). The experimental setup had been designed to find out heat transfer coefficients and friction factors of finned-tube heat exchangers. The heat transfer in finned-tube heat exchangers which depends on the parameters such as, fin type, fin height, fin thickness, diameter of tubes, tube arrangement, space between fins in horizontal and vertical direction and flow type was also examined in this study.

The heat transfer characteristics of finned tube heat exchangers under dehumidifying and dry conditions are examined both theoretically and experimentally in the study of Gemici, Eğrican & Koca (2010). Six types of heat exchangers were tested on an experimental facility. The relations between dimensionless heat transfer coefficient (Colburn j-factor) with finning factor (ratio between fins and tubes outside area to tubes outside area), fin spacing and longitudinal tube spacing with heat transfer coefficient were also examined in this study.

Another similar experimental study was made to investigate the heat transfer and pressure drop characteristics of fin-and-tube exchangers with plate, wavy and louvered fin surfaces by Yan & Sheen (2000). Results are presented as plots of friction factor-f and Colburn-j factor against Reynolds number. Additionally, the dimensional heat transfer coefficient and pressure drop are also presented against

frontal air velocity. Finally, various comparison methods were adopted to evaluate the air side performance of the plate, wavy and louver fin heat exchangers. In these studies, researchers often examined the heat exchangers and cross-flow fans separately from the device and offered suggestions for new designs and relations.

The study of Taler (2004) presents a numerical method for determining heat transfer coefficients in cross-flow heat exchangers with extended heat exchanger surfaces. The advantage of the presented method is that it can be used for determining heat transfer characteristics of different type of heat exchangers such as in use of heating, ventilating, air conditioning and refrigeration equipment. The proposed methods for identification of heat transfer, both on fluid and air sides, are effective mathematical tools in determining new heat exchanger characteristics.

Three dimensional numerical simulations were accomplished to compare both an air side and an air/water side model in the study of Borrajo-Palaez, Ortega-Casanova & Cejudo-Lopez (2010). The influence of Reynolds number, fin pitch, tube diameter, fin length and fin thickness was studied in this work. The exchanger performance was evaluated through two non-dimensional parameters: the air side Nusselt number and a friction factor

In the study of Pu, Ding, Ma, Hu, & Gao (2009), the effects of long-term intermittent operations on the air-side heat transfer and pressure drop performance of finned tube evaporators of air conditioners were investigated by experiments on an aluminum fin evaporator and a copper-fin evaporator. According to the test results, the variations of the heat transfer coefficient and the pressure drop are more obvious at lower inlet air velocity, and the influence of operations on the aluminum-fin evaporator is greater than that on the copper-fin evaporator. So, this study gives ideas about the effect of aluminum fins usage as like in our study.

The air side laminar heat transfer and fluid flow characteristics of plain fin and tube heat exchangers with large number of tube rows and large diameter of tubes were investigated numerically through three-dimensional simulations in the study of

Xie, Wang & Sunden (2009). The effects of parameters such as Reynolds number, the number of tube rows, tube diameter, tube pitches and fin pitch are examined, and the variations of heat transfer due to variations of fin materials were also observed. Based on the numerical results, the heat transfer and flow friction correlations were established in this study.

To provide experimental data for using in the optimal design of flat plate finned tube heat exchangers with large fin pitch a study was made by Kim & Kim (2005). A heat transfer correlation was developed from the measured data for flat plate finned-tubes with large fin pitch.

To improve split type air conditioner performance, not only fin and tube heat exchangers but also cross-flow fans play an important role. Cross-flow fans and their casings affect the air flow and thereby heat transfer performance of the heat exchanger inside the split air conditioner unit. So, in our literature review cross-flow studies were also taken into account.

Cross-flow fans, also called tangential or transverse fans, have a wide range of usage in air conditioners and ventilators. It was invented by Mortier in 1893 and lots of studies were made to develop the performance of the cross-flow fan by many researchers such as Eck (1973) and Coester (1959). Murata & Nisnihara (1976), investigated velocity and pressure distributions of cross-flow fans with the different casings. In that study it was found that the tip clearance of tongue, the setting angle of its suction size and the size of casing are the most effective geometrical parameters for fan performance. Another similar experimental study was made by Uskaner & Göksel (1999) which involves investigations for the following parameters; orientation of rear wall gradient, the effect of the output field magnitude, the gap between the rear wall and rotor and the rate of inlet and outlet arc. Murata & Tanaka (1995) and T. Kim, D.Kim, Park & Y.Kim (2008) also focused on the effect of the rear wall and the vortex wall on the performance of a cross-flow fan, which is higher than that of the impeller.

Dang & Bushnell (2009) showed that the other important issues beside geometry of housing and orientation for an effective fan are the position and the magnitude of the vortex which is formed with the rotation of the fan.

An experimental investigation of the flow field pattern within the impeller, the eccentricity and the strength of the vortex was made by Toffolo (2005, 2004) and Gabi, Dornstetter & Klemm (2003), thus the aerodynamics of flow and vortex regions inside the cross-flow fan were studied. In these studies, the basic step towards the formulation of a general theory on cross-flow fan operation was linked to the design parameters (the radial width of rear wall is the most important, followed by the position and the thickness of the vortex wall); flow field pattern (mainly characterized by the strength and the position of the vortex core inside the impeller) and performance (total pressure coefficient, total, volumetric and hydraulic efficiency, maximum flow coefficient).

Up to date, many researchers have made experimental and numerical investigations to find out the flow characteristics, velocity and pressure distributions in only simplified cross-flow fan housing systems. Shih, Hou & Chiang (2008), use two dimensional geometry with CFD method to simulate cross-flow fan construction in a conventional split-type air conditioner including air return grill and heat exchanger. According to the simulations' results of simple flow duct model and conventional split-type air-conditioner model, similarity laws for cross-flow fan were developed.

In the study of Chen, Li, & Huang (2008) the flow field in a cross flow fan was simulated by solving the two dimensional unsteady Reynolds-averaged Navier-Stokes equations. The calculated pressure fluctuations of the blades, the vortex wall, and the rear wall were used as noise sources to calculate the sound field. Their predictions show that the rear wall and the vortex wall sources contribute significantly to the total noise. Similar aero-acustics studies which were prepared by Noel, Farall, & Casarsa, Younsi, Bakir, Kouidri & Rey (2007) and Tsai, Tu, Li &

Wang (2006) were also investigated to apprehend the importance of cross-flow fan position's effects.

As mentioned in the literature in strongly, CFD methods are very successful for understanding the complex flow systems flow characteristics. As can be seen from the current studies, in the literature mostly two dimensional and partial analyses were made for only heat exchanger side or only fan side. The deficiency in the current literature studies about solving heat transfer and fluid flow together in CFD analyses was derived from the researches. According to literature research's estimation, for air-conditioners' air side performance determination, the requirement of three dimensional CFD analysis of complex split-type air-conditioner unit which involve cross-flow fan and fin and tube heat-exchanger in it was concluded. Namely, in this thesis, unlike other studies, three dimensional heat transfer and fluid flow analyses were made together to determinate the split air conditioner evaporator performance.

CHAPTER TWO
SPLIT AIR CONDITIONERS

2.1 History of Air Conditioners Development

In 1758, Benjamin Franklin and John Hadley, professor of chemistry at Cambridge University, conducted an experiment to explore the principle of evaporation as a means to rapidly cool an object. Franklin and Hadley confirmed that evaporation of highly volatile liquids such as alcohol and ether could be used to drive down the temperature of an object past the freezing point of water. They conducted their experiment with the bulb of a mercury thermometer as their object and with a bellows used to "quicken" the evaporation; they lowered the temperature of the thermometer bulb to -14 °C while the ambient temperature was 18 °C. Franklin noted that soon after they passed the freezing point of water (0 °C) a thin film of ice formed on the surface of the thermometer's bulb and that the ice mass was about a quarter inch thick when they stopped the experiment upon reaching -14 °C (http://en.wikipedia.org/wiki/Air_conditioner).

In 1820, British scientist and inventor Michael Faraday discovered that compressing and liquefying ammonia could chill air when the liquefied ammonia was allowed to evaporate. In 1842, Florida physician John Gorrie used compressor technology to create ice, which he used to cool air for his patients in his hospital in Apalachicola, Florida. He hoped eventually to use his ice-making machine to regulate the temperature of buildings. He even envisioned centralized air conditioning that could cool entire cities. Though his prototype leaked and performed irregularly, Gorrie was granted a patent in 1851 for his ice-making machine. His hopes for its success vanished soon afterward when his chief financial backer died; Gorrie did not get the money he needed to develop the machine. According to his biographer Vivian M. Sherlock, he blamed the "Ice King", Frederic Tudor, for his failure, suspecting that Tudor had launched a smear campaign against his invention. Dr. Gorrie died impoverished in 1855 and the idea of air conditioning faded away for 50 years.

Early commercial applications of air conditioning were manufactured to cool air for industrial processing rather than personal comfort. In 1902 the first modern electrical air conditioning was invented by Willis Haviland Carrier in Syracuse, New York. Designed to improve manufacturing process control in a printing plant, his invention controlled not only temperature but also humidity. The low heat and humidity were to help maintain consistent paper dimensions and ink alignment. Later Carrier's technology was applied to increase productivity in the workplace, and The Carrier Air Conditioning Company of America was formed to meet rising demand. Over time air conditioning came to be used to improve comfort in homes and automobiles. Residential sales expanded dramatically in the 1950s.

In 1906, Stuart W. Cramer of Charlotte, North Carolina, was exploring ways to add moisture to the air in his textile mill. Cramer coined the term "air conditioning", using it in a patent claim he filed that year as an analogue to "water conditioning", then a well-known process for making textiles easier to process. He combined moisture with ventilation to "condition" and change the air in the factories, controlling the humidity so necessary in textile plants. Willis Carrier adopted the term and incorporated it into the name of his company. This evaporation of water in air, to provide a cooling effect, is now known as evaporative cooling.

The first air conditioners and refrigerators employed toxic or flammable gases like ammonia, methyl chloride, and propane, which could result in fatal accidents when they leaked. Thomas Midgley, Jr. created the first chlorofluorocarbon gas, Freon, in 1928. The refrigerant was much safer for humans but was later found to be harmful to the atmosphere's ozone layer. Freon is a trademark name of DuPont for any chlorofluorocarbon (CFC), hydrogenated CFC (HCFC), or hydro fluorocarbon (HFC) refrigerant, the name of each including a number indicating molecular composition (R-11, R-12, R-22, R-134A). The blend most used in direct-expansion home and building comfort cooling is an HCFC known as R-22. It is to be phased out for use in new equipment by 2010 and completely discontinued by 2020. R-12 was the most common blend used in automobiles in the United States until 1994 when most changed to R-134A. R-11 and R-12 are no longer manufactured in the United

States, the only source for purchase being the cleaned and purified gas recovered from other air conditioner systems. Several non-ozone depleting refrigerants have been developed as alternatives, including R-410A, known by the brand name Puron. The most common ozone-depleting refrigerants are R-22, R-11, and R-123.

Innovation in air conditioning technologies continues, with much recent emphasis placed on energy efficiency and improving indoor air quality. As an alternative to conventional refrigerants, natural alternatives like CO_2 (R-744) have been proposed.

2.2 Split Air Conditioners

Air conditioners work in much the same way that a refrigerator does; by cooling the air in an area while also extracting the hot air from the area and removing it from the vicinity. However, unlike a refrigerator, an air conditioner must do its job on an entire house, does not need to cool the air to the same degree, and it does so with some larger, more powerful equipment.

The process of understanding an air conditioner cooling system should start with an examination of the different parts of an air conditioning unit. Each and every air conditioner has four parts: an evaporator (1), a compressor (2), a condenser (3) and expansion device (4) as shown in Figure 2.1. These four parts, in unison with a variety of chemicals that easily convert from liquids to gases and back again to liquids are what make all air conditioners work. It is essential that the fluid used in the air conditioner is in a gaseous state at room temperature (http://www.tech-faq.com/how-an-air-conditioner-works.html).

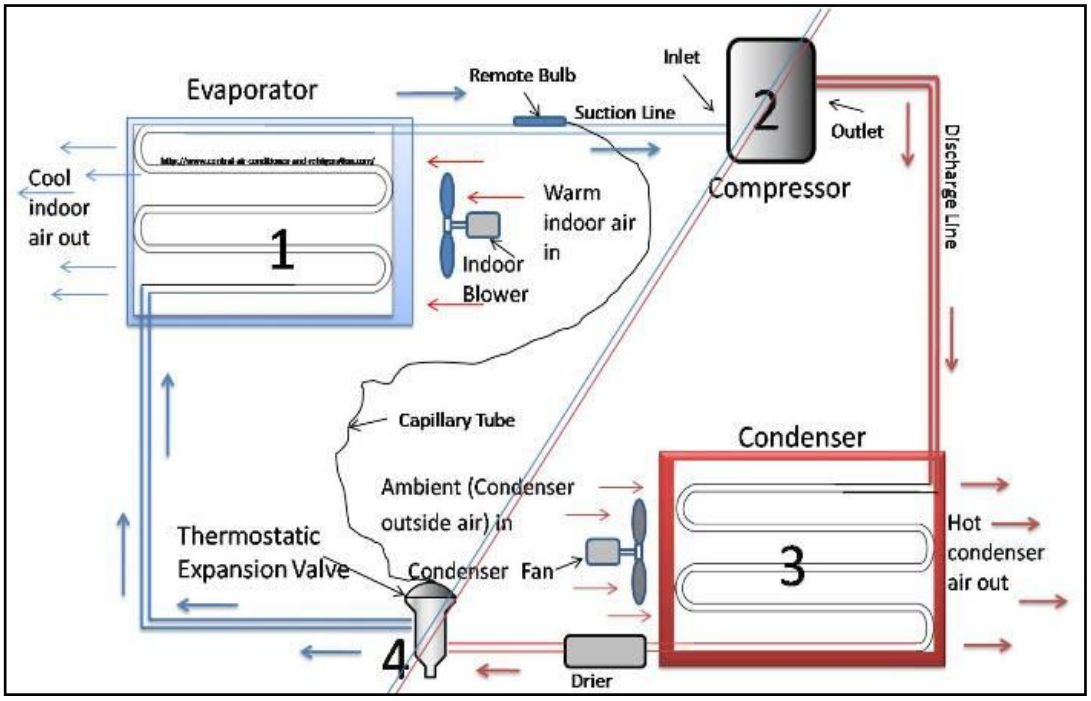


Figure 2.1 Refrigeration diagram (http://www.central-air-conditioner-and-refrigeration.com)

In this refrigeration diagram, the four major components split into two sections: Indoor and Outdoor. In indoor units, we have the air conditioner parts number 1 and 2. In outdoor units, we have the air conditioner parts number 3 and 4. These four majors' components are divided into two different pressures: high pressure and low pressure.

The high pressure side is the condenser units (outdoor) and the low pressure side is the air conditioning evaporator (indoor). The divided point between high and low pressure cut through the compressor and the expansion valve.

2.2.1 Air Conditioner Evaporator

The air conditioning evaporator is a heat exchanger that absorbs heat into the air conditioner system. Air conditioning evaporator works by absorb heat from the area (medium) that need to be cooled (Figure 2.2). It does that by maintaining the evaporator coil at low temperature and pressure than the surrounding air (Principles of home inspection: Air conditioning and heat pumps (1992), http://www.central-air-conditioner-and-refrigeration.com).

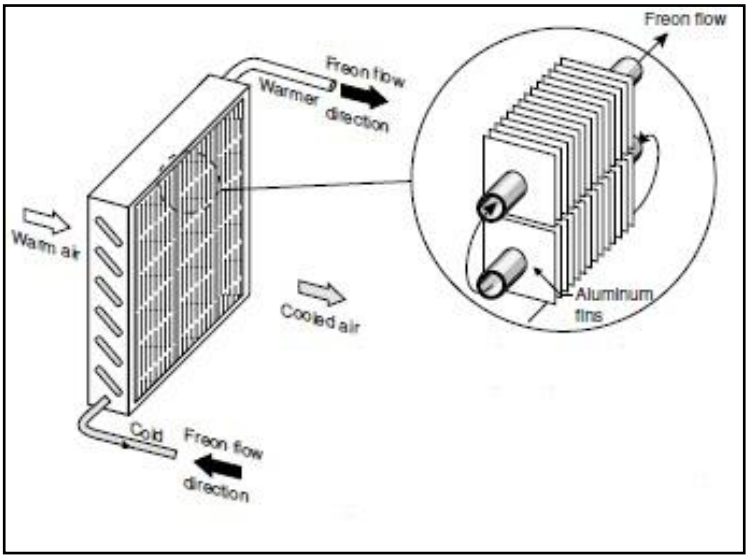


Figure 2.2 Heat transfer through the evaporator (Principles of home inspection: Air conditioning and heat pumps, 1992)

Since, the air conditioning evaporator coil contains refrigerant that absorbs heat from the surrounding air, the refrigerant temperature must be lower than the air. It takes in low temperature, low pressure liquid refrigerant from the expansion device and changes it into low-pressure, low temperature vapor refrigerant.

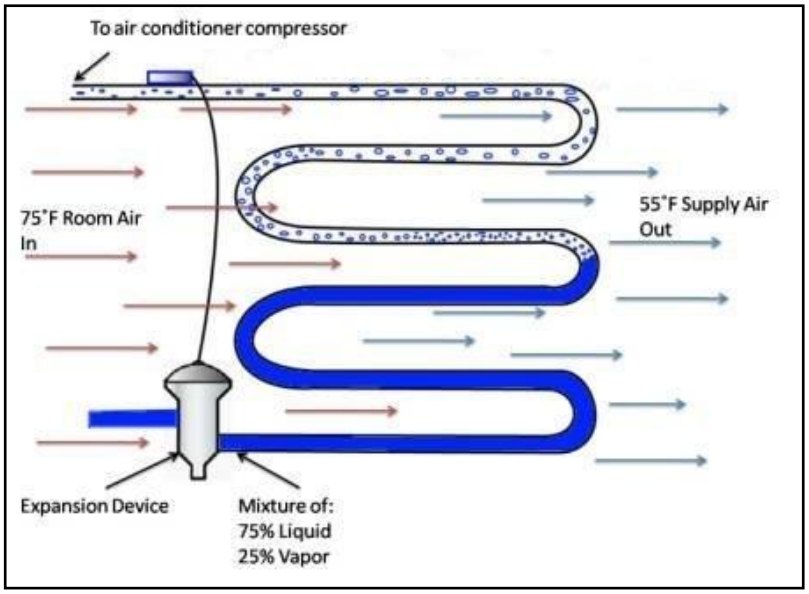


Figure 2.3 Evaporation process
(http://www.central-air-conditioner-and-refrigeration.com)

The expansion device provides a pressure reduces between the high side and the low side of the system, the saturation temperature of the refrigerant entering the air conditioning evaporator is lower than the medium to be cooled (Figure 2.3). One of the characteristic of an air conditioner refrigerant is that as the pressure is reduced the boiling point is also reduced. Therefore, as the pressure is reduced through the expansion device so is the point at which it will boil and become a vapor. As the warm air from the space passes over the evaporator, it gives up its heat to the lower temperature liquid/vapor mixture passing through the evaporator. As the liquid refrigerant absorbs this heat it boils changing from the liquid state to the vapor state.

The amount of heat the air conditioner evaporator absorbs must equal the amount of heat it lost. For instance, if the air conditioning evaporator gives up 100 Btu's of heat to the surrounding hot air, then the refrigerant within the air conditioning evaporator coil must gain 100 Btu's of heat. The amount of liquid entering the evaporator must be enough, so by the time it reaches the end of the evaporator. It will be completely boiled to the vapor state. There must be enough air flows across the air conditioning evaporator to provide heat to the refrigerant in the evaporator. This is just a safety way to ensure the air conditioner compressor doesn't have the liquid refrigerant entering it.

The air conditioning evaporator absorbs heat into the refrigerant from the warmer air passing over the surface of the evaporator. The heat absorbed causes the liquid refrigerant to boil, changing it from a liquid state to a vapor state.

Types of air conditioning evaporator:

1. Bare-tube
2. Finned-tube
3. Flat-plate

2.2.2 Air Conditioner Compressors

The air conditioning compressor is known as the heart of the air conditioner units. The air conditioning compressor is the mechanical component of the air conditioner parts that cause the air conditioner refrigerant to flows in a cycle. Its work is a vapor pump. In split air conditioner units, the compressor is located outside within the condenser units.

As shown in the refrigeration cycle diagram; the compressor has a refrigerant inlet line (low side) and refrigerant outlet line (high side). Compressors produce a pressure difference between the low side (suction pressure) and high side (discharge pressure) of the refrigeration system. The compressor absorbs vapor refrigerant from the suction line and compresses that heat to high superheat vapor. As the refrigerant flows across the compressor, it also removes heat of compression, motor winding heat, mechanical friction, and other heat absorbs in the suction line.

There are five main types of air conditioner compressors:

1. Reciprocating
2. Rotary compressor
3. Centrifugal compressor
4. screw compressors
5. Scroll compressors

Hermetic compressor is the most common air conditioner compressors found in residential air conditioner units.

2.2.3 Air Conditioner Condenser

Air conditioner condenser units are grouped according to how it rejects the heat to the medium (surround air). Here are a few condensers units.

- Air cooled condenser

- Earth cooled condenser (Geothermal Heat Pumps)
- Water cooled condenser
- Combination of air and water cooled condenser (Evaporative condensers)

In this refrigeration cycle diagram, the air conditioner condenser is air cooled condenser. Air cooled condensers are mostly used in residential air conditioner units and commercial air conditioning unit. It functions the same way as the evaporator but it does the opposite. The condenser units are located outdoor with the compressor. It purposes is to reject both sensible and latent heat of vapor absorb by the air conditioner units.

The condenser receives high pressure and high temperature superheats vapor from the compressor and rejects that heat to the low temperature air. After rejected all the vapor heat, it turns back to liquid refrigerant. The condenser has three important steps:

1. Its remove sensible heat or (de-superheat)
2. Remove latent heat or (condense)
3. Remove more sensible heat or (sub-cooled)

2.2.4 Thermostatic Expansion Valve (TEV)

All expansion device or metering device has similar function; it's responsible for providing the correct amount of refrigerant to the evaporator. This is done by creating a restriction within the thermostatic expansion valve (Figure 2.4). The restriction causes the pressure and temperature of the refrigerant entering the Evaporator to reduce.

The refrigeration cycle diagram above has a thermostatic expansion valve. This expansion device has;

1. Remote Bulb

2. Capillary Tube
3. Thermostatic Expansion Valve Body

Thermostatic expansion valve provides the correct amount of air conditioner refrigerant to the evaporator by using a remote sensing bulb as a regulator. The remote sensing bulb and capillary tube has a refrigerant inside. As you can see in the refrigeration cycle diagram above, the remote sensing bulb is tie with the suction line. The temperature from the suction line transfer heat to the sensing bulb through conduction.

Sensing bulb responds to the temperature of the suction line and as a result, it decreases or increases the temperature and pressure inside the sensing bulb due to suction line temperatures. The sensing bulb also has a diaphragm on the other end. This diaphragm is with the Thermostatic Expansion Valve body.

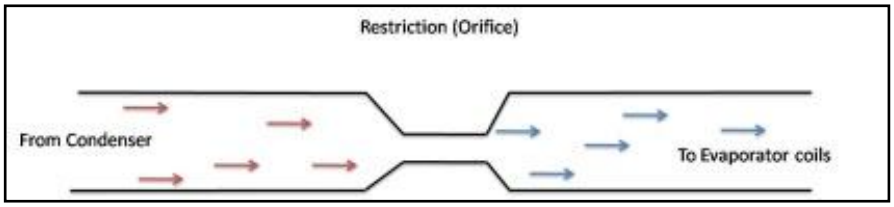


Figure 2.4 Expansion device (http://www.central-air-conditioner-and-refrigeration.com)

2.3 Air Conditioning System Basics and Theories

2.3.1 Refrigeration Cycle

In the refrigeration cycle (Figure 2.5), a heat pump transfers heat from a lower-temperature heat source into a higher-temperature heat sink. Heat would naturally flow in the opposite direction. This is the most common type of air conditioning. A refrigerator works in much the same way, as it pumps the heat out of the interior and into the room in which it stands.

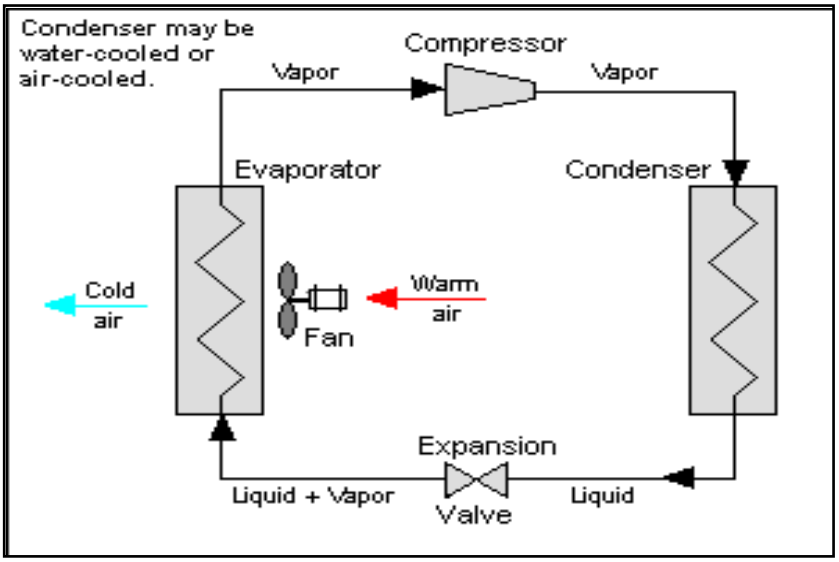


Figure 2.5 A simple stylized diagram of the refrigeration cycle.
(www.absoluteastronomy.com/topics/Heat_pump_and_refrigeration_cycle)

This cycle takes advantage of the way phase changes work, where latent heat is released at a constant temperature during a liquid/gas phase change, and where varying the pressure of a pure substance also varies its condensation/boiling point.

Cooling an area with an air conditioner begins when the fluid in an air conditioner first enters its compressor in gaseous form. The compressor increases the gas pressure causing the molecules of the gas to collide until they are a high temperature and under significant pressure. This hot and pressurized gas then enters the condenser. Because this process creates so much heat, the compressor and the condenser in a home air conditioning unit are usually located outside of the home, to prevent the exerted heat from increasing internal temperatures. Heat is dissipated from the air conditioners external unit by way of the exhaust fan and metal radiator fins.

As the gas leaves the condenser, the temperature is greatly cooled and because of the high pressure and the low temperatures, the gas turns to a liquid. The liquid then enters the evaporator through a very small hole which allows very little liquid to pass through at one time. In the evaporator, which is usually located inside the house (sometimes as an addition to a home's furnace), the liquid turns back into a gas and

begins to evaporate. While it undergoes this evaporation process, it also extracts heat from the air, cooling it. The cooled air is then blown out of the air conditioner and is left to circulate throughout the house via ducts or other vents.

The gas which extracted the heat from the air then circulates back to the compressor as a low pressure gas where it can begin its journey through the air conditioning system yet again. This cooling process will continue until the built in thermostat on the air conditioning unit detects that the room is at the proper temperature (http://www.tech-faq.com/how-an-air-conditioner-works.html.).

There are two laws that are significant to understand the basic refrigeration cycle and air conditioning. Thermodynamics' first law explains that energy cannot be neither created nor destroyed, but can be changed from one form to another. Thermodynamics second law can help us better understand how the basic refrigeration cycle works. Once of these laws state that heat always flows from a material at a high temperature to a material at a low temperature.

The air conditioning (the refrigeration cycle) is a process that simply removes heat from an area that is not wanted and transfers that heat to an area that makes no difference. The air conditioner itself does not create heat, it just transfers heat. For heat to transfer there has to be a temperature and pressure difference. In the refrigeration process there are two sections which produce a pressure difference: a high-pressure, high temperature section (condenser) and a low-pressure, low temperature section (evaporator). The refrigeration system removes heat from an area that is low-pressure, low temperature (evaporator) into an area of high-pressure, high temperature (condenser).

Air conditioning is a way to keep home comfortable by controlling the temperature, air movement, cleanliness, humidity, or dehumidify for our comfort.

To move heat from the evaporator to the condenser we need refrigerant, and other mechanical components, therefore we need to understand how heat transfers. There

are three methods of heat transfer. They are conduction, convection, and radiation or any combination of the three methods. Heat transfer is the movement of heat from solid, liquid or gas materials to other solid, liquid and gas materials. According to the second law of thermodynamics, heat always flows from a material at a high temperature to a material at a low temperature. For heat to transfer there has to be a temperature difference between the two materials. Heat transfer by conduction is when we heat a copper pipe to 100°F and grab that hot copper with our bare hand. That is molecule to molecule heat transfer. Radiation is the transfer of heat in an invisible ray, for example, sun ray. We cannot see it, but we can feel the sun ray hits our skin. Convection is the transfer of heat from one place to a different location by circulating it with a fan (force movement) or natural movement.

Basic refrigeration cycle principles:

1. As refrigerant in the latent state or as vapor refrigerant in the process of changed state to liquid, this is the phase where it absorbs or rejects large quantities of heat. The quantities of heat absorbed or rejected can be managed by controlling the pressure and temperature of the refrigerant.
2. The boiling point of closed-system liquid can be controlled by changing the vapor pressure above it.
3. Gauge pressure is used to determine the pressure inside the closed refrigeration cycle system. It's expressed in pounds per square inch gauge (psig).
4. Heat flows from a material at a higher temperature to a material at low temperature.
5. Heat energy is not created but converted and transferred.

2.3.2 The P-h Diagram

The Ph chart graphically shows where the physical states of these five mechanical components are and what is happening to the refrigerant within these components (Figure 2.6).

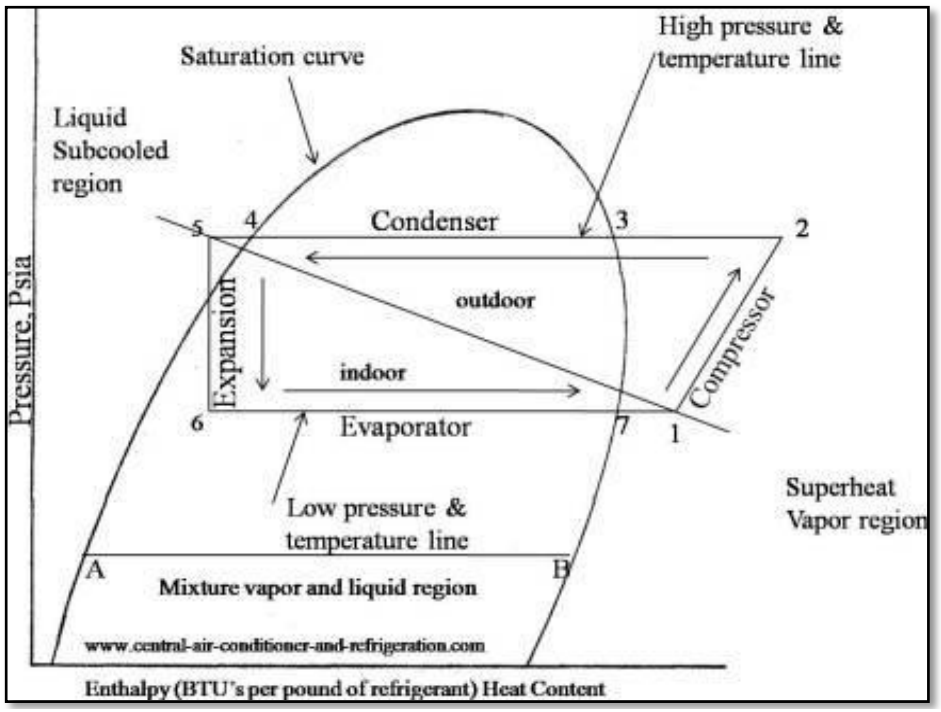


Figure 2.6 P-h diagram (http://www.central-air-conditioner-and-refrigeration.com)

First, we can start the basic refrigeration cycle diagram discussion on evaporator section. The evaporator and condenser act as a heat exchanges in the air conditioning system. There are two pressure lines and two heat exchangers. The low-pressure line is an evaporator (it absorbs heat) and the high pressure line is the condenser (it rejects heat). The first heat exchange that occurs in this basic refrigeration cycle is the evaporator. The air conditioner evaporator is locating between points 6 and 1 in the basic refrigeration cycle diagram.

The evaporator is a heat exchange that is responsible for absorbing heat from whatever place (medium) that needs to be cooled; for our discussion it's indoor. Since the evaporator is at a low temperature than the air surrounding it, it will absorb the surrounding heat until the refrigerant liquid inside the evaporator coils starts boiling as result of absorb that heat. As the evaporator refrigerant has boiled completely to vapor it's now saturated vapor at point 7. Some compressors cannot pump liquid; if it does pump liquid, it will damage it. This is why we need the entire liquid refrigerant to boil at point 7.

After, the entire liquid refrigerant turns to vapor and passes point 7. Superheat occurs. Superheat is between point 7 and 1. Superheat is life insurance for the compressor. It makes sure the compressor does not pull in liquid refrigerant from the evaporator.

The air conditioner compressors located between points 1 and 2 has two important lines: a suction line (low side pressure and back pressure) and discharge pressure (high side pressure, head pressure). The suction line is the line that pulls the low-pressure and temperature from the evaporator and the discharge line is the line that compresses and pushes that superheat vapor to the condenser. Its creates a pressure difference in the air conditioning system by pulling in low-pressure, low temperature vapor from the evaporator suction line and increasing it to high-pressure, high temperature superheat. This pressure difference what makes the refrigerate flow in a refrigeration cycle. The compressor is also known as the heart of the refrigeration system. The compressor is known as the vapor pump.

The air conditioner condenser locate between points 2 and 5 is a heat exchange; it rejects both sensible (measurable) and latent (hidden) heat absorbed by the indoor evaporator plus heat of compression from the compressor. There are three important states that take place in the condenser heat rejection. The first state points 2 and 3 it de-superheat or simply rejects hot superheat vapor (it removes sensible heat). At points 3 and 4 this the state where it rejects so many saturated vapors heat, it starts changing phase from vapor to liquid; as the refrigerant reaches point 4 it is 100 percent saturated liquid refrigerant. From points 4 and 5 it removes sensible heat from the saturated liquid refrigerant. This is where you could use a thermometer and tell how much heat it has removed; as more heat is removed it’s now in the sub-cooled region.

The expansion device is normally installed in the liquid line between condenser and evaporator (points 5 and 7). In a regular split central air conditioners system it’s located indoors with or near the evaporator coils.

2.4 Refrigerants

Refrigerants are the working fluids in refrigeration, air- conditioning, and heat-pumping systems. They absorb heat from one area, such as an air-conditioned space, and reject it into another, such as outdoors, usually through evaporation and condensation. These phase changes occur both in absorption and mechanical vapor compression systems, but not in systems operating on a gas cycle using a fluid such as air. The design of the refrigeration equipment depends strongly on the properties of the selected refrigerant (ASHRAE, 2005).

Refrigerant selection involves compromises between conflicting desirable thermo physical properties. A refrigerant must satisfy many requirements, some of which do not directly relate to its ability to transfer heat. Chemical stability under conditions of use is an essential characteristic. Safety codes may require a nonflammable refrigerant of low toxicity for some applications. Cost, availability, efficiency, and compatibility with compressor lubricants and equipment materials are other concerns.

The environmental consequences of refrigerant leaks must also be considered. The air conditioner refrigerants and ozone layer important relation was discovered in the mid 1980s that the commonly used air conditioner refrigerant has a damaging impact on the ozone layer. At that time, the refrigerants that used then were known as CFC (chlorofluorocarbons) and HCFCs (hydro chlorofluorocarbons). CFCs are a family of chemicals that contain chlorine, fluorine and carbon. The chlorine content in these compounds causes the depletion of the ozone layer (Wikipedia).

This discovery prompted the signing of Montreal Protocol of 1987, an agreement signed by 180 nations that target to phase out the production of CFCs by 1995 and HCFCs by 2030. New refrigerants that are being used to replace these CFCs are HFCs (hydro fluorocarbons) and refrigerant blends (Azeotropic, Zeotropic). In summary, the four commonly used refrigerants that we can find today are:

- CFCs
- HCFCs
- HFCs
- Refrigerant blends

The future commonly used refrigerants will be in the last two categories. Among the currently widely used ones are R-134a, R407C and R410A.

2.4.1 CFC Refrigerants

These refrigerants were developed more than 70 years ago and are harmful to our respiratory systems and the ozone layer. Their production was stopped since 1995 but is still being used widely in existing residential air conditioning units as many types of equipment have a lifetime of up to 30 years. Today's refrigerants used are from reclaimed units that are no longer in operation. The common ones still used are: R-11, R-12, R-113, R-114, R-115.

2.4.2 HCFC Refrigerants

These air conditioner refrigerants are considered partially halogenated as they consists of methane or ethane in combination with chlorine and fluorine. They are shorter lifespan and are less destructive to the ozone layer compared to CFCs. They are an interim solution to a totally "free from chlorine" refrigerant that are being developed. Their production is scheduled to be phased out totally in 2030. The common ones used are:

- R-22
- R-123

R-22 is used extensively in residential, commercial and industrial applications.

2.4.3 HFC Refrigerants

These air conditioner refrigerants contain no chlorine atom and are not destructive to the ozone layer though they have a slight effect on global warming. R-134a is used in new systems that are specially designed for its use. The common HFCs are:

- R-134a
- R-124

The 1997 Kyoto Protocol puts R-134a as one of the 6 greenhouse gases that must be reduced. There is no phase-out date for this refrigerant and it is expected to be highly used in the HVAC industry.

2.4.4 Refrigerant Blends

These air conditioner refrigerants are also known as "azeotropic" and "zeotropic". Their use is increasing as they are environmental friendly. The setback is that the total air conditioning systems production cost is higher. However, as more manufacturers switch to this type of refrigerants, the cost/unit will drop eventually. The common refrigerant blends used in the air conditioning industry are:

- R-410A
- R-407c

R-410A is used as a replacement refrigerant for residential air conditioning applications and R-407C is used as R-22 replacement.

CHAPTER THREE
HEAT EXCHANGERS

A heat exchanger is a device that is used to transfer thermal energy (enthalpy) between two or more fluids, between a solid surface and a fluid, or between solid particulates and a fluid, at different temperatures and in thermal contact. In heat exchangers, there are usually no external heat and work interactions. Typical applications involve heating or cooling of a fluid stream of concern and evaporation or condensation of single or multi component fluid streams. In other applications, the objective may be to recover or reject heat, or sterilize, pasteurize, fractionate, distill, concentrate, crystallize, or control a process fluid (Shah & Sekulic, 2003).

3.1 Classification of Heat Exchangers

Heat exchangers are used in a wide variety of applications such as in power production, industrial processes, environmental engineering, space applications, air-conditioning and refrigeration. So, heat exchangers take various shapes, sizes etc. through their usage. In Figure 3.1, classification of heat exchangers according to 5 main criteria is shown (Kakaç & Liu, 1998):

1. Recuperators and regenerators
2. Transfer processes: direct contact and indirect contact
3. Geometry of construction: tubes, plates, and extended surfaces
4. Heat transfer mechanisms
5. Flow arrangements: parallel, counter, and cross flows

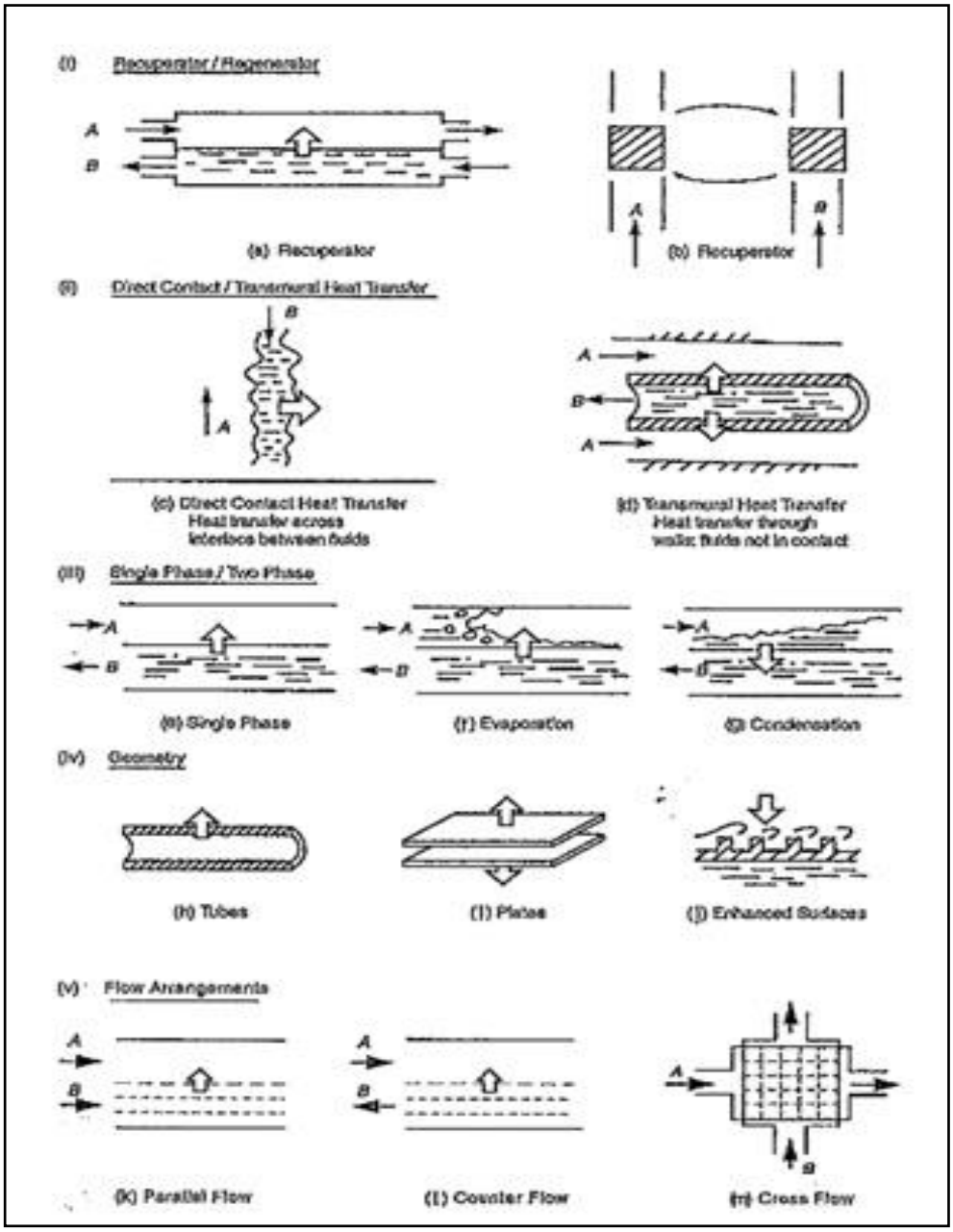


Figure 3.1 Classification of heat exchangers (Kakaç & Liu, 1998)

3.1.1 Recuperation and Regeneration

A recuperator, with heat transfer between two fluids is shown in Figure 3.1a. The hot stream A recuperates some of the heat from stream B. As shown in Figure 3.1c, the heat transfer occurs through a separating wall or through the interface between the streams as in the case of direct contact type of heat exchangers. Some of the recuperative-type exchangers are shown in Figure 3.2 (Kakaç & Liu, 1998)

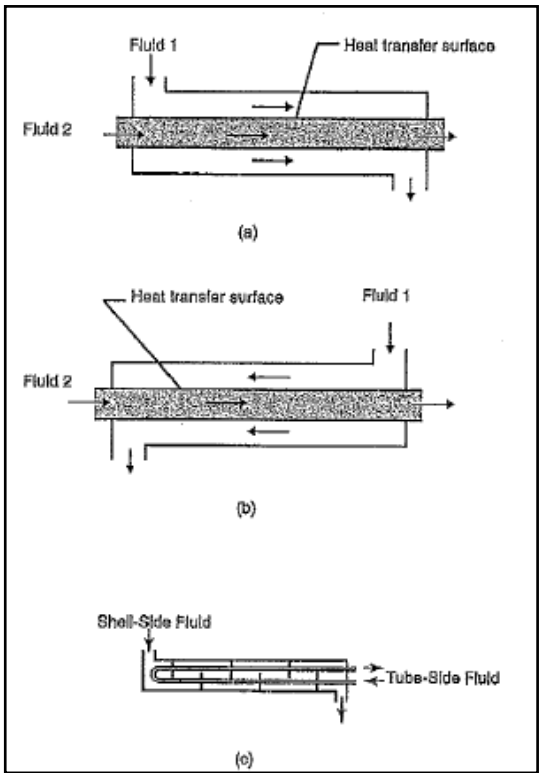


Figure 3.2 Indirect contact types of heat exchangers.
(a) and (b) Double-pipe type, (c) Shell and tube type
(Kakaç & Liu, 1998)

The same flow passage (matrix) is alternately occupied by one of the two fluids in regenerators or storage-type heat exchangers. The hot fluid stores the thermal energy in the matrix; during the cold fluid flow through the same passage at a later time, stored energy will be extracted from the matrix. Therefore, as shown in Figure 3.1b, thermal energy is not transferred through the wall as in a direct transfer type heat exchanger. While the solid is in the cold stream A, it losses heat; while it is in the hot stream B, it gains heat, so it is regenerated.

Regenerators can be classified as:

1. Rotary regenerator (a. Disk-type, b. Drum-type)
2. Fixed-matrix regenerator

The disk-type and drum-type regenerators are shown in Figure 3.3, schematically. In a disk type regenerator, heat transfer surface is in a disk form and fluids flow axially. In drum-type regenerators, the matrix is in a hollow drum form and fluids flow radially.

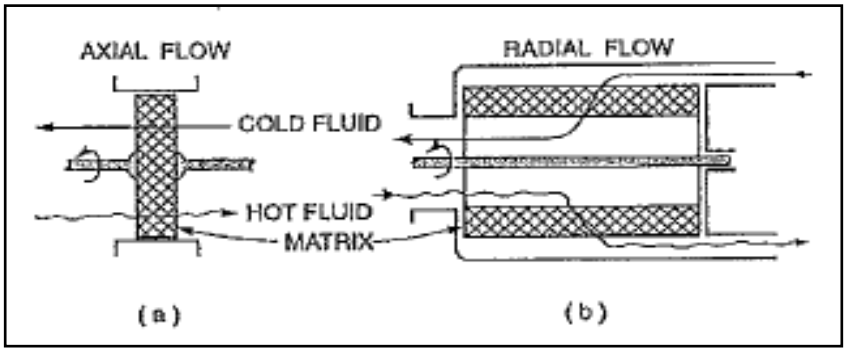


Figure 3.3 Rotary regenerators. (a) Disk type. (b) Drum type (Kakaç & Liu, 1998)

Rotary regenerators are used in preheating air in large coal-fired steam power plants, gas turbines, fixed-matrix air preheating for blast furnace stoves, steel furnaces, open-hearth steel melting furnaces, and glass furnaces.

3.1.2 Transfer Processes

According to the transfer processes, heat exchangers are classified as direct contact type and indirect contact type (Kakaç & Liu, 1998). In direct contact heat exchangers, heat is transferred between the cold and hot fluids through direct contact between these fluids. As shown in Figure 3.1.c, there is no wall between hot and cold streams, and the heat transfer occurs through the interface of two streams. The streams are two immiscible liquids, a gas-liquid pair, or a solid particle fluid combination in direct contact type heat exchangers. Cooling towers, spray and tray condensers are good examples of such heat exchangers.

In indirect contact type heat exchangers, heat is transferred through a heat transfer surface between the cold and hot fluids, as shown in Figure 3.1.d. A wall is separating the fluids so they are not mixed. This type of heat exchanger examples are shown in Figure 3.2.

Indirect contact and direct contact type heat exchangers are also called recuperators. Tubular (double-pipe, shell and tube), plate, and extended surface heat exchangers; cooling towers; and tray condensers are examples of recuperators.

Compared to indirect contact recuperators and regenerators, in direct-contact heat exchangers, (1) very high heat transfer rates are achievable, (2) the exchanger construction is relatively inexpensive, and (3) the fouling problem is generally nonexistent, due to the absence of a heat transfer surface (wall) between the two fluids. However, the applications are limited to those cases where a direct contact of two fluid streams is permissible (Shah & Sekulic, 2003).

3.1.3 Geometry of Construction

Direct transfer type heat exchangers are often described in terms of their construction features. Tubular, plate and extended surface heat exchangers are the major construction types (Shah & Sekulic, 2003 and Kakaç & Liu, 1998)

3.1.3.1 Tubular Heat Exchangers

These exchangers are generally built of circular tubes, although elliptical, rectangular, or round/flat twisted tubes have also been used in some applications. There is considerable flexibility in the design because the core geometry can be varied easily by changing the tube diameter, length, and arrangement. Tubular heat exchangers can be classified as:

1. Double-pipe
2. Shell and tube
3. Spiral-tube

3.1.3.1.1 Double-Pipe Heat Exchangers. A typical double-pipe heat exchanger consists of two concentric pipes with the inner pipe plain or finned, as shown in Fig. 3.4. Double-pipe heat exchangers can be arranged in various series and parallel arrangements to meet pressure drop and mean temperature difference requirements. Double-pipe exchangers are generally used for small-capacity applications where the total heat transfer surface area required is 50 m^2 or less because it is expensive on a cost per unit surface area basis.

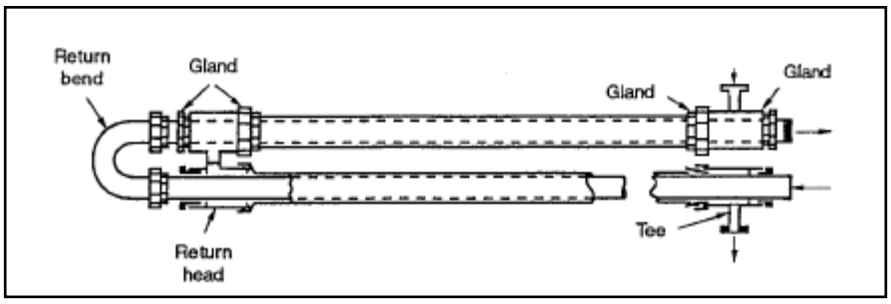


Figure 3.4 Double-pipe heat exchanger (Shah & Sekulic, 2003)

3.1.3.1.2 Shell and Tube Heat Exchangers. Shell and tube heat exchangers are generally built of a bundle of round tubes mounted in a cylindrical shell with the tube axis parallel to that of the shell. One fluid flows inside the tubes, the other flows across and along the tubes. The major components of this exchanger are tubes (or tube bundle), shell, frontend head, rear-end head, baffles, and tube sheets. They are used as oil coolers, power condensers, preheaters in power plants, steam generators in nuclear power plants, and in process and chemical industry applications, extensively.

A horizontal shell and tube condenser is shown in Figure 3.5 and 3.6. One fluid flows through the tubes while the other flows on the shell side, across or along the tubes.

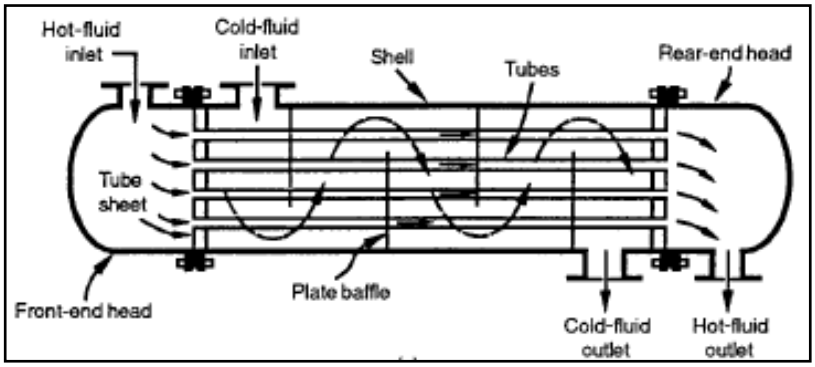


Figure 3.5 Shell and tube heat exchanger with one shell pass for the tube pass (Shah & Sekulic, 2003)

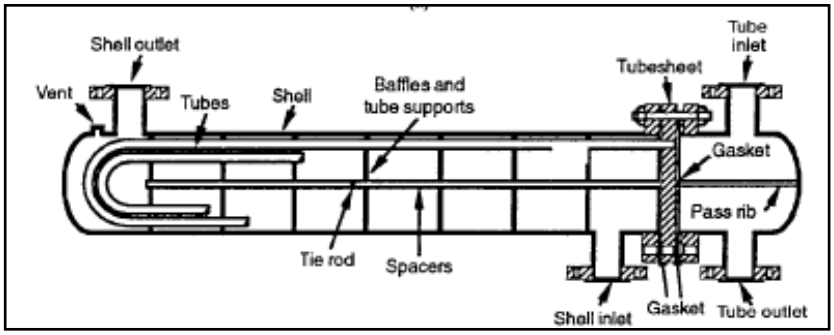


Figure 3.6 Shell and tube heat exchanger with one shell pass and two tube passes (Shah & Sekulic, 2003)

A variety of different internal constructions are used in shell-and-tube exchangers, depending on the desired heat transfer and pressure drop performance and the methods employed to reduce thermal stresses, to prevent leakages, to provide for ease of cleaning, to contain operating pressures and temperatures, to control corrosion, to accommodate highly asymmetric flows, and so on.

3.1.3.1.3 Spiral-Tube Heat Exchangers. Spiral-tube heat exchangers consist of one or more spirally wound coils fitted in a shell. Heat transfer rate associated with a spiral tube is higher than that for a straight tube. In addition, a considerable amount of surface can be accommodated in a given space by spiraling. Thermal expansion is no problem, but cleaning is almost impossible.

3.1.3.2 Plate Heat Exchangers

Plate-type heat exchangers are usually built of thin plates (all prime surface). The plates are either smooth or have some form of corrugation, and they are either flat or wound in an exchanger. Generally, these exchangers cannot accommodate very high pressures, temperatures, or pressure and temperature differences. Plate heat exchangers can be classified as gasketed, welded (one or both fluid passages), or brazed, depending on the leak tightness required. Other plate-type exchangers are spiral plate, lamella, and plate coil exchangers.

3.1.3.2.1 Gasketed-Plate Heat Exchangers. A typical gasketed-plate heat exchanger and the flow paths are shown in Figure 3.7. A gasketed plate consists of a series of corrugated or wavy thin plates that separates the fluids. Gaskets are used to prevent the leakage to the outside and direct the fluids in the plates. The counter current flow pattern is generally selected 31ort he fluids. Because of the small flow passages, strong eddying gives high heat transfer coefficients, high-pressure drops, and high local shear that minimize fouling. Gasketed-plate heat exchangers provide relatively compact and light weight heat transfer surface. They are typically used for heat exchange between two liquid streams. Because of easy cleaning and sterilization, they are extensively used in the food processing industry.

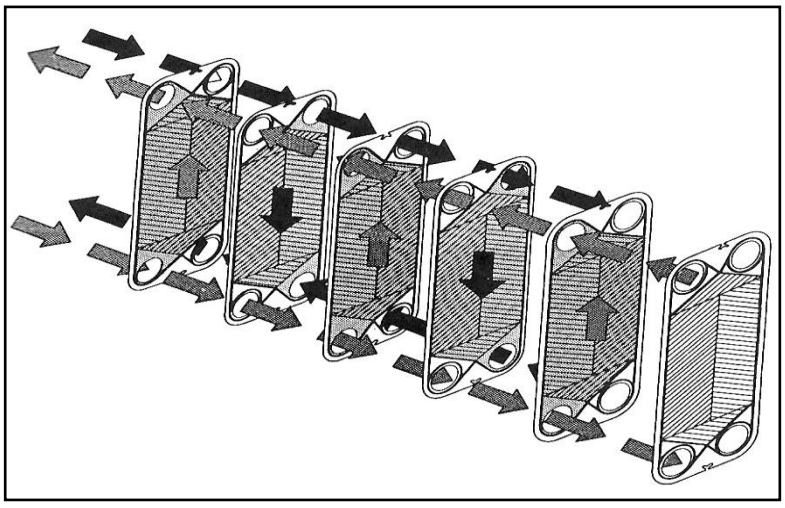


Figure 3.7 Gasketed-plate heat exchanger and flow paths (Kakaç & Liu, 1998)

3.1.3.2.2 Welded and Other Plate Heat Exchangers. One of the limitations of the gasketed plate heat exchanger is the presence of gaskets, which restricts their use to compatible fluids (noncorrosive fluids) and which limits operating temperatures and pressures. To overcome this limitation, a number of welded plate heat exchanger designs have surfaced with welded pairs of plates on one or both fluid sides. To reduce the effective welding cost, the plate size for this heat exchanger is usually larger than that of the gasketed plate heat exchangers. The disadvantage of such a design is the loss of disassembling flexibility on the fluid sides where the welding is done.

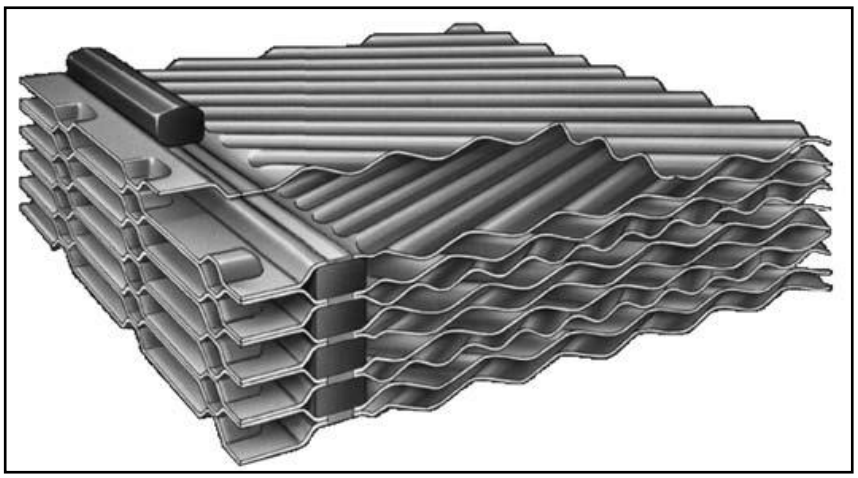


Figure 3.8 Section of welded plate heat exchanger (Shah & Sekulic, 2003)

A Bavex welded-plate heat exchanger with welded headers is shown in Figure 3.9. A Stacked Plate Heat Exchanger is another welded plate heat exchanger design (from Packinox), in which rectangular plates are stacked and welded at the edges. Some applications of this exchanger are for catalytic reforming, hydrosulfurization, and crude distillation, and in a synthesis converter feed effluent exchanger for methanol and for a propane condenser.

A vacuum brazed plate heat exchanger is a compact plate heat exchanger for high-temperature and high-pressure duties, and it does not have gaskets, tightening bolts, frame, or carrying and guide bars. The applications include water-cooled evaporators and condensers in the refrigeration industry, and process water heating and heat recovery.

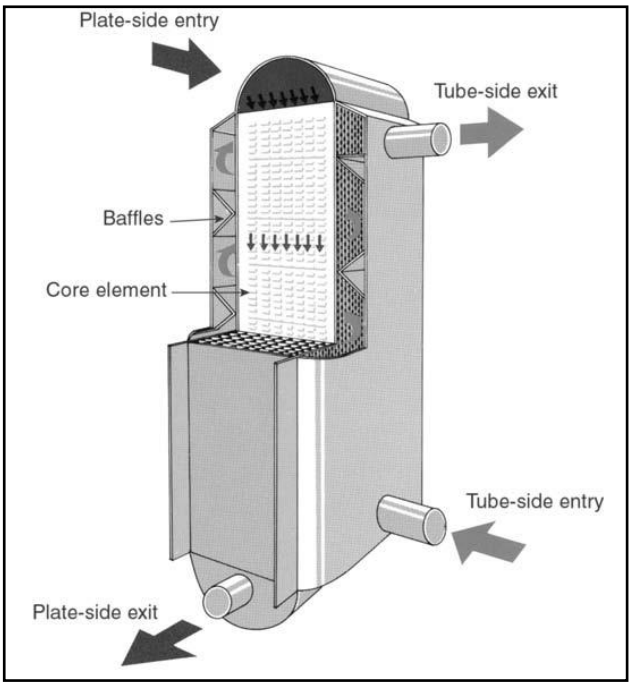


Figure 3.9 Bavex welded-plate heat exchanger (Shah & Sekulic, 2003)

3.1.3.2.3 Spiral Plate Heat Exchangers. A spiral plate heat exchanger consists of two relatively long strips of sheet metal, normally provided with welded studs for plate spacing, wrapped helically around a split mandrel to form a pair of spiral channels for two fluids, as shown in Figure 3.10.

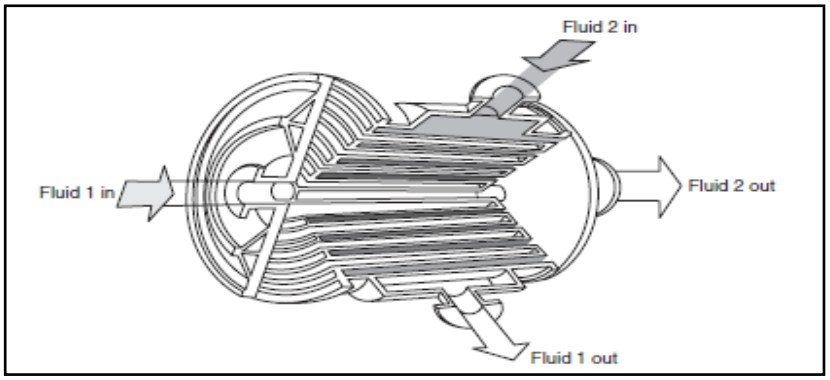


Figure 3.10 Spiral plate heat exchanger with both fluids in spiral counter flow (Shah & Sekulic, 2003)

The heat transfer coefficients are not as high as in a plate exchanger if the plates are not corrugated. However, the heat transfer coefficient is higher than that for a

shell-and-tube exchanger because of the curved rectangular passages. Hence, the surface area requirement is about 20% lower than that for a shell-and-tube unit for the same heat duty.

3.1.3.2.4 Lamella Heat Exchangers. A lamella heat exchanger consists of an outer tubular shell surrounding an inside bundle of heat transfer elements. These elements, referred to as lamellas, are flat tubes (pairs of thin dimpled plates, edge welded, resulting in high-aspect-ratio rectangular channels), shown in Figure 3.11.

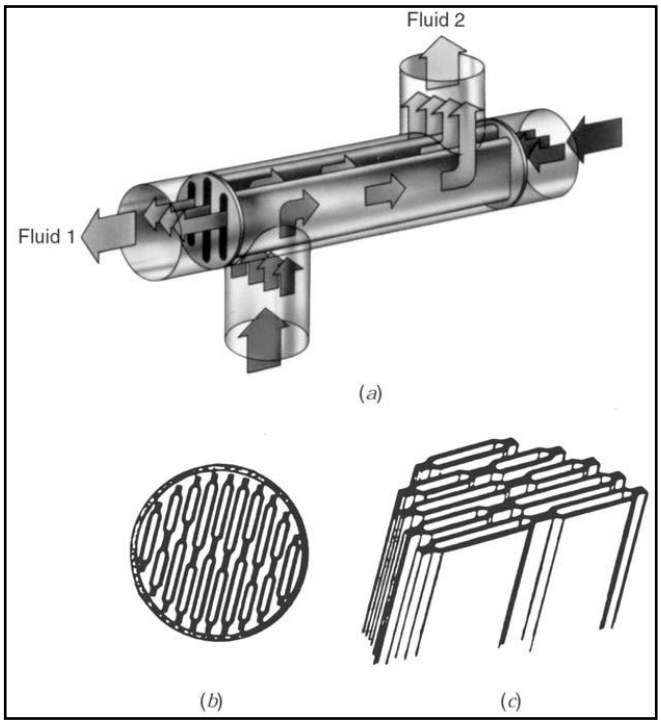


Figure 3.11 (a) Lamella heat exchanger; (b) cross section of a lamella heat exchanger; (c) lamellas (Shah & Sekulic, 2003)

3.1.3.3 Extended Surface Heat Exchangers

In some applications, much higher (up to about 98%) exchanger effectiveness is essential, and the box volume and mass are limited so that a much more compact surface is mandated. Also, in a heat exchanger with gases or some liquids, the heat transfer coefficient is quite low on one or both fluid sides. This results in a large heat transfer surface area requirement. One of the most common methods to increase the surface area and exchanger compactness is to add the extended surface (fins) and use fins with the fin density (fin frequency, fins/m or fins/in.) as high as possible on one or both fluid sides, depending on the design requirement. Addition of fins can increase the surface area by 5 to 12 times the primary surface area in general, depending on the design. The resulting exchanger is referred to as an extended surface exchanger. Plate-fin and tube-fin geometries are the two most common types of extended surface heat exchangers.

3.1.3.3.1 Plate-Fin Heat Exchangers. Plate-fin type of heat exchanger has corrugated fins (most commonly having triangular and rectangular cross sections) or spacers sandwiched between paralel plates. Plate fins are categorized as (1) plain (i.e., uncut) and straight fins, such as plain triangular and rectangular fins, (2) plain but wavy fins (wavy in the main fluid flow direction), and (3) interrupted fins, such as offset strip, louver, perforated, and pin fins. Examples of commonly used fins are shown in Figure 3.12.

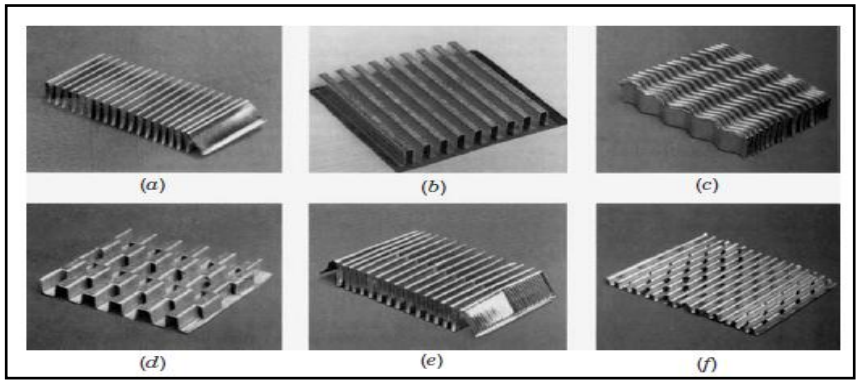


Figure 3.12 Corrugated fin geometries for plate-fin heat exchangers: (a) plain triangular fin;(b) plain rectangular fin; (c) wavy fin; (d) no strip fin; (e) multi louver fin; (f) perforated fin (Shah & Sekulic, 2003)

3.1.3.3.2 Tube-Fin Heat Exchangers. These exchangers may be classified as conventional and specialized tube-fin exchangers. In a conventional tube-fin exchanger, heat transfer between the two fluids takes place by conduction through the tube wall. However, in a heat pipe exchanger (a specialized type of tube-fin exchanger), tubes with both ends closed act as a separating wall, and heat transfer between the two fluids takes place through this ‘‘separating wall’’ (heat pipe) by conduction, and evaporation and condensation of the heat pipe fluid.

In a tube-fin exchanger, round and rectangular tubes are most common, although elliptical tubes are also used. Fins are generally used on the outside, but they may be used on the inside of the tubes in some applications. Depending on the fin type, tube-fin exchangers are categorized as follows: (1) an individually finned tube exchanger or simply a finned tube exchanger, as shown in Figures 3.13.a and 3.14, having normal fins on individual tubes; (2) a tube-fin exchanger having flat (continuous) fins, as shown in Figures 3.13.b and 3.15; the fins can be plain, wavy, or interrupted, and the array of tubes can have tubes of circular, oval, rectangular or other shapes; and (3) longitudinal fins on individual tubes, as shown in Figure 3.16. A tube fin exchanger with flat fins has been referred to variously as a plate-fin and tube, plate finned tube and tube in-plate fin exchanger in the literature.

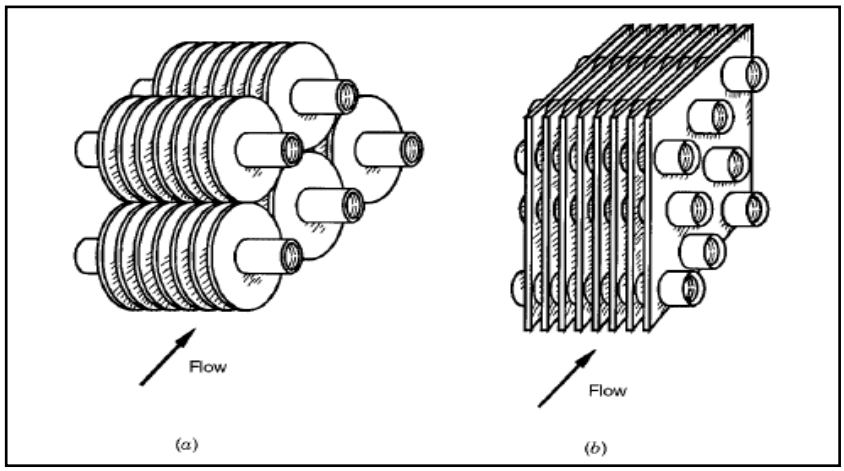


Figure 3.13 (a) Individually finned tubes; (b) flat (continuous) fins on an array of tubes. The flat fins are shown as plain fins, but they can be wavy, louvered, or interrupted (Shah & Sekulic, 2003)

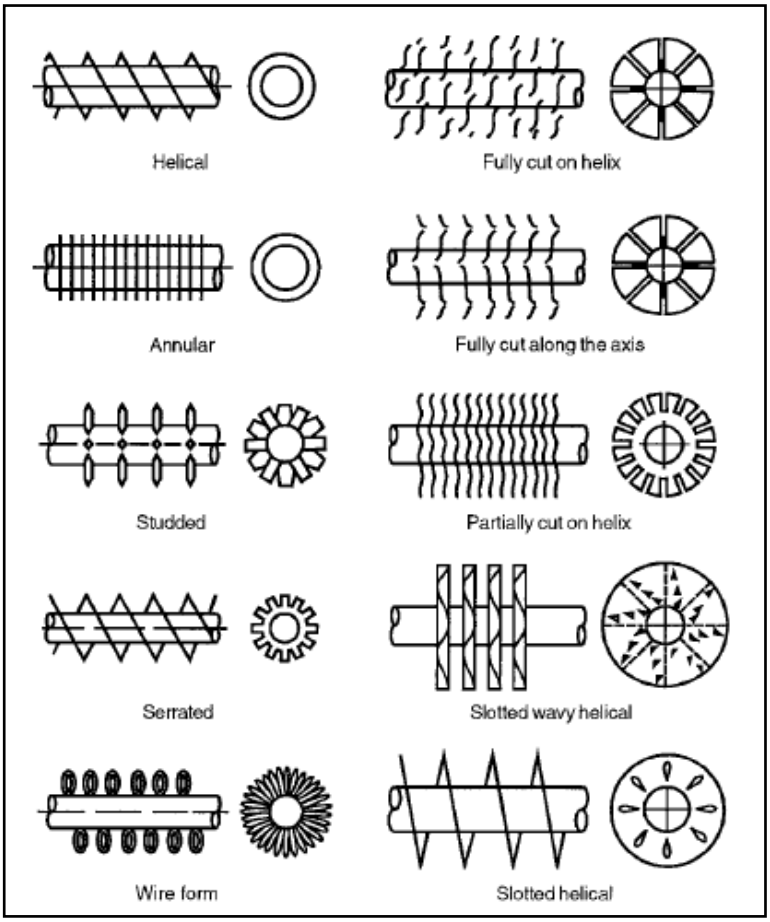


Figure 3.14 Individually finned tubes (Shah & Sekulic, 2003)

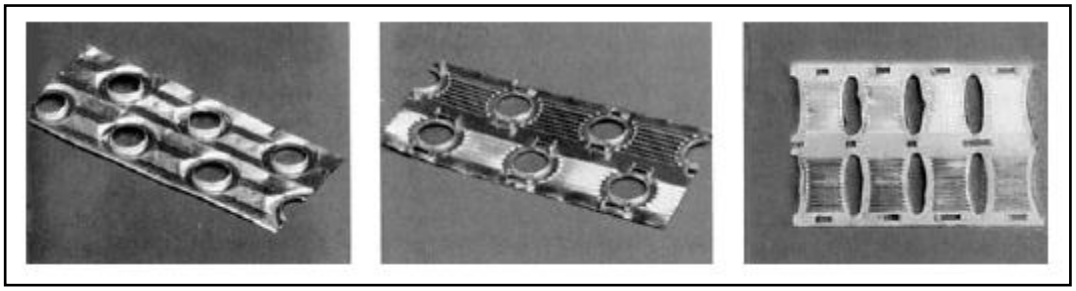


Figure 3.15 Flat fins on an array of round, flat, or oval tubes: (a) wavy fin; (b) multilouver fin; both fins with staggered round tubes; (c) multilouver fin with inline elliptical tubes (Shah & Sekulic, 2003)

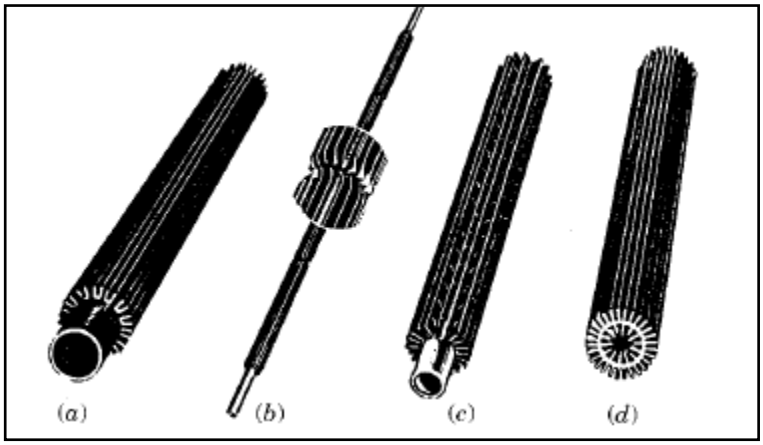


Figure 3.16. Longitudinal fins on individual tubes: (a) continuous plain; (b) cut and twisted; (c) perforated; (d) internal and external longitudinal fins (Shah & Sekulic, 2003)

3.1.4 Heat Transfer Mechanism

The basic heat transfer mechanisms employed for transfer of thermal energy from the fluid on one side of the exchanger to the wall (separating the fluid on the other side) are single-phase convection (forced or free), two-phase convection (condensation or evaporation, by forced or free convection), and combined convection and radiation heat transfer. Any of these mechanisms individually or in combination could be active on each fluid side of the exchanger (Shah & Sekulic, 2003).

Single-phase convection occurs on both sides of the following two-fluid exchangers: automotive radiators and passenger space heaters, regenerators, intercoolers, economizers, and so on. Single -phase convection on one side and two-phase convection on the other side (with or without desuperheating or superheating, and sub cooling, and with or without noncondensables) occur in the following two-fluid exchangers: steam power plant condensers, automotive and process / power plant air-cooled condensers, gas or liquid heated evaporators, steam generators, humidifiers, dehumidifiers and so on. Two-phase convection could occur on each side of a two-fluid heat exchanger, such as condensation on one side and evaporation on the other side, as in an air-conditioning evaporator. Multicomponent two-phase

convection occurs in condensation of mixed vapors in distillation of hydrocarbons. Radiant heat transfer combined with convective heat transfer plays a role in liquid metal heat exchangers and high temperature waste heat recovery exchangers. Radiation heat transfer is a primary mode in fossil-fuel power plant boilers, steam generators, coal gasification plant exchangers, incinerators, and other fired heat exchangers.

3.1.5 Flow Arrangement

Heat exchangers may be classified according to the fluid-flow path through the heat exchanger (Kakaç & Liu, 1998). Three basic flow arrangements are;

1. Parallel flow
2. Counter flow
3. Cross flow

As shown in Figure 3.17.a, in parallel flow heat exchangers, the two fluid streams enter together at one end, flow through the same direction, and leave together at the other end. In counter flow heat exchangers, two fluid streams flow in opposite direction (Figure 3.17.b). In single-cross flow heat exchangers, one fluid flows through the heat exchanger surface at right angles to the flow path of the other fluid. Cross flow arrangements with both fluids unmixed, and one fluid mixed and the other fluid unmixed are shown in Figures 3.17.c and 3.17.d, respectively.

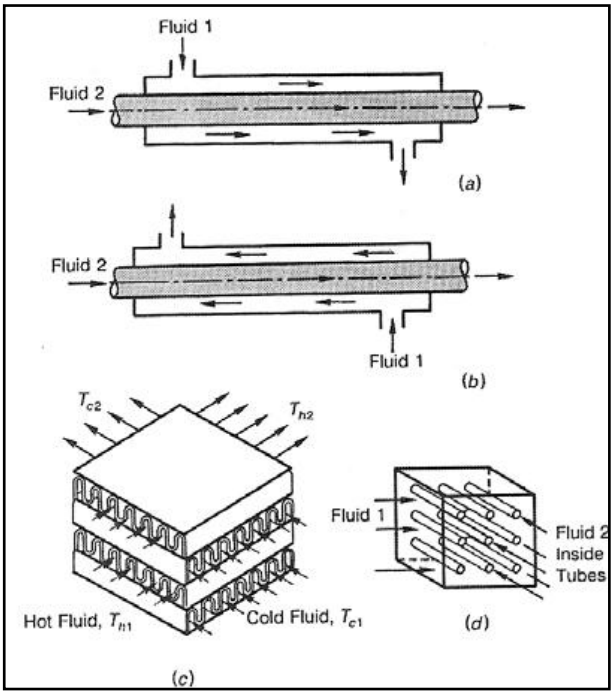


Figure 3.17 Heat exchanger classification according to flow arrangement. (a) Parallel-flow, (b) counter flow, (c) cross flow-both fluids unmixed, (d) cross flow fluid-1 mixed, fluid-2 unmixed (Kakaç & Liu, 1998)

3.2 Evaporators

The most common type air-conditioning evaporator or condenser is the type in which air flows over a circular tube bank that has been finned with continuous plates as shown in Figure 3.18; hence it is known as plate fin and tube heat exchanger. The evaporating or condensing refrigerant flows through tubes that are mounted perpendicular to the air flow and arranged in staggered rows. The end views in Figure 3.18 show that the tubes can be connected and coiled to form any number of passes, rows, and parallel paths, hence the name evaporator and condenser. Evaporators use round tubes for the most part. The fins and tubes are generally made of aluminum and copper respectively. The fins are connected to the tubes by inserting the tubes into holes stamped in the fins and then expanding the tubes by either mechanical or hydraulic means.

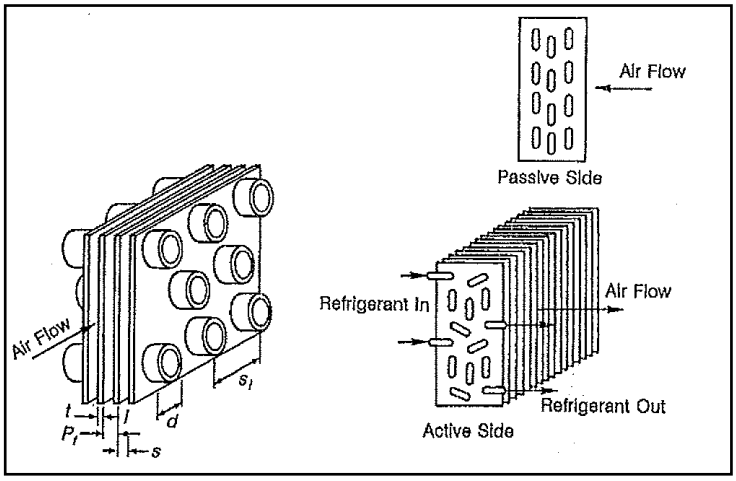


Figure 3.18 Evaporator (Kakaç &Liu, 1998)

Most refrigeration and air-conditioning air coils, whether evaporators or condensers, use circular-finned tubes rather than plate fin and tubes (the exception is evaporators in automotive air-conditioning). The fin plates used on the air side can be flat or plain surfaces, standard or sine-wave corrugated surfaces, or louvered surfaces. Examples of some of these fin surfaces are shown in Figure 3.19. The order presented represents increasing heat transfer performance; however, additional manufacturing effort is required to either deform or shape the surface or, in the case of louvering, to cut slits in the surface. It should also be noted that even though the heat transfer performance increases, the pressure drop on the air side, and, hence, required fan power, also increases.

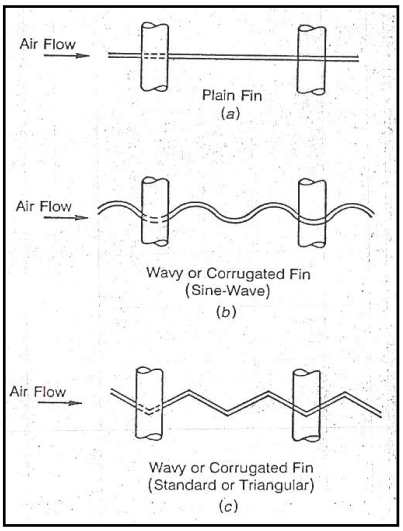


Figure 3.19 Several fin plates used on the air side. (Kakaç &Liu, 1998)

A typical fin and tube heat exchanger type evaporator for air conditioner indoor unit was shown in Figure 3.20.

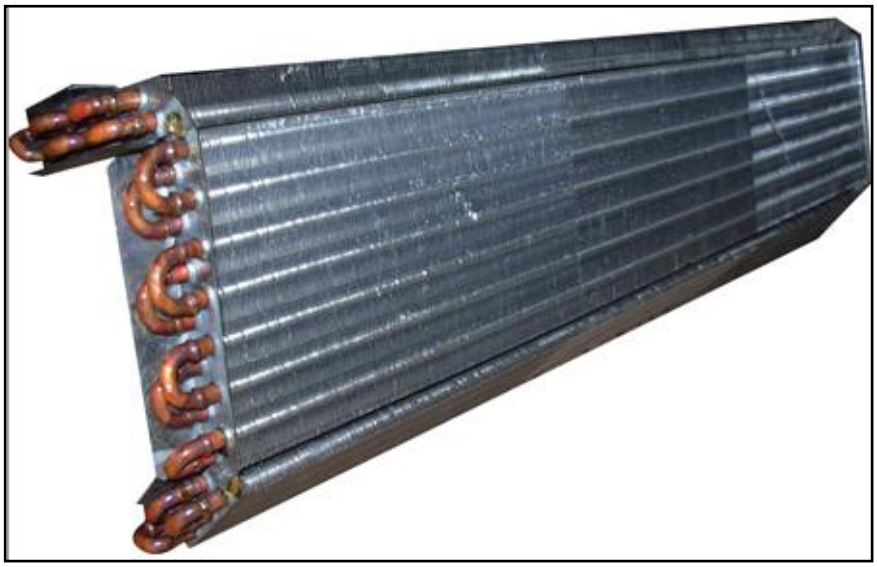


Figure 3.20 Air conditioner indoor unit evaporator (fin and tube heat exchanger) (http://maxellgroup.tradeindia.com/Exporters_Suppliers/Exporter16275.247966/Evaporator-Coil-for-Split-Indoor-Unit.html)

CHAPTER FOUR
NUMERICAL METHODS

4.1 Computational Fluid Dynamics (CFD)

Computational Fluid Dynamics (CFD) is a computer-based tool for simulating the behavior of systems involving fluid flow, heat transfer, and other related physical processes. It works by solving the equations of fluid flow over a region of interest, with specified (known) conditions on the boundary of that region. Computers are used to perform the millions of calculations required to simulate the interaction of fluids and gases with the complex surfaces used in engineering. However, even with simplified equations and high-speed supercomputers, only approximate solutions can be achieved in many cases. More accurate software that can accurately and quickly simulate even complex scenarios such as transonic or turbulent flows are an ongoing area of research. Validation of such software is often performed using a wind tunnel (Ansys CFD user manuel, CFD-Wiki).

Usage of CFD technique leads reduction of time and costs. The cost of an experiment is proportional to the variations at the number of data points and configurations. This may lead increase or decrease at the expense. CFD codes can produce large volumes of results depending on hardware configuration with no added expense. Whilst optimizing an equipment performance in other words performing a parametric study, CFD code is very cheap according to experiments.

Computational Fluid Dynamics (CFD) provides a qualitative prediction of fluid flows by means of;

- Mathematical modeling (partial differential equations)
- Numerical methods (discretization and solution techniques)
- Software tools (solvers, pre and post processing utilities)

CFD enables scientists and engineers to perform ‘numerical experiments’ (i.e. computer simulations) in a ‘virtual flow laboratory’. Numerical simulations of fluid flow (will) enable;

• Architects to design comfortable and safe living environments,
• Designers of vehicles to improve the aerodynamic characteristics,
• Chemical engineers to maximize the yield from their equipment,
• Petroleum engineers to devise optimal oil recovery strategies,
• Surgeons to cure arterial diseases (computational hemodynamic),
• Meteorologists to forecast the weather and warn of natural disasters,
• Safety experts to reduce health risks from radiation and other hazards,
• Military organizations to develop weapons and estimate the damage.

4.1.1 The History of CFD

Computers have been used to solve fluid flow problems for many years. Numerous programs have been written to solve either specific problems, or specific classes of problems. From the mid-1970's, the complex mathematics required to generalize the algorithms began to be understood, and general purpose CFD solvers were developed. These began to appear in the early 1980's and required what were then very powerful computers, as well as an in-depth knowledge of fluid dynamics, and large amounts of time to set up simulations. Consequently, CFD was a tool used almost exclusively in research (Ansys CFD user manuel).

Recent advances in computing power, together with powerful graphics and interactive 3D manipulation of models have made the process of creating a CFD model and analyzing results much less labor intensive, reducing time and, hence, cost. Advanced solvers contain algorithms which enable robust solutions of the flow field in a reasonable time.

As a result of these factors, Computational Fluid Dynamics is now an established industrial design tool, helping to reduce design time scales and improve processes

throughout the engineering world. CFD provides a cost-effective and accurate alternative to scale model testing, with variations on the simulation being performed quickly, offering obvious advantages.

4.1.2 The Mathematics of CFD

Fluid Dynamics is the investigation of the interactive motion of a large number of individual particles (molecules or atoms). That means, the density of the fluid is high enough, so that it can be approximated as a continuum. It implies that even an infinitesimally small (in the sense of differential calculus) element of the fluid still contains a sufficient number of particles, for which we can specify mean velocity and mean kinetic energy. In this way, we are able to define velocity, pressure, temperature, density and other important quantities at each point of the fluid (Blazek, 2001 and Anderson, 1995).

All of CFD, in one form or another, is based on the fundamental governing equations of fluid dynamics the continuity, momentum, and energy equations. These equations speak physics. They are the mathematical statements of three fundamental physical principles upon which all of fluid dynamics is based on following conservation laws:

1. The conservation of mass,
2. The conservation of momentum,
3. The conservation of energy.

The set of equations which describe the processes of momentum, heat and mass transfer are known as the Navier-Stokes equations. These partial differential equations were derived in the early nineteenth century and have no known general analytical solution but can be discredited and solved numerically.

There are a number of different solution methods which are used in CFD codes. After selecting the mathematical model, one has to choose a suitable discretization

method, i.e. a method of approximating the differential equations by a system of algebraic equations for the variables at some set of discrete locations in space and time. There are many approaches, but the most important of which are: finite difference (FD), finite volume (FV) and finite element (FE) methods. The most common and the one on which ANSYS CFD is based, is known as the finite volume technique.

In this technique, the region of interest is divided into small sub-regions, called control volumes. The equations are discredited and solved iteratively for each control volume. As a result, an approximation of the value of each variable at specific points throughout the domain can be obtained.

4.1.2.1 Finite Control Volume

A general flow field as represented by the streamlines in Figure 4.1.a and a closed volume drawn within a finite region of the flow. This volume defines a control volume U; a control surface S is defined as the closed surface which bounds the volume. The control volume may be fixed in space with the fluid moving through it, as shown at the left of Figure 4.1.a. Alternatively, the control volume may be moving with the fluid such that the same fluid particles are always inside it, as shown at the right of Figure 4.1.a. In either case, the control volume is a reasonably large, finite region of the flow. The fundamental physical principles are applied to the fluid inside the control volume and to the fluid crossing the control surface (if the control volume is fixed in space). Therefore, instead of looking at the whole flow field at once, with the control volume model we limit our attention to just the fluid in the finite region of the volume itself. The fluid-flow equations that we directly obtain by applying the fundamental physical principles to a finite control volume are in integral form. These integral forms of the governing equations can be manipulated to indirectly obtain partial differential equations. The equations so obtained from the finite control volume fixed in space (left side of Figure 4.1.a), in either integral or partial differential form, are called the conservation form of the governing equations. The equations obtained from the finite control volume moving with the fluid (right side of

Figure 4.1.a), in either integral or partial differential form, are called the nonconservation form of the governing equations (Blazek, 2001).

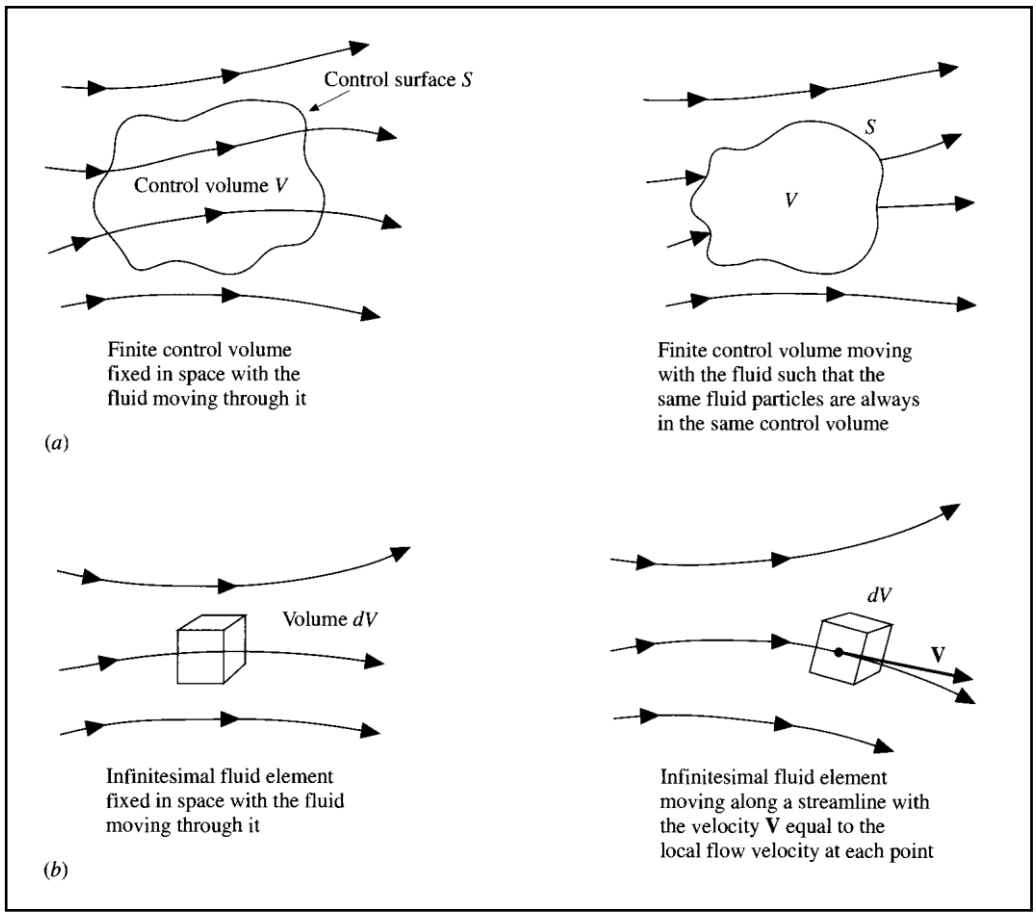


Figure 4.1 Models of flow (a) Finite control volume approach; (b) infinitesimal fluid element approach (Blazek, 2001)

4.1.2.2 Infinitesimal Fluid Element

General flow field represented by the streamlines in Figure 4.1.b and it is an infinitesimally small fluid element in the flow with a differential volume dU. The fluid element is infinitesimal in the same sense as differential calculus; however, it is large enough to contain a huge number of molecules so that it can be viewed as a continuous medium. The fluid element may be fixed in space with the fluid moving through it, as shown at the left of Figure 4.1.b. Alternatively, it may be moving along a streamline with a velocity vector V equal to the flow velocity at each point. Again, instead of looking at the whole flow field at once, the fundamental physical

principles are applied to just the infinitesimally small fluid element itself. This application leads directly to the fundamental equations in partial differential equation form. Moreover, the particular partial differential equations obtained directly from the fluid element fixed in space (left side of Figure 4.1.b) are again the conservation form of the equations. The partial differential equations obtained directly from the moving fluid element (right side of Figure 4.1.b) are again called the nonconservation form of the equations (Blazek, 2001).

4.2 Conservation Laws

4.2.1 The Continuity Equation

In order to derive the continuity equation, consider the model of a finite control volume fixed in space, as sketched in Figure 4.2. At a point on the control surface, the flow velocity is $\vec{v}$, the unit normal vector is $\vec{n}$ and dS denotes an elemental surface area. The conserved quantity in this case is the density ρ. For the time rate of change of the total mass inside the finite volume U we have;

$$\frac{\partial}{\partial t}\int_{U} \rho dU \qquad \ldots(4.1)$$

The mass flow of a fluid through some surface fixed in space equals to the product of (density) x (surface area) x (velocity component perpendicular to the surface). Therefore, the contribution from the convective flux across each surface element dS becomes**;**

$$\rho(\vec{v}.\vec{n}).\,dS \qquad \ldots(4.2)$$

Since by convection $\vec{n}$ always points out of the control volume, we speak of inflow if the product $(\vec{v}.\vec{n})$ is negative, and of outflow if it is positive and hence the mass flow leaves the control volume. As stated above, there are no volume or surface

sources present. Thus, by taking into account the general formulation of Eq. (4.3), we can write;

$$\frac{\partial}{\partial t}\int_{\upsilon} \rho d\mathrm{U} + \oint_{\partial \upsilon} \rho(\vec{v}.\vec{n})dS = 0 \qquad \ldots (4.3)$$

This represents the integral form of the continuity equation - the conservation law of mass.

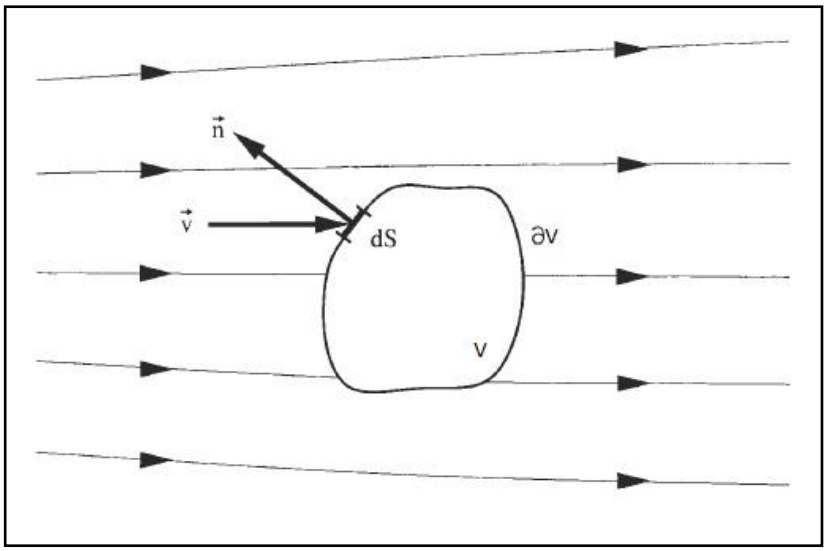


Figure 4.2 Definition of a finite control volume (fixed in space) (Blazek, 2001)

4.2.2 The Momentum Equation

The derivation of the momentum equation can start by recalling the particular form of Newton's second law which states that the variation of momentum is caused by the net force acting on a mass element. For the momentum of an infinitesimally small portion of the control volume U (Figure 4.2) we have;

$$\rho\vec{v}d\mathrm{U} \qquad \ldots (4.4)$$

The variation in time of momentum within the control volume equals;

$$\frac{\partial}{\partial t}\int_{\upsilon} \rho\vec{v}d\mathrm{U} \qquad \ldots (4.5)$$

Hence, the conserved quantity is here the product of density times the velocity, i.e,

$$\rho.\vec{v} = [\,\rho u, \rho v, \rho\omega]^T \qquad \ldots(4.6)$$

The convective flux tensor, which describes the transfer of momentum across the boundary of the control volume, consists in the Cartesian coordinate system of the following three components;

x-component: $\rho u\vec{v}$
y-component : $\rho v\vec{v}$
z-component : $\rho\omega\vec{v}$

The contribution of the convective flux tensor to the conservation of momentum is then given by;

$$-\oint_{\partial\upsilon} \rho\vec{v}(\vec{v}.\vec{n})\,dS \qquad \ldots(4.7)$$

The diffusive flux is zero, since there is no diffusion of momentum possible for a fluid at rest. We can identify two kinds of forces acting on the control volume:

1. External volume or body forces, which act directly on the mass of the volume. These are for example gravitational, buoyancy, Coriolis or centrifugal forces. In some cases, there can be electromagnetic forces present as well.

2. Surface forces, which act directly on the surface of the control volume. They result from only two sources:
(a) the pressure distribution, imposed by the outside fluid surrounding the volume,
(b) the shear and normal stresses, resulting from the friction between the fluid and the surface of the volume.

The body force per unit volume, denoted as $\rho.\vec{f}$, the surface sources consist of two parts - an isotropic pressure component and a viscous stress tensor $\vec{\vec{\tau}}$ .The effect of the surface sources on the control volume is sketched in Figure 4.3**.**

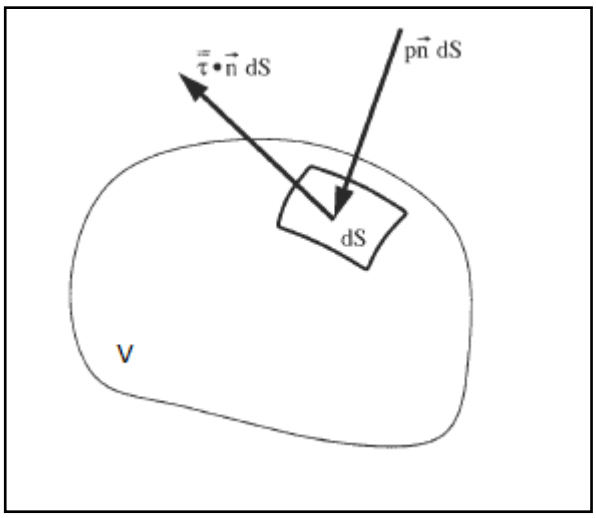


Figure 4.3 Surface forces acting on a surface element of the control volume (Blazek, 2001)

Sum up all the above contributions according to the general conservation law; we finally obtain the expression in Eq. 4.8;

$$\frac{\partial}{\partial t}\int_{\upsilon} \rho\vec{v}dU + \oint_{\partial\upsilon} \rho\vec{v}(\vec{v}.\vec{n})dS = \int_{\upsilon} \rho\vec{f}dU - \oint_{\partial\upsilon} p\vec{n}dS + \oint_{\partial\upsilon} \left(\vec{\vec{\tau}}.\vec{n}\right) dS \quad \text{... (4.8)}$$

4.2.3 The Energy Equation

The first law of thermodynamics is the main principle for the energy equation. As displayed in Figure 4.2, any changes in time of the total energy inside the volume are caused by the rate of work of forces acting on the volume and by the net heat flux into it. The total energy per unit mass *E* of a fluid is obtained by adding its internal energy per unit mass, *i*, to its kinetic energy per unit mass, $|\vec{v}|^2/2$. Thus, we can write for the total energy;

$$\mathrm{E} = i + \frac{|\vec{\mathrm{v}}|^2}{2} = i + \frac{\mathrm{u}^2+\upsilon^2+\omega^2}{2} \quad \ldots(4.9)$$

The conserved quantity is in this case the total energy per unit volume, i.e., ρE. Its variation in time within the volume U can be expressed as;

$$\frac{\partial}{\partial t}\int_{\upsilon} \rho E d\mathrm{U} \quad \ldots(4.10)$$

We can readily specify the contribution of the convective flux as **;**

$$-\oint_{\partial\upsilon} \rho\mathrm{E}(\vec{\mathrm{v}}.\vec{\mathrm{n}})\mathrm{dS} \quad \ldots(4.11)$$

In contrast to the continuity and the momentum equation, there is now a diffusive flux $\vec{F}_D$ is defined in general written in the form of Fourier's law of heat conduction with k standing for the thermal conductivity coefficient and T for the absolute static temperature;

$$\vec{\mathrm{F}}_{\mathrm{D}} = -\mathrm{k}\nabla\mathrm{T} \quad \ldots.(4.12)$$

The other part of the net heat flux into the finite control volume consists of volumetric heating due to absorption or emission of radiation, or due to chemical reactions. We will denote the heat sources - the time rate of heat transfer p y unit mass - as $\dot{q}_h$. Together with the rate of work done by the body forces $\vec{f}$**,** which we have introduced for the momentum equation, it completes the volume sources;

$$\mathrm{Q_V} = \rho\,\vec{\mathrm{f}}.\vec{\mathrm{v}} + \dot{\mathrm{q}}_{\mathrm{h}} \quad \ldots(4.13)$$

The last contribution to the conservation of energy, which we have yet to determine, is the surface sources Q_S. They correspond to the time rate of work done by the pressure as well as the shear and normal stresses on the fluid element;

$$\overrightarrow{Q_S} = -p\vec{v} + \vec{\vec{\tau}} . \vec{v} \qquad \dots (4.14)$$

Sorting now all the above contributions and terms, we obtain for the energy conservation equation (4.3) the expression;

$$\frac{\partial}{\partial t}\int_{\upsilon} \rho E d\upsilon + \oint_{\partial\upsilon} \rho E(\vec{v}.\vec{n})dS = \oint_{\partial\upsilon} k(\nabla T . \vec{n}).dS + \int_{\upsilon} (\rho \vec{f}. \vec{v} + \dot{q}h) d\upsilon - \oint_{\partial\upsilon} p(\vec{v}.\vec{n})dS + \oint_{\partial\upsilon} \left(\vec{\vec{\tau}}.\vec{n}\right).\vec{n} dS \qquad \dots (4.15)$$

4.3 Conservative Form of the Governing Equations of Fluid Flow

The governing equations can be summarize in Table 4.1 the conservative or divergence form of the system of equations which governs the time-dependent three-dimensional fluid flow and heat transfer of a compressible Newtonian fluid (Versteeg& Malalasekera, 1995).

Table 4.1 Governing equations of a compressible fluid flow (Versteeg & Malalasekera, 1995)

MASS	$\frac{\partial \rho}{\partial t} + \text{div}(\rho v) = 0$
X-MOMENTUM	$\frac{\partial \rho u}{\partial t} + \text{div}(\rho u v) = -\frac{\partial p}{\partial x} + \text{div}(\mu \text{ grad } u) + S_{Mx}$
Y-MOMENTUM	$\frac{\partial \rho v}{\partial t} + \text{div}(\rho v v) = -\frac{\partial p}{\partial x} + \text{div}(\mu \text{ grad } v) + S_{My}$
Z-MOMENTUM	$\frac{\partial \rho \omega}{\partial t} + \text{div}(\rho \omega v) = -\frac{\partial p}{\partial x} + \text{div}(\mu \text{ grad } \omega) + S_{Mz}$
INTERNAL ENERGY	$\frac{\partial (\rho i)}{\partial t} + \text{div}(\rho i v) = -p \text{ div } v + \text{div}(k \text{ grad } T) + \phi + S_i$
EQUATIONS OF STATE	p = p(ρ,T) and i=i(ρ,T) for perfect gas; p= ρRT and i =$C_v T$

4.4 The Control Volume

ANSYS CFD uses an element-based finite volume method, which first involves discretizing the spatial domain using a mesh. The mesh is used to construct finite volumes, which are used to conserve relevant quantities such as mass, momentum, and energy (ANSYS CFD theory guide).

The Figure 4.4 shows a typical three-dimensional mesh. All solution variables and fluid properties are stored at the nodes (mesh vertices). A control volume (the shaded area) is constructed around each mesh node using the median dual (defined by lines joining the centers of the edges and element centers surrounding the node).

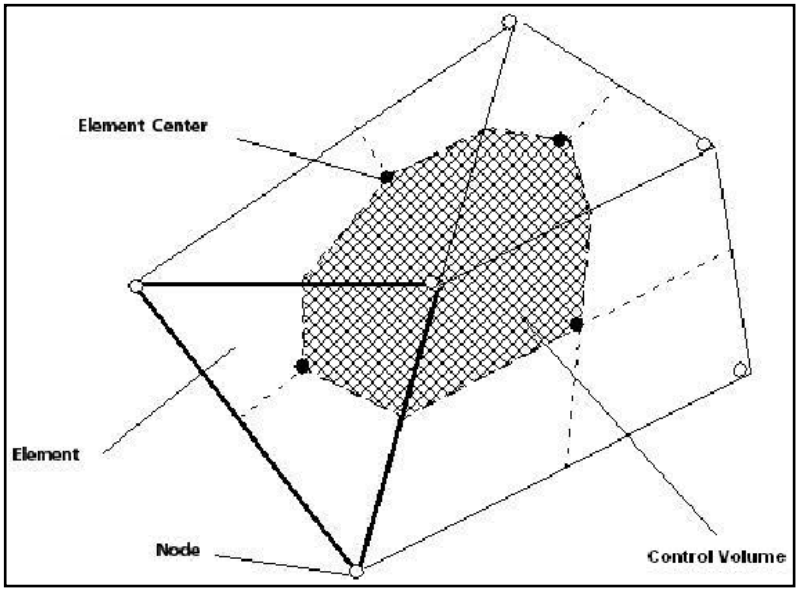


Figure 4.4 Control volume definition

4.5 General Solution Procedure of CFD

To solve governing equations above numerically, the solution procedure can be summarize as the following steps (Çengel, 2008).

1. A computational domain is chosen, and a grid (also called a mesh) is generated; the domain is divided into many small elements called cells. For two-dimensional (2D) domains, the cells are areas, while for three-dimensional (3D) domains the cells

are volumes. We can think of each cell as a tiny control volume in which discretized versions of the conservation equations are solved. We limit our discussion here to cell-centered finite volume CFD codes. The quality of a CFD solution is highly dependent on the quality of the grid.

2. Boundary conditions are specified on each edge of the computational domain (2D flows) or on each face of the domain (3D flows).

3. The type of fluid (water, air, gasoline, etc.) is specified, along with fluid properties (temperature, density, viscosity, etc.).

4. Numerical parameters and solution algorithms are selected. These are specific to each CFD code and the default settings of or user specified codes can be use.

5. Starting values for all flow field variables are specified for each cell. These are initial conditions, which may or may not be correct, but are necessary as a starting point, so that the iteration process may proceed. We note that for proper unsteady-flow calculations, the initial conditions must be correct.

6. Beginning with the initial guesses, discretized forms of governing equations are solved iteratively, usually at the center of each cell. If one were to put all the terms of Navier-Stokes equation on one side of the equation, the solution would be “exact” when the sum of these terms, defined as the residual, is zero for every cell in the domain. In a CFD solution, however, the sum is never identically zero, but decreases with progressive iterations. A residual can be thought of as a measure of how much the solution to a given transport equation deviates from exact, and one monitors the average residual associated with each transport equation to help determine when the solution has converged. Sometimes hundreds or even thousands of iterations are required to converge on a final solution, and the residuals may decrease by several orders of magnitude.

7. Once the solution has converged, flow field variables such as velocity and pressure are plotted and analyzed graphically. Users can also define and analyze additional custom functions that are formed by algebraic combinations of flow field variables. Most commercial CFD codes have built in postprocessors, designed for quick graphical analysis of the flow field. There are also stand-alone postprocessor software packages available for this purpose.

8. Global properties of the flow field, such as pressure drop, and integral properties, such as forces (lift and drag) and moments acting on a body, are calculated from the converged solution.

For unsteady flow, a physical time step is specified, appropriate initial conditions are assigned, and an iteration loop is carried out to solve the transport equations to simulate changes in the flow field over this small span of time. Since the changes between time steps are small, a relatively small number of iterations (on the order of tens) is usually required between each time step. Upon convergence of this "inner loop," the code marches to the next time step. If a flow has a steady-state solution, that solution is often easier to find by marching in time after enough time has past, the flow field variables settle down to their steady-state values.

4.5.1 Solution Strategy of ANSYS CFD - The Coupled Solver

Segregated solvers employ a solution strategy where the momentum equations are first solved, using a guessed pressure, and an equation for a pressure correction is obtained. Because of the 'guess-and-correct' nature of the linear system, a large number of iterations are typically required in addition to the need for judiciously selecting relaxation parameters for the variables (ANSYS CFD Theory Guide).

ANSYS CFD uses a coupled solver, which solves the hydrodynamic equations (for *u, v, w and p*) as a single system. This solution approach uses a fully implicit discretization of the equations at any given time step. For steady state problems, the time-step behaves like an 'acceleration parameter', to guide the approximate

solutions in a physically based manner to a steady-state solution. This reduces the number of iterations required for convergence to a steady state, or to calculate the solution for each time step in a time-dependent analysis.

The flow chart shown below illustrates the general field solution process used in the CFD Solver (Figure 4.5). The solution of each set of field equations shown in the flow chart consists of two numerically intensive operations. For each time step:

1. Coefficient Generation: The non-linear equations are linearized and assembled into the solution matrix.

2. Equation Solution: The linear equations are solved using an Algebraic Multigrid method.

When solving fields in the CFD-Solver, the outer (or time step) iteration is controlled by the physical time scale or time step for steady and transient analyses, respectively. Only one inner (linearization) iteration is performed per outer iteration in steady state analyses, whereas multiple inner iterations are performed per time step in transient analyses.

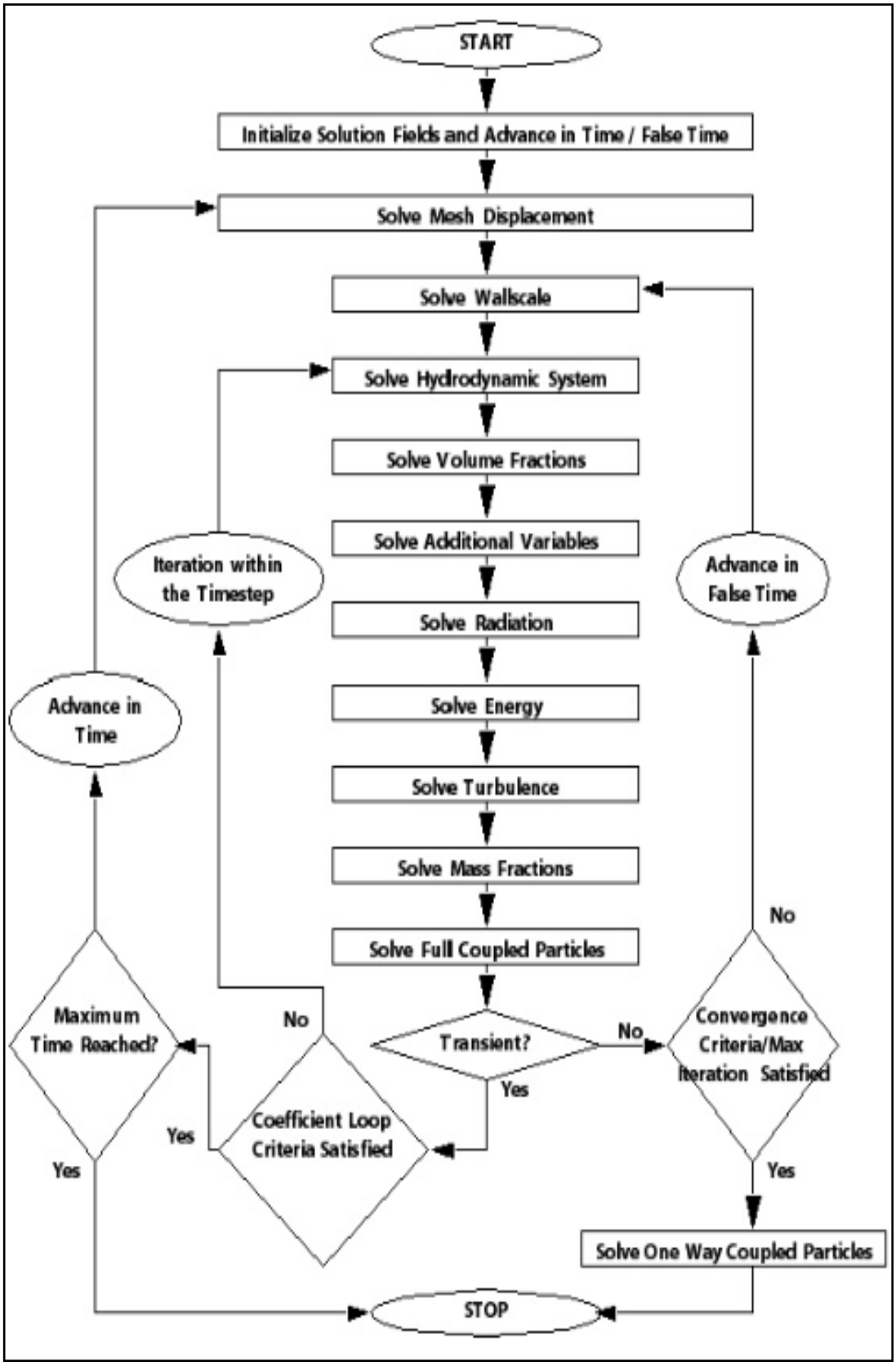


Figure 4.5 ANSYS CFD general solution strategy (ANSYS CFD Theory Guide)

4.6 CFD with Heat Transfer

By coupling the differential form of the energy equation with the equations of fluid motion, we can use a computational fluid dynamics code to calculate properties associated with heat transfer (e.g., temperature distributions or rate of heat transfer from a solid surface to a fluid). Since the energy equation is a scalar equation, only one extra transport equation (typically for either temperature or enthalpy) is required, and the computational expense (CPU time and RAM requirements) is not increased significantly. Heat transfer capability is built into most commercially available CFD codes, since many practical problems in engineering involve both fluid flow and heat transfer. Additional boundary conditions related to heat transfer need to be specified. At solid wall boundaries, we may specify either wall temperature T_{wall} (K) or the wall heat flux $\dot{q}_{wall}$ (W/m^2), defined as the rate of heat transfer per unit area from the wall to the fluid. When we model a zone in a computational domain as a solid body that involves the generation of thermal energy via electric heating (as in electronic components) or chemical or nuclear reactions (as in nuclear fuel rods), we may instead specify the heat generation rate per unit volume $\dot{g}$ (W/m^3) within the solid since the ratio of the total heat generation rate to the exposed surface area must equal the average wall heat flux. In that case, neither T_{wall} nor $\dot{q}_{wall}$ is specified; both converge to values that match the specified heat generation rate. In addition, the temperature distribution inside the solid object itself can then be calculated. Other boundary conditions (such as those associated with radiation heat transfer) may also be applied in CFD codes (Çengel, 2008).

CHAPTER FIVE
THEORETICAL STUDY

6.1 Air Side Heat Transfer Coefficient

In this chapter, the air side heat transfer coefficient and pressure drop of the heat exchanger of an air-conditioner unit calculated, theoretically. The geometrical characteristics for plain flat fins on circular tubes type heat exchanger were given below (Figure 5.1);

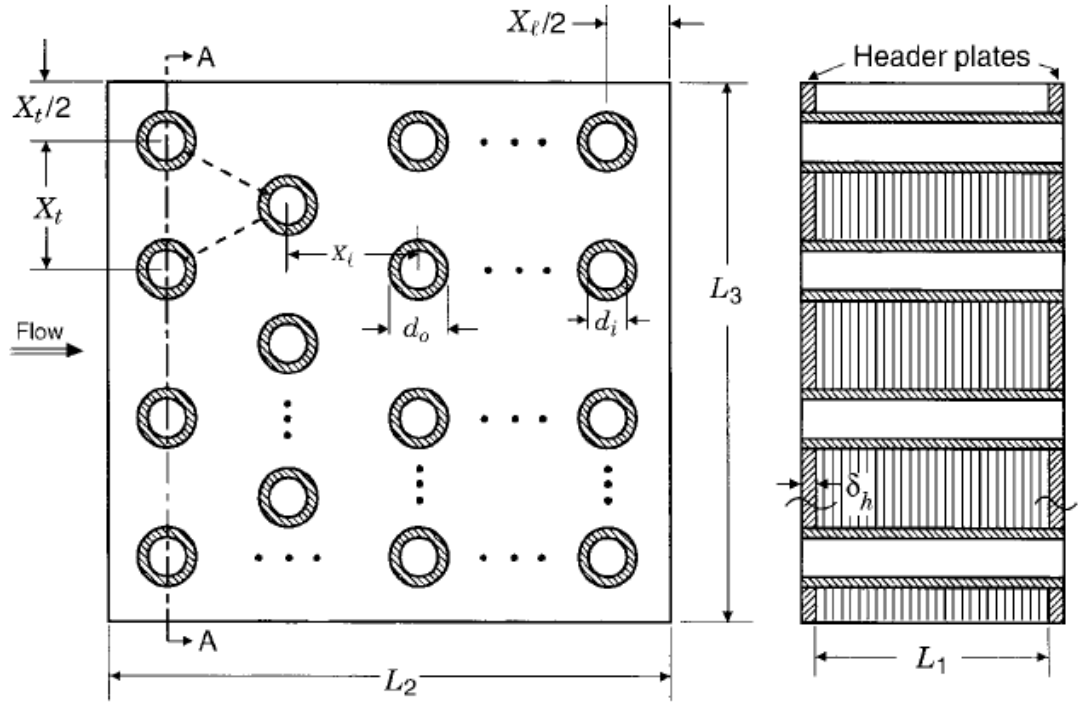


Figure 5.1 Flat fin and tube heat exchanger geometrical parameters (Shah & Sekulic, 2003)

The split air conditioner indoor unit heat exchanger geometry has aluminum fins with δ thicknesses, d_0 tube diameter and L_1 evaporator length. Each fin construction consist of specially designated configurations with longitudinal pitch (X_L) through the L_2 length, transverse pitch (X_T) through the L_3 length, diagonal pitch (X_D) and gap between two fins (s) by the manufacturer. Although the geometrical structure of heat exchanger has been shown in Figure 5.2, numerical data for notations wasn't given here due to the confidentiality of commercial information.



Figure 5.2 Geometry of air-conditioner heat exchanger and fin

Number of fins per unit length (N_f) calculated as the ratio of 1/ fin pitch. The fin pitch (p_f) equals the sum of gap between two fins (s) and fin thickness (δ). The total number of tubes entitled as N_t and to calculate this, the following equation (Eq. 5.1) was used.

$$N_t = \frac{\mathrm{L_2}.\mathrm{L_3}}{\mathrm{X_T}.\mathrm{X_L}} \quad \ldots (5.1)$$

The total heat transfer area (Eq. 5.2) consists of the area associated with the exposed tubes (primary surface area) and the fins (secondary surface area) (Shah & Sekulic, 2003, p.571).

$$\mathrm{A} = \mathrm{A_p} + \mathrm{A_f} \quad \ldots (5.2)$$

$$A_p = \pi.d_o.\left(\mathrm{L_1} - \delta.N_f.\mathrm{L_1}\right).N_t \quad \ldots (5.3)$$

$$A_f = 2.\left(\mathrm{L_2}.\mathrm{L_3} - \frac{\pi.d_o^2}{4}.N_t\right).N_f.L_1 + 2.L_3.N_f.L_1.\delta \quad \ldots (5.4)$$

The minimum free-flow area is calculated from Eq. 5.5 (Shah & Sekulic, 2003, p.573),

$$A_0 = [\left(\frac{L_3}{X_T} - 1\right).c" + (X_T - d_0) - (X_T - d_0).\delta.N_f].L_1 \quad \text{... (5.5)}$$

For the staggered tube arrangement, the minimum free-flow area could occur either through the front row or through the diagonals and it is determined from Eq. 5.6 (Shah & Sekulic, 2003, p.573);

$$c" = \begin{cases} 2a" & \text{if } 2a" < 2b" \\ 2b" & \text{if } 2b" < 2a" \end{cases} \quad \text{... (5.6)}$$

Modified dimensions, referred to as 2a" and b", are given by Eq. 5.7 and 5.8.

$$2a" = (X_T - d_0) - (X_T - d_0).\delta.N_f \quad \text{... (5.7)}$$

$$b" = [(\frac{X_T}{2})^2 + X_L^2]^{1/2} - d_0 - (X_T - d_0).\delta.N_f \quad \text{... (5.8)}$$

Air-side heat transfer coefficient (h) is calculated from Eq. 5.9 (Incropera & DeWitt, 2001, p.202),

$$h = \frac{Nu \,.\, k}{D_h} \quad \text{... (5.9)}$$

h: Heat transfer coefficient (W/m^{2}K)
Nu: Nusselt number
k: Conduction heat transfer coefficient of the air (W/mK)
D_h: Hydraulic diameter (m)

Hydraulic diameter is calculated from Eq. 5.10 (Kakaç & Liu, 1998, p.307).

$$D_h = 4.L.\frac{A_o}{A} \quad \text{... (5.10)}$$

Air-side Nusselt number is calculated from Eq. 5.11 (VDI Heat Atlas),

$$\mathrm{Nu} = 0.38.Re^{0.6}.\mathrm{Pr}^{\frac{1}{3}}.(\frac{A}{A_p})^{-0.15} \quad \ldots (5.11)$$

Reynolds number is calculated from Eq. 5.12 (Incropera & DeWitt, 2001, p.664). Air flows over collar diameter between fins. Mass velocity in minimum area is represented as G and calculated from Eq. 5.13 (Incropera & DeWitt, 2001, p.664).

$$Re = \frac{G.D_h}{\mu} \quad \ldots (5.12)$$

$$G = \rho.u_{max} \quad \ldots (5.13)$$

Air velocity in minimum free flow area is u_{max} (Incropera & DeWitt, 2001, p.406);

$$\mathrm{u_{max}} = \mathrm{u}.\frac{\mathrm{X_T}}{\mathrm{X_T} - \mathrm{d_o}} \quad \ldots (5.14)$$

Re: Reynolds number
G: Mass flux (kg/m^2s)
μ: Air dynamic viscosity at average temperature (Ns/m^2)
u_{max}: Maximum velocity (m/s)

The air velocity at heat exchanger inlet is determined according to cross-flow fan rotational velocity (1200 rpm) and measured from the numerical results as 3 m/s.

For u = 3 m/s, heat transfer coefficient is calculated as;

h = 111.878 W/m^2K

6.1.1 Colburn-j Factor

Dimensionless heat transfer coefficient in terms of Colburn-j factor was calculated from the Eq. 5.15 (Incropera & DeWitt, 2001, p.664).

$$j = \frac{Nu}{Re.Pr^{\frac{1}{3}}} \quad \ldots (5.15)$$

j= 0.014679202

Heat transfer characteristics have been determined for specific velocities and they are presented in Figure 5.3 with the relation of Reynolds numbers.

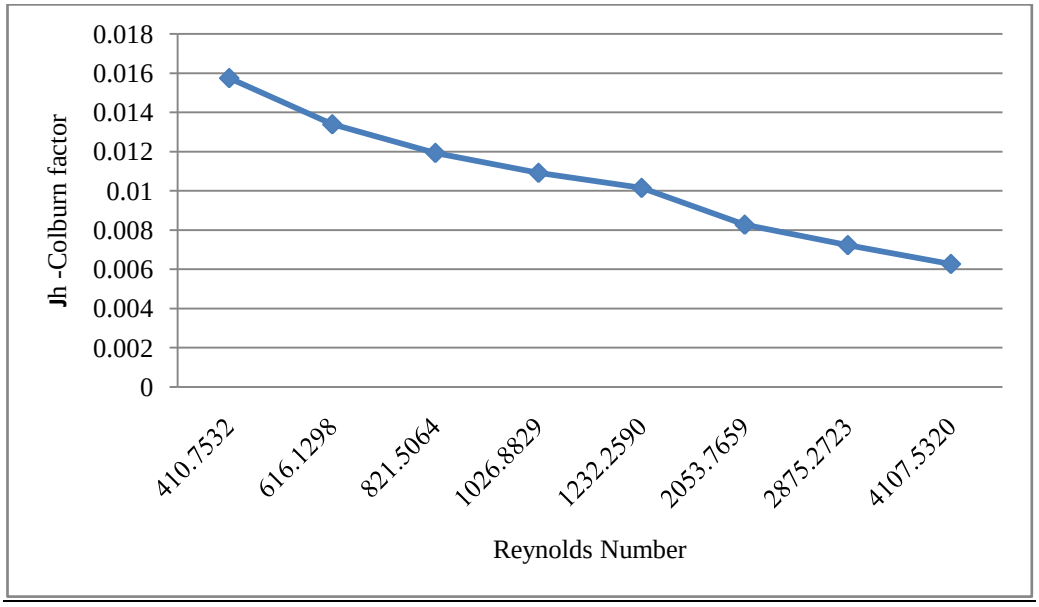


Figure 5.3 Colburn-j factor due to Reynolds number

6.2 Pressure Drop

Air side pressure drop through the heat exchanger fins calculated from Eq. 5.16 (Kakaç & Liu, 1998, p.310),

$$\Delta P = \frac{G^2}{2.\rho_i}.\left[f.\frac{A}{A_0}.\frac{\rho_i}{\rho} + \frac{1}{\sigma^2}\left(\frac{\rho_i}{\rho_0} - 1\right)\right] \quad \dots (5.16)$$

The ratio between minimum flow area to frontal are called as σ and shown in Eq. 5.17 (Kakaç & Liu, 1998, p.310),

$$\sigma = \frac{A_o}{A_{fr}} \quad \dots (5.17)$$

The average air density is calculated from Eq. 5.18 (Kakaç & Liu, 1998, p.311),

$$\frac{1}{\rho} = \frac{1}{2}.\left(\frac{1}{\rho_i} + \frac{1}{\rho_0}\right) \quad \dots (5.18)$$

ρ: average air density (kg/m^3)
ρ_i: air density at inlet temperature (kg/m^3)
ρ_o: air density at film temperature (kg/m^3)

6.2.1 f-Friction Factor

For the calculation of pressure drop in the heat exchanger, f-friction factor was required. Wang and Chi (2000) provided the following correlations for the friction factor in Eq. 5.19 (Shah & Sekulic, 2003, p.521).

$$f = 0.0267.Re^{c7}.\left(\frac{X_T}{X_L}\right)^{c8}.\left(\frac{p_f}{d_0}\right)^{c9} \quad \dots (5.19)$$

$$c_7 = -0.764 + 0.739\left(\frac{X_T}{X_L}\right) + 0.177\left(\frac{p_f}{d_0}\right) - \left(\frac{0.00758}{N_r}\right) \quad \dots (5.20)$$

$$c_8 = -15.689 + \frac{64.021}{lnRe} \quad \dots (5.21)$$

$$c_9 = 1.696 - \frac{15.695}{\ln Re} \quad \ldots (5.22)$$

f = 0.073026

The flow characteristics expression f-friction factor have been calculated for various Reynolds numbers and shown in Figure 5.4.

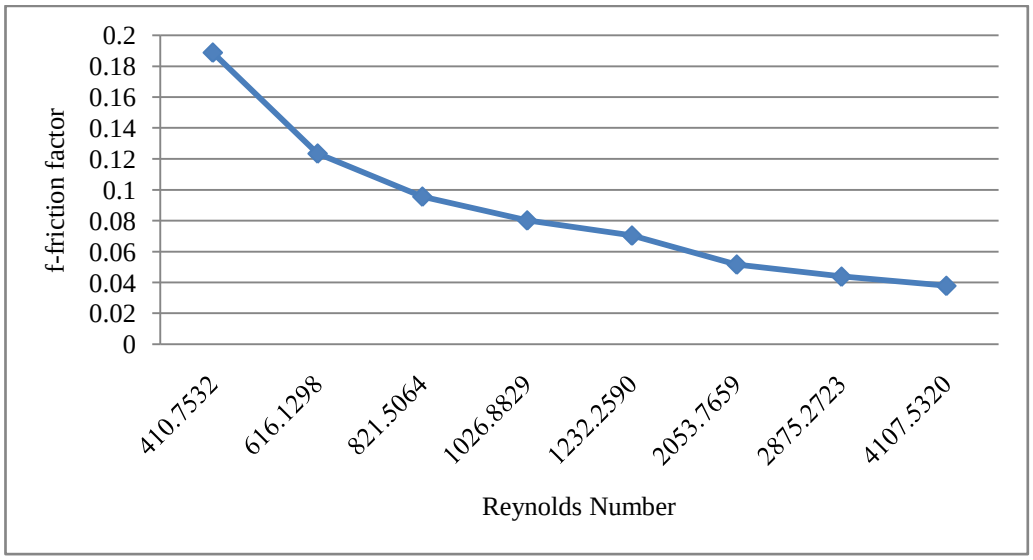


Figure 5.4 Friction factor due to Reynolds number

After calculations of all parameters, pressure drop through the heat exchanger calculated as;

ΔP = 43.355589 Pa

CHAPTER SIX
NUMERICAL STUDY

6.1 Preparing Cad Model for Numerical Study

For numerical study, the Cad model of split type air-conditioner inside unit which was taken from a commercial air conditioner producer company was re-modeled with a commercial engineering Cad program (Figure 6.1, Figure 6.2.a). To ease of solution the proper minimum section of the assembly was determined (Figure 6.2.b) and a symmetrical geometry of air conditioner was modeled according to this section sketch.

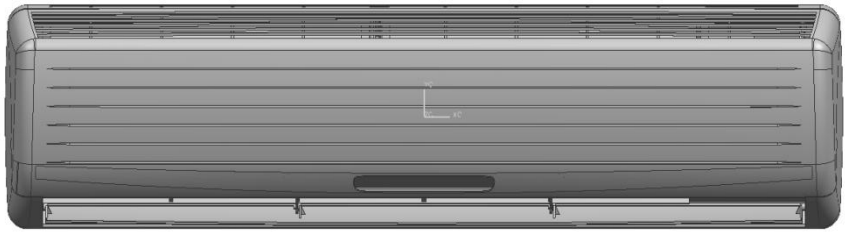
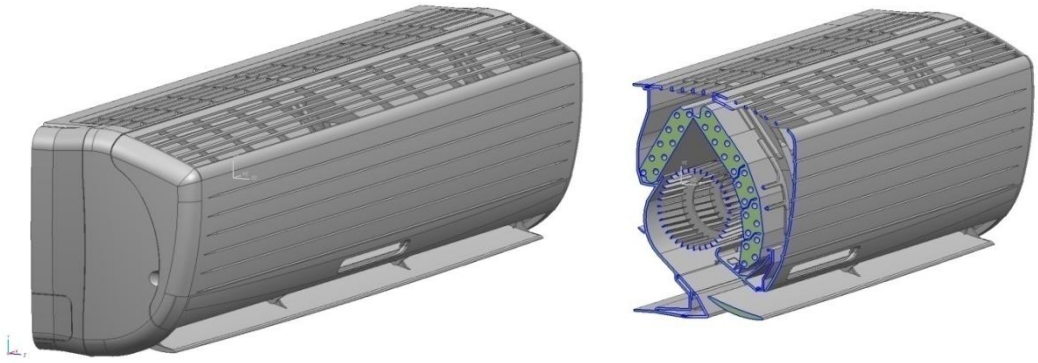


Figure 6.1 The assembly view of the air conditioner inside unit

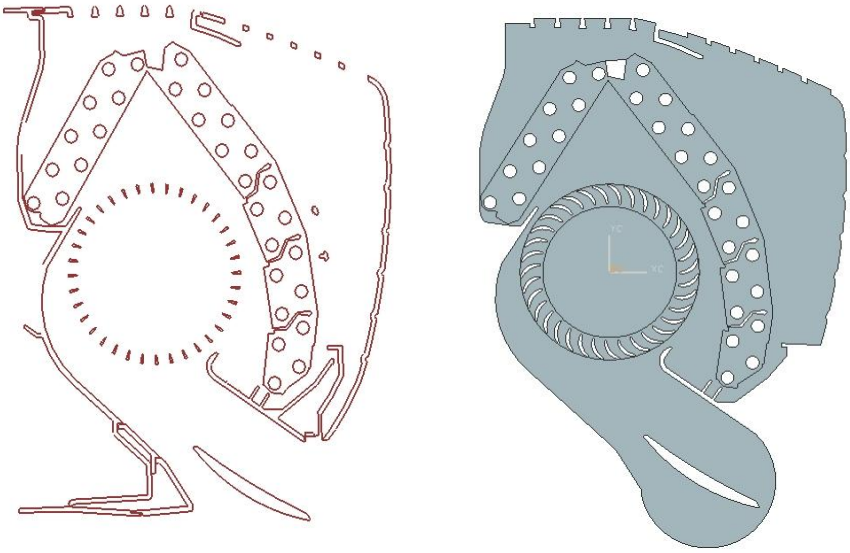


a. b.

Figure 6.2 Air conditioner indoor unit assembly views: (a) Perspective view, (b) Section view

After the determination of most common minimum section sketch, heat exchangers and the air side geometries of air conditioner was modeled (Figure 6.3.a and b). In this geometry, the effects of drain tray, dust filter, outer shell of section and some little assembly parts weren't modeled for simplification. This prediction

was made according to their neglectable effects and also for having a high mesh quality.



a. b.

Figure 6.3 Selected section sketch (a) and prepared air side section model (b), for air conditioner inside unit

The cross flow fan geometry (Figure 6.4) was modeled through the dimensions of real fan model which was taken from the producer company and this prepared fan section added to the air conditioner geometry.

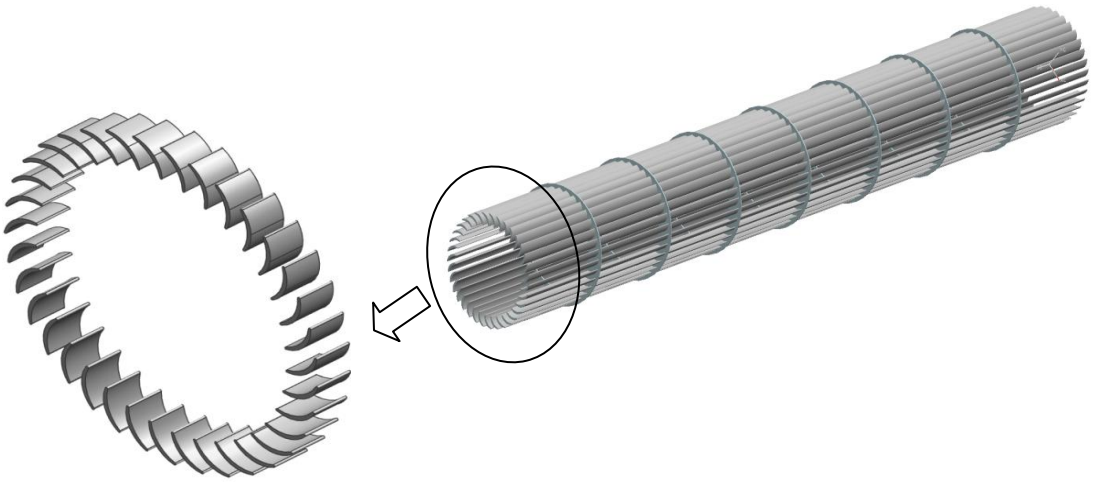


Figure 6.4 Cross flow fan Cad geometry

The thickness of symmetrical section's 3D model was determined through the information of fin thickness and the gap between two fins (Figure 6.5). The prepared

model involves five geometrical regions; two half thickness fin, air inside the section, the air between cross-flow fan's impellers which is also rotating region of the model, the air inside fan and the air outside the section model by the mean of ambient air (Figure 6.6).

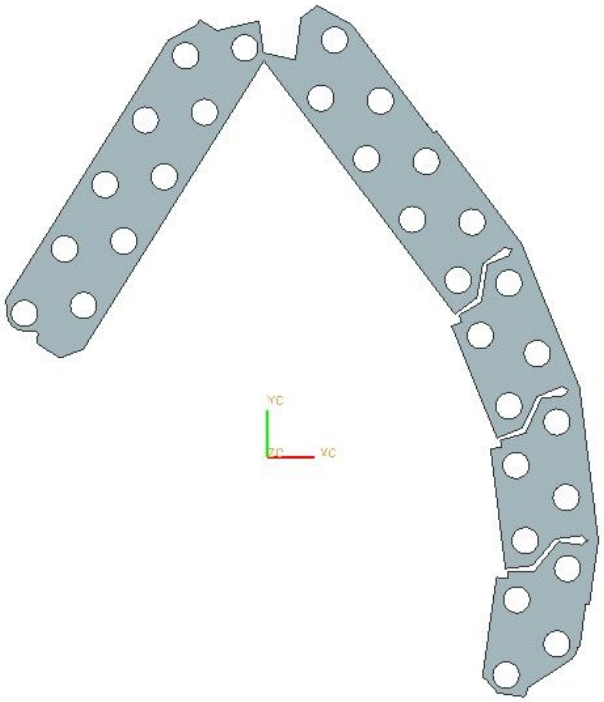


Figure 6.5 Fin geometry

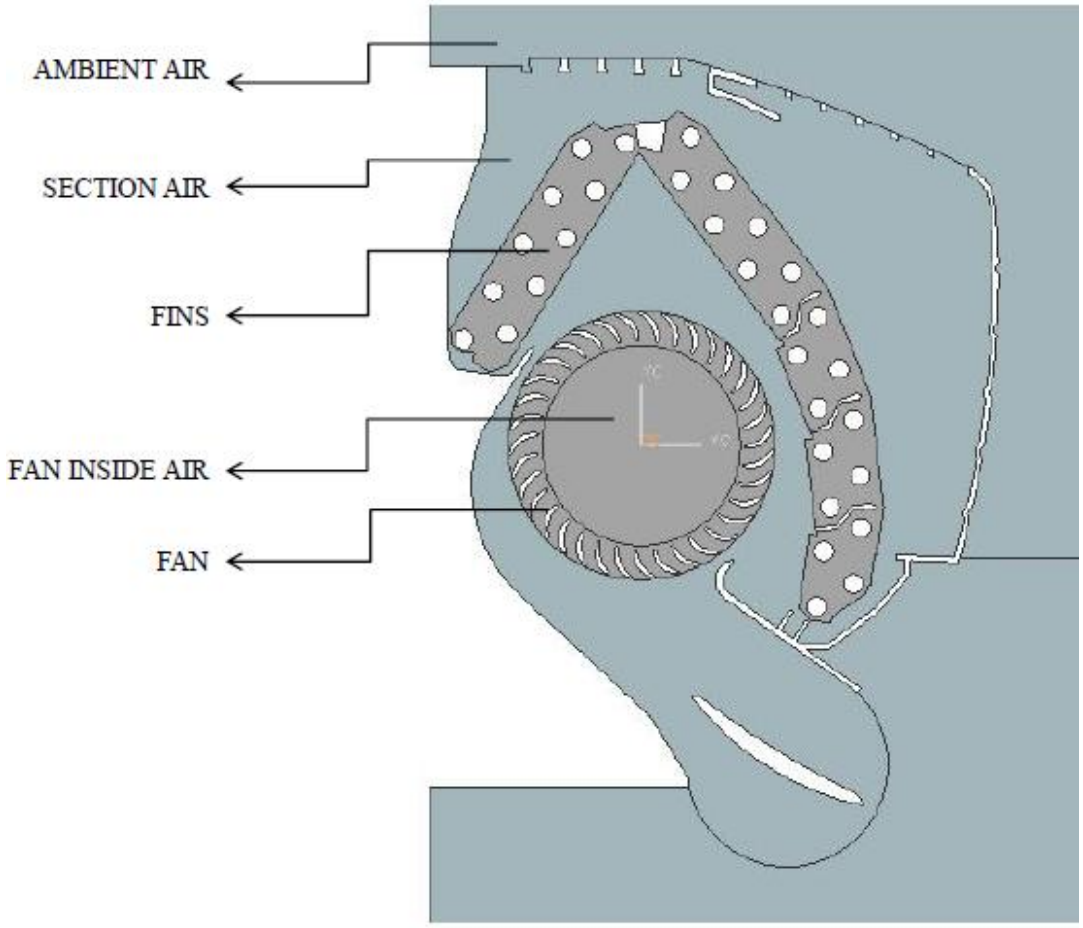
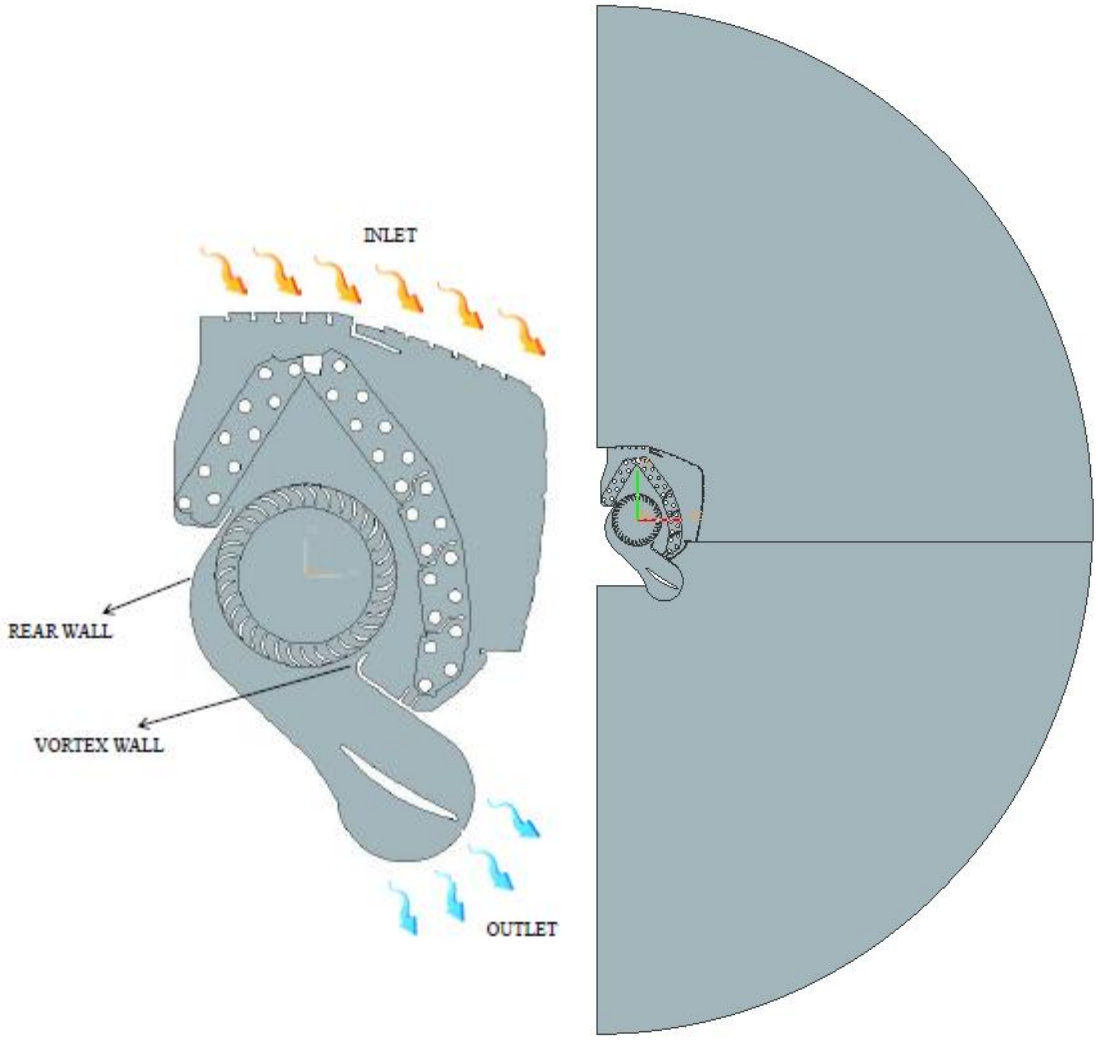


Figure 6.6 Regions of 3D model

The internal construction of a conventional split-type air conditioner which is mainly made of four parts: cross-flow fan, rear wall, vortex wall, and evaporator is shown in Figure 6.7.a, also, the inlet and the outlet regions are illustrated with colored arrows in the figure. Not only the geometry of heat exchanger but also the form of the cross-flow fan and its cavity are the most important parameters for air-conditioner's performance. The flow characteristics and fan performance are as important as heat exchanger effectiveness in heat transfer. While preparing the simplified 3D air conditioner section and ambient airs for the numerical study, these geometrical parameters and their important effects was taken into account.



a. b.

Figure 6.7 Simplified, 3D air-conditioner air side model, (a) Section air, (b) Section air with ambient air

As shown in Figure 6.7.b, the ambient air was chosen as a semi-circular area and its diameter was determined according to twenty times the diameter of the fan through the information of reference study of Shih, Hou & Chiang (2008). Moreover, for the ease of boundary conditions definitions and to increase the speed of numerical convergence, the ambient air geometry divided into two parts.

6.2 Meshing

The most important steps to reach the closest results to real life in a Computational Fluid Dynamics (CFD) analysis are generating a proper numerical grid model and defining boundary conditions correctly. This pre-processing of the numerical study was performed at commercial CFD analysis program. The prepared computer aided design (CAD) model is imported to the package program's mesh module and the names of air conditioner section air model's fluid and solid regions were selected for the ease of definitions.

CFD-Mesh is a mesh generator aimed at producing high quality meshes for use in computational fluid dynamics simulations. Computational fluid dynamics require meshes that can resolve boundary layer phenomena and satisfy more stringent quality criteria than structural analyses. CFD-Mesh produces meshes containing tetrahedral, prisms, and pyramids in standard 3D meshing mode, and additionally can include hexahedra in the Extruded 2D meshing mode (Figure 6.8). Extensive advanced surface and volume mesh generation controls are available in CFD-Mesh, including: Inflation for resolving the mesh in near wall regions, controls for mesh refinement, proximity for detecting edges and surfaces during mesh refinement, parallel mesh generation for volume meshes.

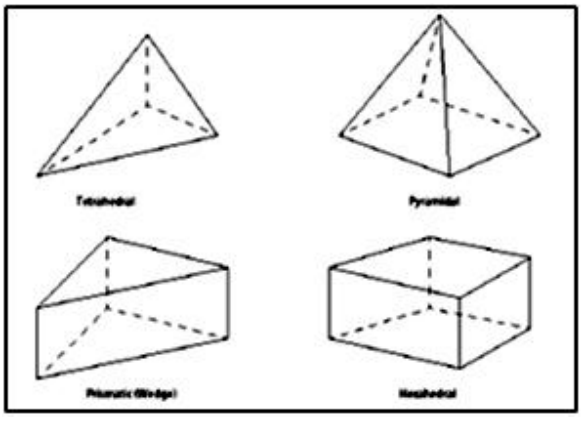


Figure 6.8 CFD Meshing elements types

Different types and sizes of grids were generated for pre-study of the numerical model and extruded tetrahedral mesh was applied to our model. The investigation of

the effect of extruded layers' numbers' difference through the thickness and element numbers change on the surface were also taken into consideration and these studies were summarized at Table 6.1 and 6.2.

Table 6.1 The study of mesh optimization through the thickness

NUMBER OF EXTRUDED LAYERS THROUGH THE THICKNESS	MODEL	NUMBER OF ELEMENTS & NODES	VELOCITY AT OUTLET [m/s]	TEMPERATURE AT OUTLET [C]	TIME [Hours]	CONVERGENCE CRITERIA
12		E: 1495988 N:1018735	10.1962	19.400	Not converged	Iteration:>4000 RMS :1.E^{-5}
14		E:1700042 N:1130745	10.1286	19.603	29	Iteration:511 RMS :1.E^{-5}
16		E:1903880 N:1242663	10.2747	19.701	25	Iteration:408 RMS :1.E^{-5}
18		E:2108678 N:1355085	10.0542	19.718	25	Iteration:392 RMS :1.E^{-5}
20		E:2312996 N:1467255	9.9702	19.751	27	Iteration:381 RMS :1.E^{-5}

The extruded layers were positioned as increasing from fin to air through the thickness. The number of finite volume elements were redound and the size of them were made smaller for air around the fan impellers, inlet, outlet regions and especially, the air near the fin to find out the heat transfer more effectively.

Table 6.2 The study of mesh optimization through surface elements sizes and types

SURFACE MESH OPTIMIZATION	MODEL	NUMBER OF ELEMENTS & NODES	VELOCITY AT OUTLET [m/s]	TEMPERATURE AT OUTLET [C]	TIME [Hours]	CONVERGENCE CRITERIA
TETREHEDRAL MESH-1		E:1756060 N:1149802	9.9848	19.69	48	Iteration:746 RMS :1.E^{-5}
TETREHEDRAL MESH-2		E:1152384 N:783304	9.8051	19.79	17	Iteration:432 RMS :1.E^{-5}
HEXAHEDRAL MESH-1		E:281052 N:377431	9.2565	19.87	36	Iteration:>3500 RMS :1.E^{-5}

These meshing type and size determination studies were made for the geometry without ambient air to ease of analysis. So, these studies have been done in terms of giving ideas. According to the mesh optimization studies, specified mesh spacings for the regions were shown in the Table 6.3.

Table 6.3 Mesh spacings

	CONSTANT LENGTH [m]	**RADIUS OF INFLUENCE**
BODY SPACING	0.018	-
FACE SPACING / AMBIENT AIR	0.018	0.001
FACE SPACING / SECTION AIR	0.006	0.001
FACE SPACING / AIR INSIDE FAN	0.0024	0.001
FACE SPACING / FIN	0.0012	0.001
FACE SPACING / FAN AIR	0.0012	0.001
EDGE SPACING / FAN BLADES	0.0006	0.001
EDGE SPACING / PIPE	0.0006	0.001
TOTAL NUMBER OF EXTRUDED LAYERS THROUGH THE THICKNESS	16	
TOTAL ELEMENTS NUMBER	2482876	
TOTAL NODES NUMBER	1614599	

The created numerical model composed of 2482876 tetrahedral elements and 1614599 nodes (Figure 6.8 and Figure 6.9). The total number of extruded layers through the thickness is determined as 16.



Figure 6.8 Numerical model

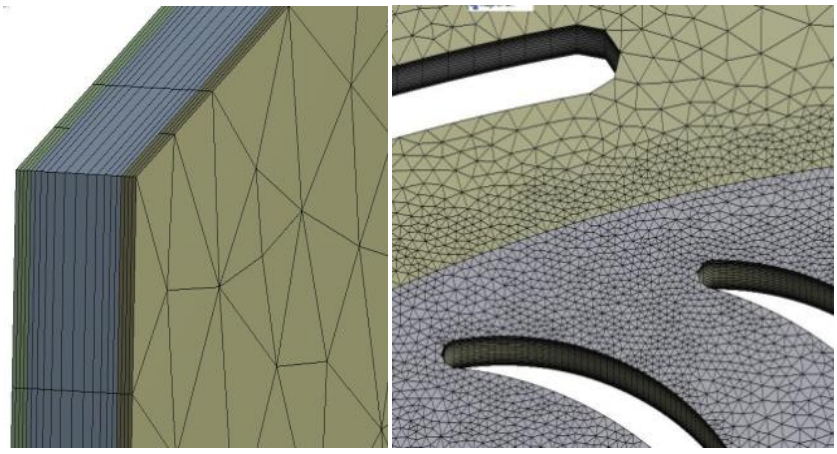
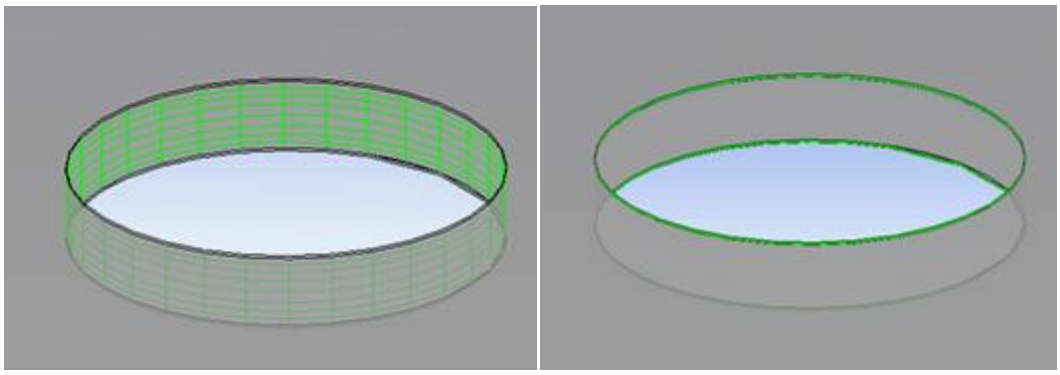


Figure 6.9 Extruded layers through the thickness

6.3 Boundary Conditions

The prepared numerical model was transferred to the CFD program for the pre-processing. Solid (fin) and fluid (air) domains were introduced to the program. To alleviate the solver process only fins were modeled as a solid and their material selected as aluminum. The other solid domains like the shell of the section, fan's impellers weren't modeled but these regions' effects were added as adiabatic walls. Boundary conditions were applied same as the testing room conditions for the absolute comparison. Analyses were made for summer conditions. The inlet and outlet boundary conditions were given to the inlet and outlet as 27 C outside temperature and 0 Pa relative pressures. In the definition of boundary conditions, the direction of the flow wasn't specified to the program. So that, the control of the description of the cross-flow fan rotation was made.

The air's thermo physical properties such as density (kg/m^3), specific heat (J/kgK), dynamic viscosity (Ns/m^2) were given according to its film temperature 17 C. The effect of cooling fluid R22 (Freon) from evaporator's pipes was applied to the fins' and air's pipe side surfaces as a 7 C constant temperature (Figure 6.10 a and b).



a. b.

Figure 6.10 Pipe surface definitions, (a) air side, (b) fin side

The rotating region's boundary conditions were given as 1200 rpm and this region's interfaces were defined. As mentioned before, while the repeating model had been determined, the model's symmetry surfaces' boundary conditions were

defined as symmetry. The proper interface models between fluid and solid domains or rotating and stationary domains were also specified in the program.

6.4 Solver

After the definitions of boundary conditions (material types, domain motion, temperature, pressure, heat transfer mechanisms, turbulence models etc.) and initial conditions, solver control definitions were made.

To simulate the characteristics of turbulent flow, the standard k–ε turbulence model was used because of its wide capability. This model has been implemented in most general purpose CFD codes and is considered the industry standard model. It has proven to be stable and numerically robust and has a well established regime of predictive capability. k–ε turbulence model, provide good predictions for many flows of engineering interest such as flows with boundary layer separation, flows with sudden changes in the mean strain rate, flows in rotating fluids and flows over curved surfaces (ANSYS CFD - Solver modeling guide).

Three dimensional, steady-state analyses' iterations have continued until residuals reach $10*E^{-4}$ and domain imbalances come below % 0.0001. This took 6 days, 18 hours and 44 minutes with 5344 iterations. Heat transfer, momentum and mass and turbulence residuals were shown in Figure 6.11, 6.12 and 6.13.

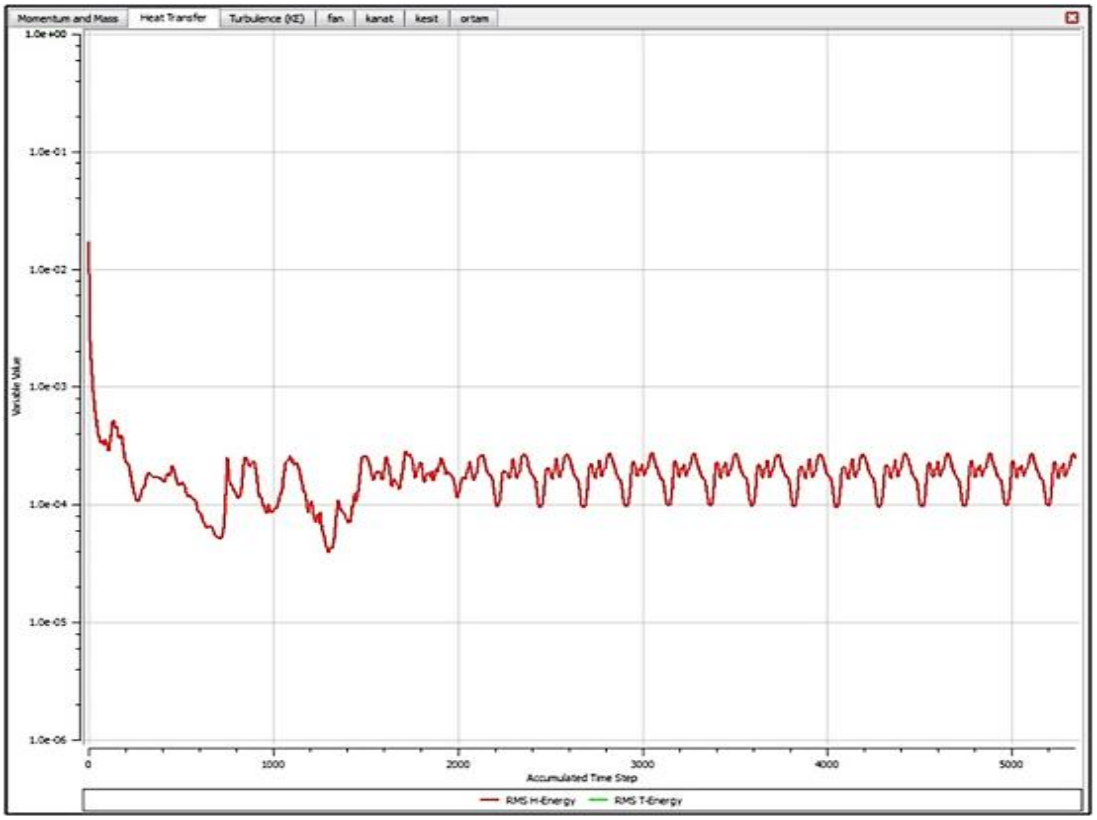


Figure 6.11 Heat transfer residuals

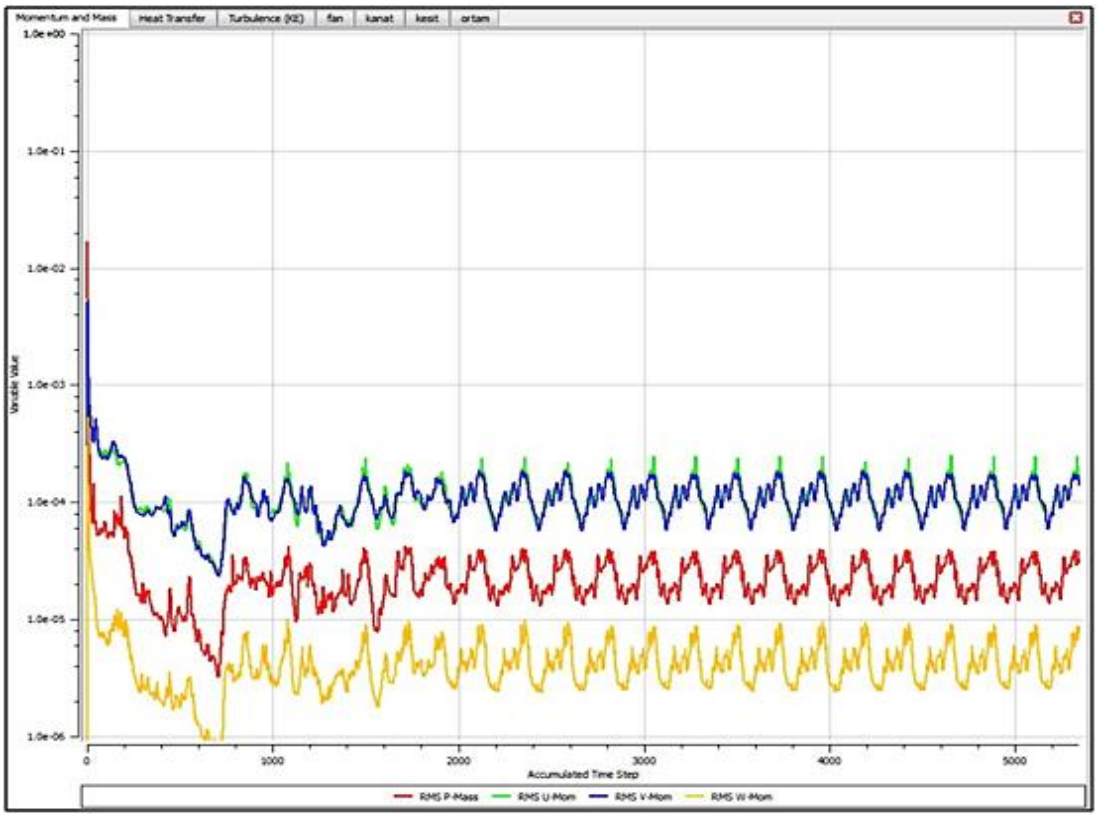


Figure 6.12 Momentum and mass residuals

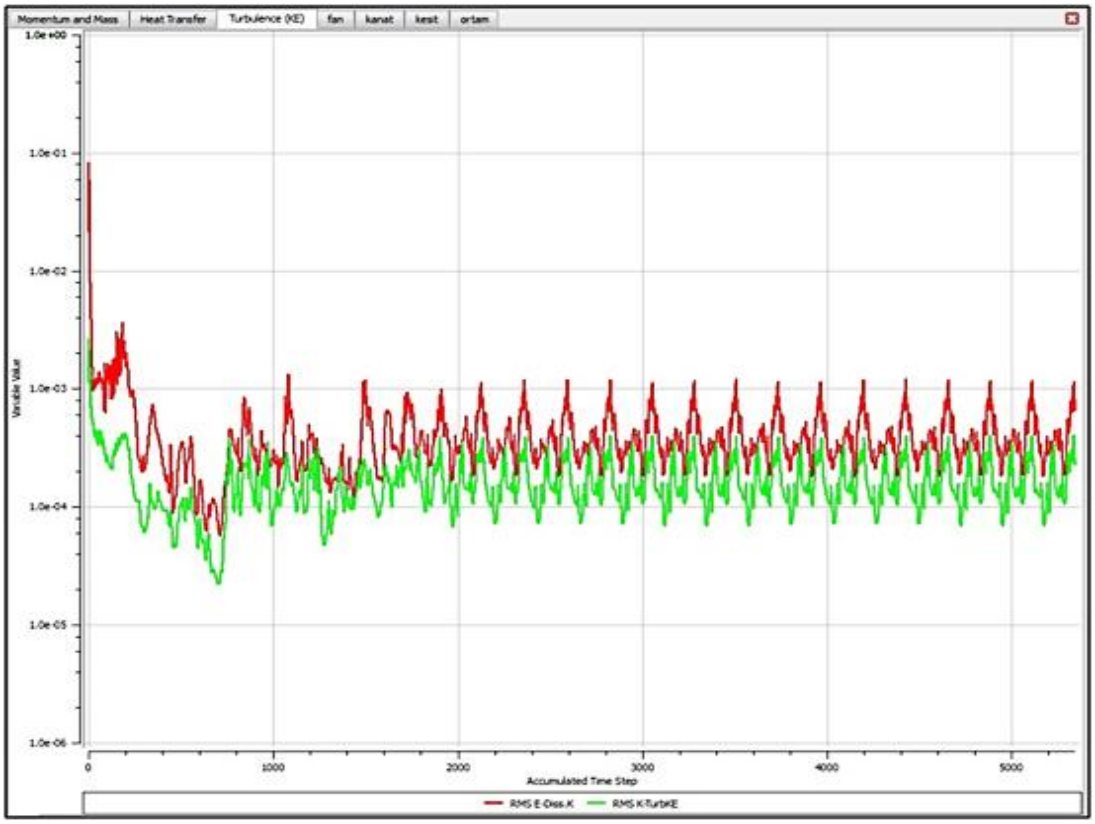


Figure 6.13 Turbulence residuals

Heat transfer, pressure drop and flow analyzes were made through the governing equations from the computational fluid dynamics package program solver tool.

After solution was converged; temperature and pressure contours, velocity vectors were displayed for visual consideration of the results. To calculate pressure drop, heat transfer rate etc. solutions reports and surface plots differences were also used.

CHAPTER SEVEN
RESULTS AND DISCUSSIONS

7.1 Results and Discussions

The air side heat transfer performance of an evaporator inside the split type air conditioner is investigated theoretically and numerically in this study. According to detailed literature surveys, it is confirmed that no similar study was made before which involves heat transfer and flow analysis together. The air side heat transfer performance of the evaporator is analyzed with almost real model of air conditioning inside unit with fan and ambient air.

The aim of this study is to develop a numerical method for a split type air conditioner evaporator heat transfer calculations with a commercial computational package program and provide ease for performance and design process improvement.

5275 Watt and 700 m^3/h air flow capacity split type air conditioner was used in our study. The assembly model (CAD geometry) of the air conditioner unit, boundary and initial conditions inputs were taken from Vestel Air-Conditioner Product Company. To compare the accuracy of the numerical results with the existing real air conditioner performance measurements, the test room data were also taken from the company (Figure 7.1). A 17584 Watt capacity Psychrometric type testing room for determining capacity with air-enthalpy test method and a 10550 Watt capacity calorimetric type testing room for determining the capacity with thermal balance test method are available within the company (Figure 7.2 and 7.3). All these tests are performed according to TS EN 14511:2007 and ISO 5151 Standards.

Psychrometric Test Room — **COOLING CAPACITY REPORT** — Page 1 of 2

UUT Model Number:	18 K R22 HITACHI (SHV33MC4-U)	Date:	24 Oca 2006 Sal
UUT Serial Number:	Kond: 18K 7mm (1.5 Row - 4 Cycle + Subcool)	Time:	1:40 AM
Engineering Number:	Evap : 18K (5 Cycle)	Test ID:	060123_225653
Operator Initials:	Od Fan : 18K (980 RPM) - Id Set : 18K	Test Name:	Standard_Cooloing_230
Test Facility:	Od : Plastik Dış Ünite	Run No. :	AVERAGE

	INDOOR ROOM MEASURED DATA		OUTDOOR ROOM MEASURED DATA	
	ENGLISH	SI	ENGLISH	SI
Entering Dry Bulb Temperature:	80,56 Deg. F	26,98 Deg. C	94,93 Deg. F	34,96 Deg. C
Entering Wet Bulb Temperature:	66,22 Deg. F	19,01 Deg. C	75,10 Deg. F	23,94 Deg. C
Leaving Dry Bulb Temperature:	59,25 Deg. F	15,14 Deg. C	111,60 Deg. F	44,22 Deg. C
Leaving Wet Bulb Temperature:	55,95 Deg. F	13,31 Deg. C	79,25 Deg. F	26,25 Deg. C
Delta Dry Bulb:	21,31 Deg. F	11,84 Deg. C	16,67 Deg. F	9,26 Deg. C
Delta Wet Bulb:	10,27 Deg. F	5,70 Deg. C	4,15 Deg. F	2,31 Deg. C
UUT Discharge Air Static Pressure:	-0,01 " WC	-2,0 Pa	0,00 " WC	-0,2 Pa
AirFlow Tunnel Nozzles Diff. Pressure:	1,59 " WC	395,8 Pa	1,75 " WC	435,6 Pa
Barometric Pressure:	29,95 " HgA	101,43 kPa	30,05 " HgA	101,77 kPa

UUT Power:	1759,9 Watts	UUT Evap. Fan RPM:	1,3 RPM
UUT Voltage:	230,3 Volts	UUT Cond. Fan RPM:	0,8 RPM
UUT Current:	7,94 Amps		
Line Frequency:	0,2 Hz		

PSYCHROMETRIC CALCULATIONS

	INDOOR COIL CAPACITY		OUTDOOR COIL CAPACITY	
UUT Airflow (Actual):	428,9 cfm	728,7 CMH	1208,6 cfm	2053,7 CMH
UUT Airflow (Standard):	435,2 cfm	739,4 CMH	1118,0 cfm	1899,8 CMH
Sampling Duct Loss:	374,0 BTU/H	109,6 Watts	270,1 BTU/H	79,1 Watts
Rated Capacity:	18000,0 BTU/H	5273,1 Watts	1,0 BTU/H	0,3 Watts
Tested Capacity:	14523,6 BTU/H	4254,7 Watts	20995,4 BTU/H	6150,6 Watts
% Rated Capacity:	80,69 %	80,69 %	2099536,88 %	2099536,88 %
Tested Sensible Capacity:	10476,5 BTU/H	3069,1 Watts	20995,4 BTU/H	6150,6 Watts
Tested Latent Capacity:	4047,1 BTU/H	1185,6 Watts	0,0 BTU/H	0,0 Watts
Sensible to Total Ratio:	72,14 %	72,14 %	100,00 %	100,00 %
Rated EER:	1,000 BTU/W	0,293 W/W	1,000 BTU/W	0,293 W/W
Tested EER:	8,253 BTU/W	2,418 W/W	11,930 BTU/W	3,495 W/W
% Rated EER:	825,27 %	825,27 %	1193,02 %	1193,02 %
Tested Sensible EER:	6,0 BTU/W	1,7 W/W	11,9 BTU/W	3,5 W/W

ID to OD BALANCE %: -3,20 %

Statistically Valid: Yes _____ No _____

Comments: R22 : 1200 gr
Cap : 2*1000 mm

Figure 7.1 Vestel air-conditioner product company psychrometric test room cooling test results



Figure 7.2 Vestel air-conditioner product company test room



Figure 7.3 Air-conditioner indoor unit with testing equipments and measurement thermocouples

7.1.1 Flow Characteristics (Streamlines) Results

According to the detailed literature surveys it is infirmed that to simulate an air-conditioner working performance properly, flow characteristic should be the same as possible as the real conditions. It means that the simulation of fan work and its appropriate description in the CFD pre-processing tool is really important. Therefore, as can be seen from the literature researches, cross-flow fan flow characteristics inside their fan cavity were investigated. But it must be indicated that none of these studies involves air conditioner inside unit with whole elements' heat transfer and fluid flow analysis together.

As shown in Figure 7.4, the streamline contour was taken from the numerical results. This streamlines show us the flow direction, flow characteristics and vortexes inside and outside the air-conditioner unit.

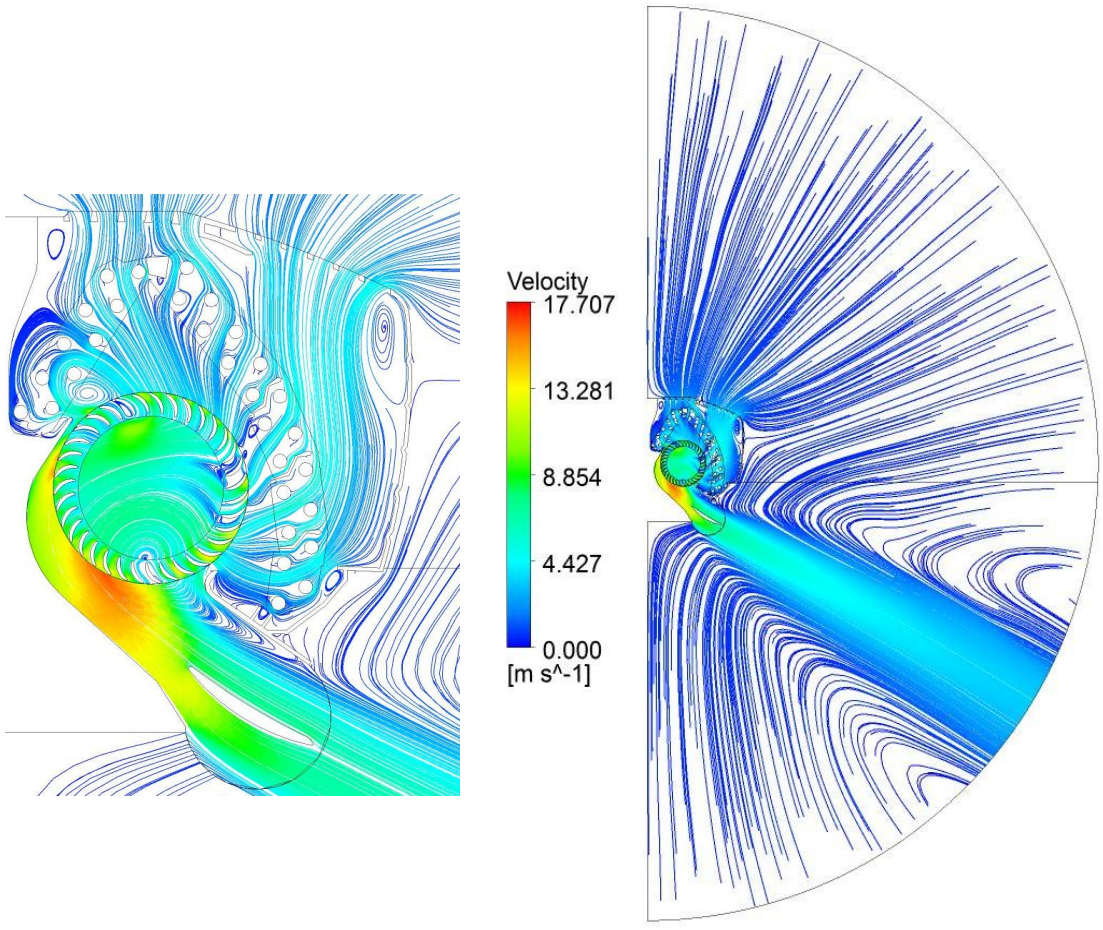


Figure 7.4 Streamlines

Flow enters the blade row in the radially inward direction on the upstream side, passing through the interior of the impeller, and then passes radially outward through the blading a second time. The flow is characterized by the formation of an eccentric vortex. Figure 7.5 shows flow field inside the fan according to the CFD analyzes. Fan rotation is counter-clockwise.

7.1.2 Pressure Drop Results

With the effect of the casing elements (rear wall and vortex wall) two important eccentric vortexes were formed inside the fan impellers and these vortexes generate a low pressure region which provide the air suction. According to the study of Dang & Bushnell (2009), these vortexes show us that fan work is proper.

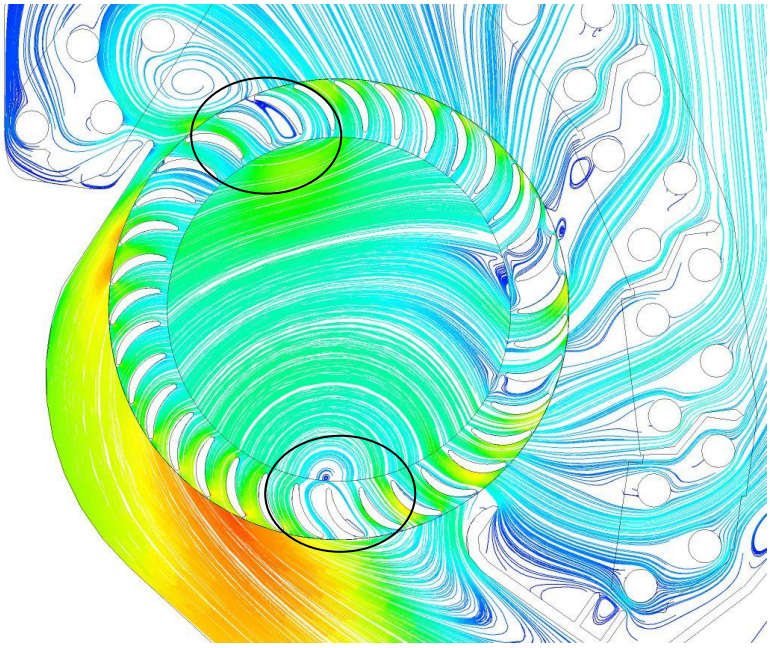


Figure 7.5 Streamline visualization of eccentric vortex inside the fan

Pressure distribution inside the air conditioner is shown in Figure 7.6. As showed below, maximum negative pressure region occurred in the centre of the eccentric vortex or in other words between the fan blades.

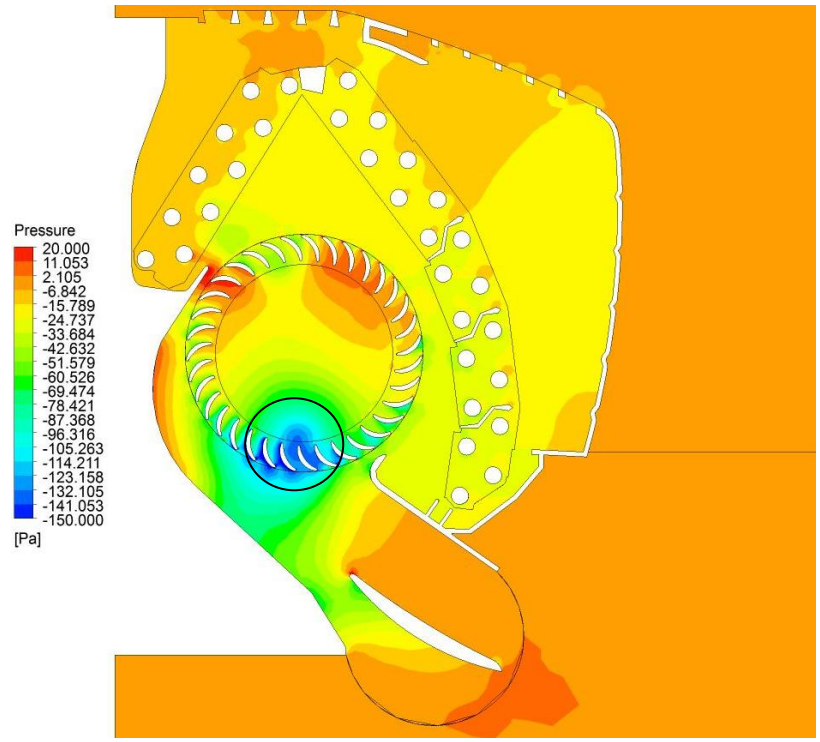


Figure 7.6 Pressure contour

Pressure distribution of the air passing through the heat exchangers fins calculated manually from post process results. Also, theoretical and numerical pressure loss calculations' are compared to find out the accuracy of the results. It is shown in Table 7.1 and Figure 7.7.

Table 7.1 Theoretical and numerical results of pressure losses through the fins

	PRESSURE DROP (Pa)		
VELOCITY (m/s)	**NUMERICAL ANALYSIS**	**THEORETICAL STUDY**	**RELATIVE DIFFERENCE**
1	8.1033	13.3689	5.2656
1,5	14.3757	19.4050	5.0293
2	22.0165	26.4768	4.4603
2,5	30.9252	34.4764	3.5512
3	40.9901	43.3555	2.3654
5	90.6956	87.1996	3.4960
7	151.3141	143.7818	7.5323
10	257.4454	251.6585	5.7869

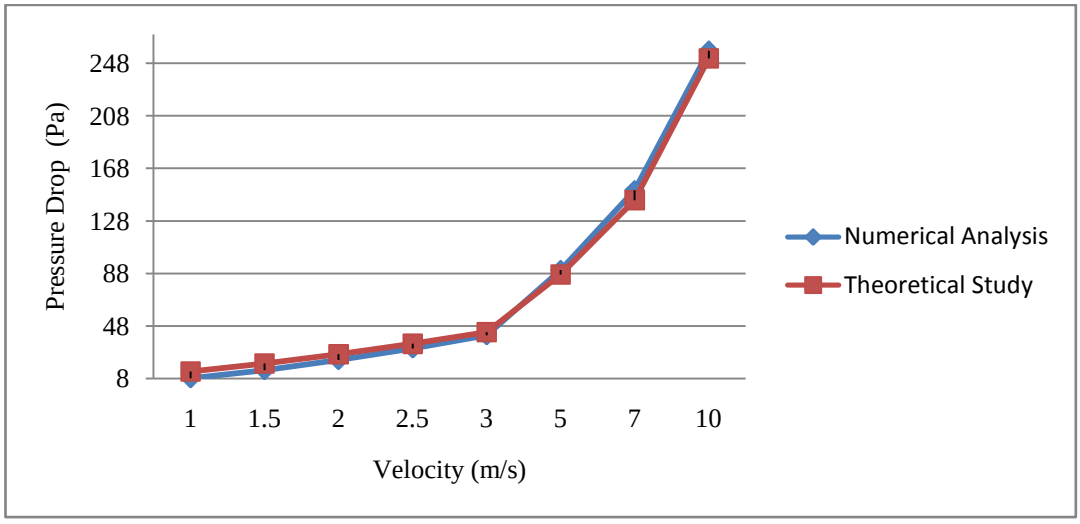


Figure 7.7 Pressure drop results comparison between CFD and theoretical studies

7.1.3 Velocity Distribution Results

Flow directions and flow characteristics of the air inside and outside zone of the air conditioner unit were shown in Figure 7.8 with velocity vectors. These velocity vector distributions are important to understand and calculate the heat transfer performance of the heat exchanger. The velocity or mass flow rate of the air flow through the heat exchanger's fins is directly effective for the convective heat transfer performance of the evaporator. Velocity vector characteristics such as their rates and directions give us a wide range of performance investigation at inside section air and at ambient air. Velocity vector magnitudes and flow paths from inlet to outlet zones are providing us to understand the conditioned air flow effects easily. These velocity vectors plots also give ideas to us for further refinement studies such as using heat exchanger surface area more efficiently.

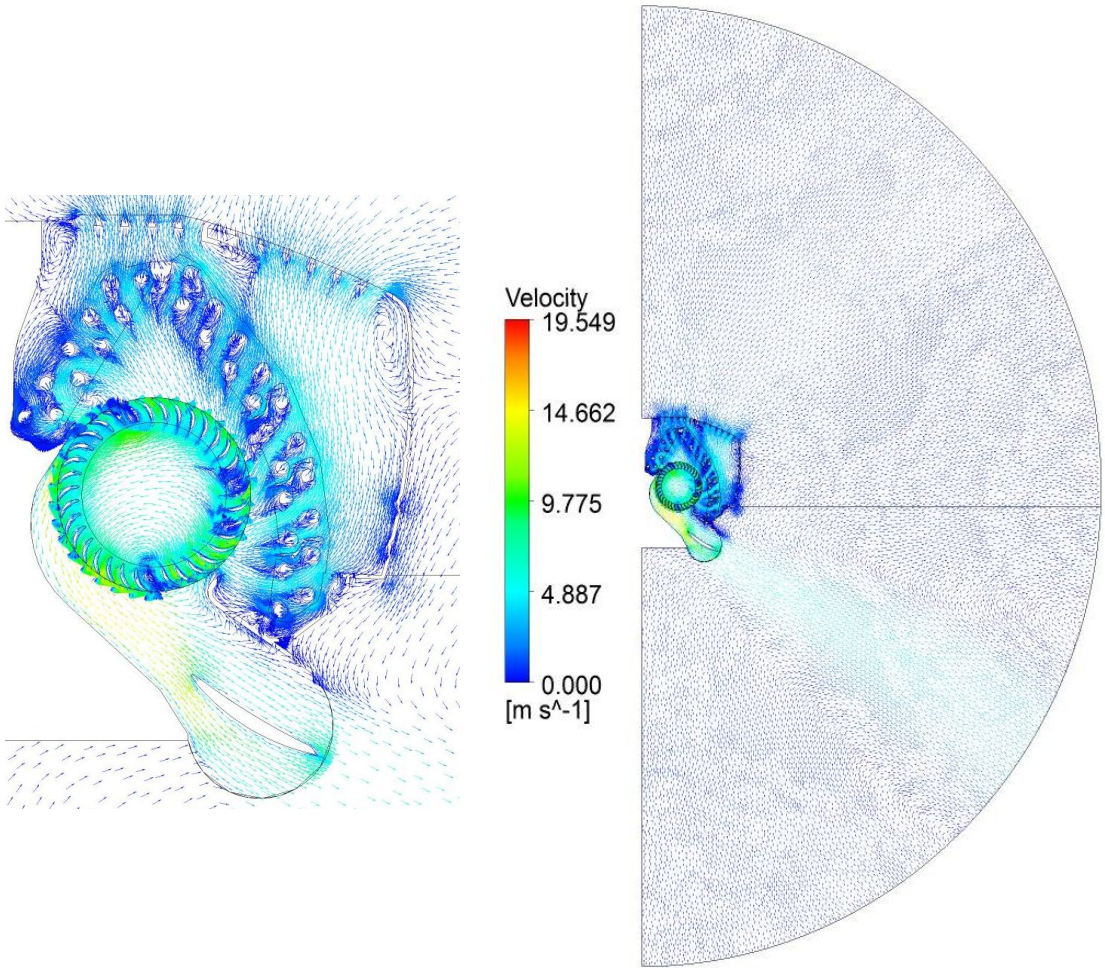


Figure 7.8 Velocity vectors

In Figure 7.9 and 7.10 the inlet and the outlet zones of the air conditioner unit were shown closely. Investigation of the air flow characteristic respectively at inlet, between the fins, between the fan and its casing, at outlet and also at ambient is possible with the vector plots. As shown in Figure 7.9, with the effect of fan suction, velocity vectors came into the air conditioner section from the inlet holes. Vectors keep going between the heat exchangers fins, pipes and air flow behave proper to the fluid dynamics principles. Flow separations through the pipe surfaces, vortexes which were occurred behind the pipes and reverse flow at the corners of the air conditioner section can be seen from these vector plots.

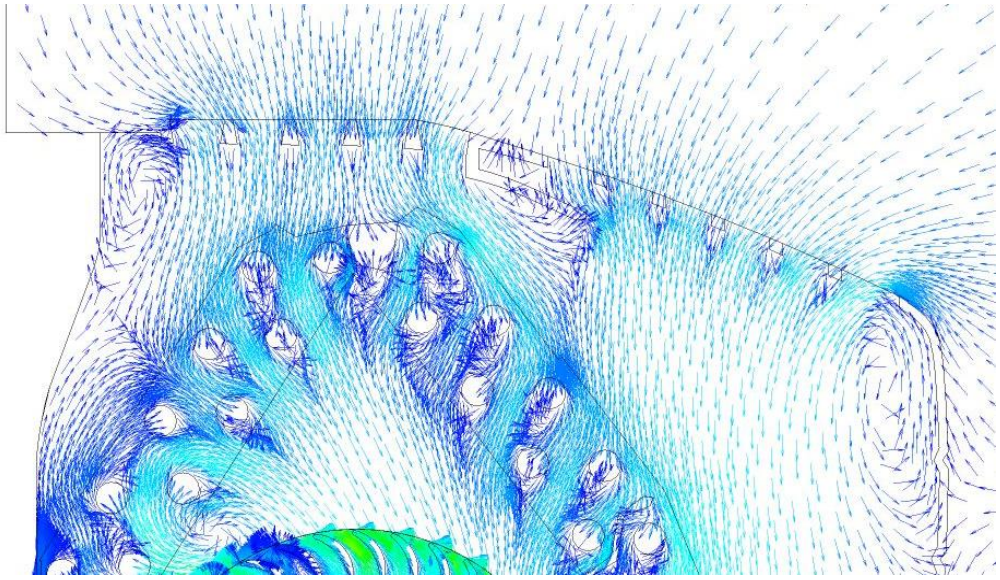


Figure 7.9 Inlet zone of the air conditioner unit

As described in streamline result part, air flow passes through the fan and its impellers proper to the cross flow fan characteristics and it is blown out from the outlet zone to the ambient air. In this region, with the effect of the fan casing, form of the outlet and router wing, conditioned air gain its effective flow form and magnitude. The blowing air also creates vortexes near the exit because of the jet fluid flow from the outlet of the air conditioner section to ambient air.

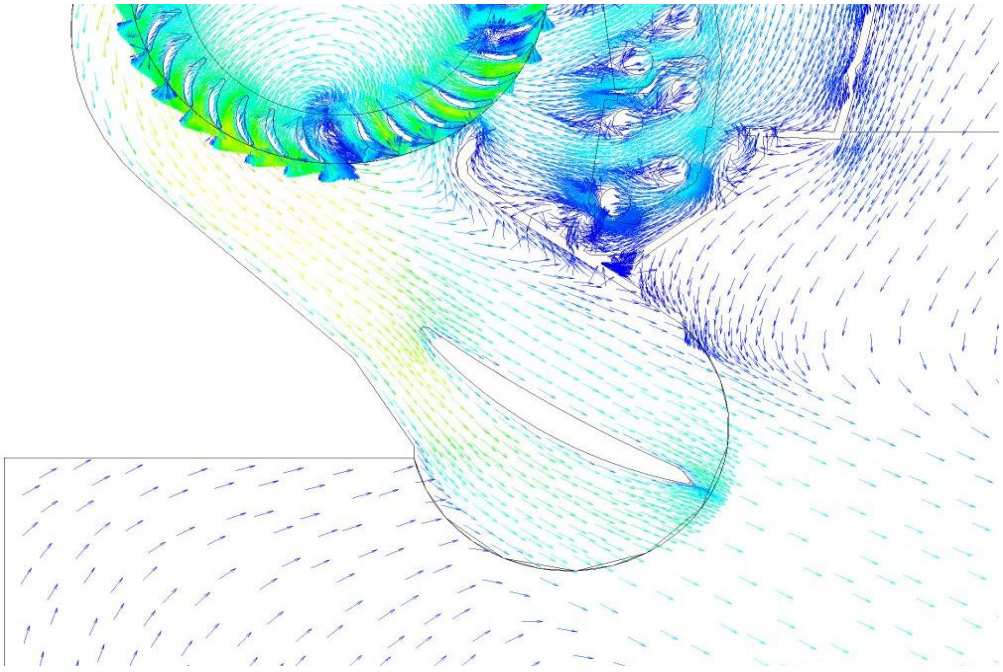


Figure 7.10 Outlet zone of the air conditioner unit

The magnitude of the air velocity at outlet zone taken from the air conditioner producer company's test results which were made in their test room for comparison. The value of the measured velocity was given as 4.62 m/s which was detected through the average of the thermo-anemometer probe's data. For comparison, CFD results taken from a path which was shown in Figure 7.11 for having average values of velocities or temperatures at outlet zone. As can be seen from the velocity range scale and also Table 7.2, average velocity magnitude at outlet obtained as 5.646 m/s from CFD results.

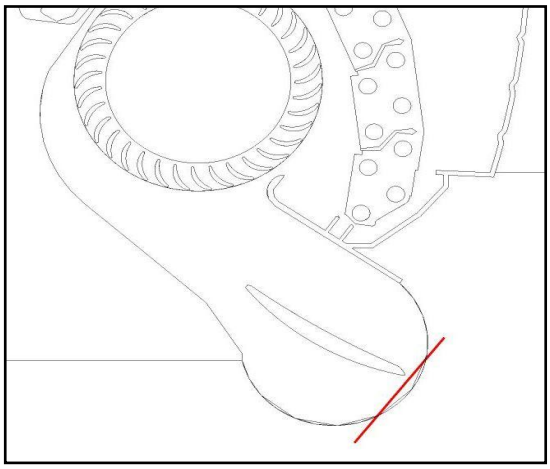


Figure 7.11 The prepared path at the outlet region of the air-conditioner model for taking average CFD data

Table 7.2 Velocity values through a path at CFD

CFD data path through x direction (m)	Velocity (m/s)
0.080041	3.389
0.084269	4.843
0.088497	6.321
0.092725	7.544
0.096953	7.050
0.101182	5.993
0.105410	6.488
0.109638	5.921
0.113866	5.124
0.118094	3.788
AVERAGE	**5,646**

From CFD results, the average volumetric flow rate for outlet section area was obtained as 1.76 m^3/ h. To compare this result with the test room data report (Figure 7.1), the total volumetric flow rate calculated and found as 1106 m^3/h. As shown in test room report the standart airflow rate was given as 739.4 m^3/ h and this difference sourced velocity difference.

The air conditioner model we are working on which was taken from the air conditioner product company is open to the developments. As can be seen from the vector plots inside the air conditioner unit, it is obtained that reverse flows and cooled air passing through the heat exchanger again caused to the energy losses. To improve efficiency, engineering investigations about the air conditioner structure, heat exchanger form and the positions of the air conditioner unit elements must be made. In this thesis, a numerical study was made and computational fluid dynamics and heat transfer analyses were developed for the ease of engineering studies.

7.1.4 Temperature Distribution Results

Heat transfer results were shown in Figure 7.12 with temperature contours. This contours generated on the mid-plane which involves only air temperature distributions. The 27 C ambient air comes through the heat exchanger with same temperature and starts to become cooler while it is passing between heat exchanger's fins and tubes. The cooled air with the effect of heat transfer from the 7 C pipe surfaces and aluminum fins' surfaces was blown out from the outlet zone by the cross-flow fan.

Air was conditioned with the effect of convective heat transfer from the heat exchanger aluminum fins and temperature distributions through the fins and pipe circumferences showed that proper heat transfer and fluid flow descriptions were made in the CFD program.

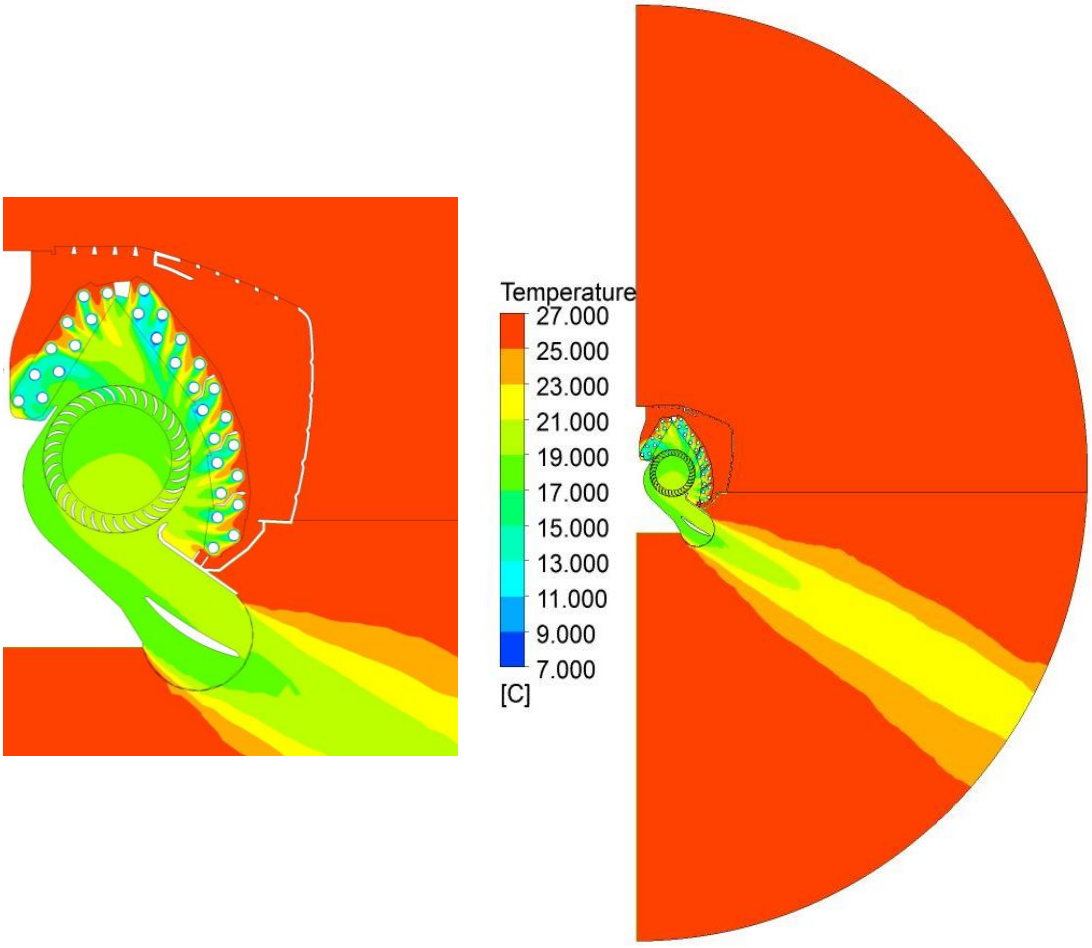


Figure 7.12 Air side temperature contour

The accuracy of the temperature distributions results proved by the comparison of the test room measurements and CFD results. All the measurements taken from the same outlet zone for absolute comparison. Despite this, test room data was taken by point measurements and CFD results consist an average temperature through a path at outlet. So, blowing air temperature difference between CFD and real is within the acceptable limits to have an idea about the temperature. According to the CFD results, the average temperature value of the air at the outlet is obtained 19.155 C (Table 7.3) and as given in the test room measurements report (Figure 7.1), conditioned air temperature is 15.14 C.

To control results complience between test room report data and CFD data, tested sensible capasity and calculated capacity comparasion was made. From CFD results, the average mass flow rate for outlet section area was obtained as $5.87*10^{-4}$ kg/s.

With temperature difference between inlet and outlet and specific heat capacity, the total heat transfer capacity was calculated and found as 3061.15 Watt. As shown in test room report the tested sensible capasity was given as 3069.1 Watt (Figure 7.1) and this difference show that CFD study is nearly same with test room.

Table 7.3 Temperature values through a path at CFD

CFD data path through x direction (m)	Temperature (C)
0.080041	19.4631
0.084269	19.9071
0.088497	19.4746
0.092725	18.3575
0.096953	18.4246
0.101182	18.5195
0.105410	19.0908
0.109638	19.1168
0.113866	19.3649
0.118094	19.8361
AVERAGE	**19,155**

Temperature distributions through the aluminum fin, pipe surfaces and air between fins were shown in Figure 7.13 and 7.14.

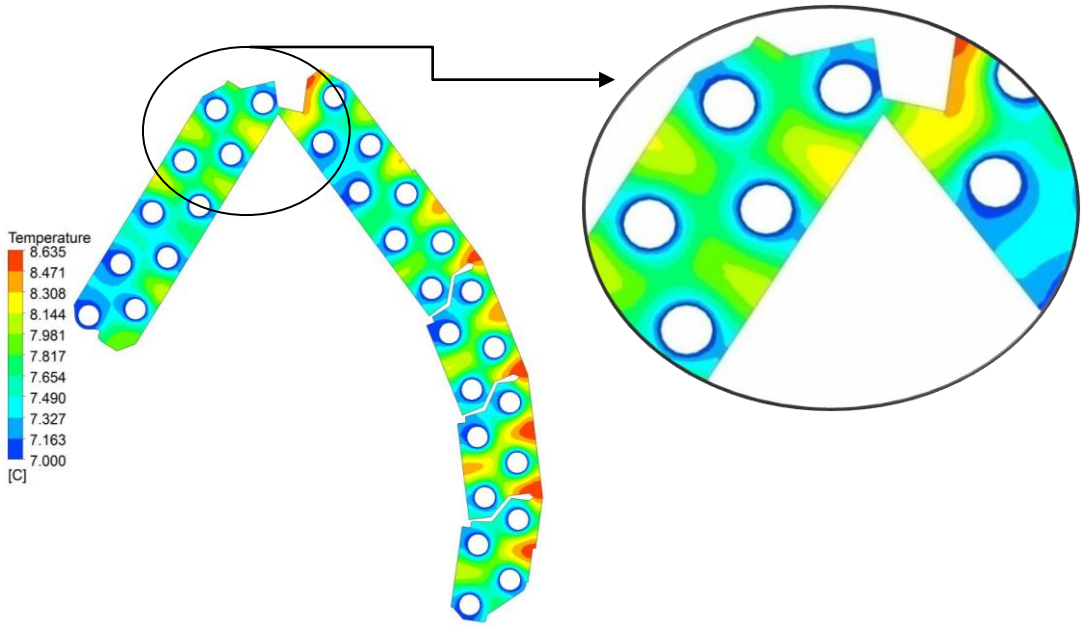


Figure 7.13 Temperature distributions through the aluminum fin

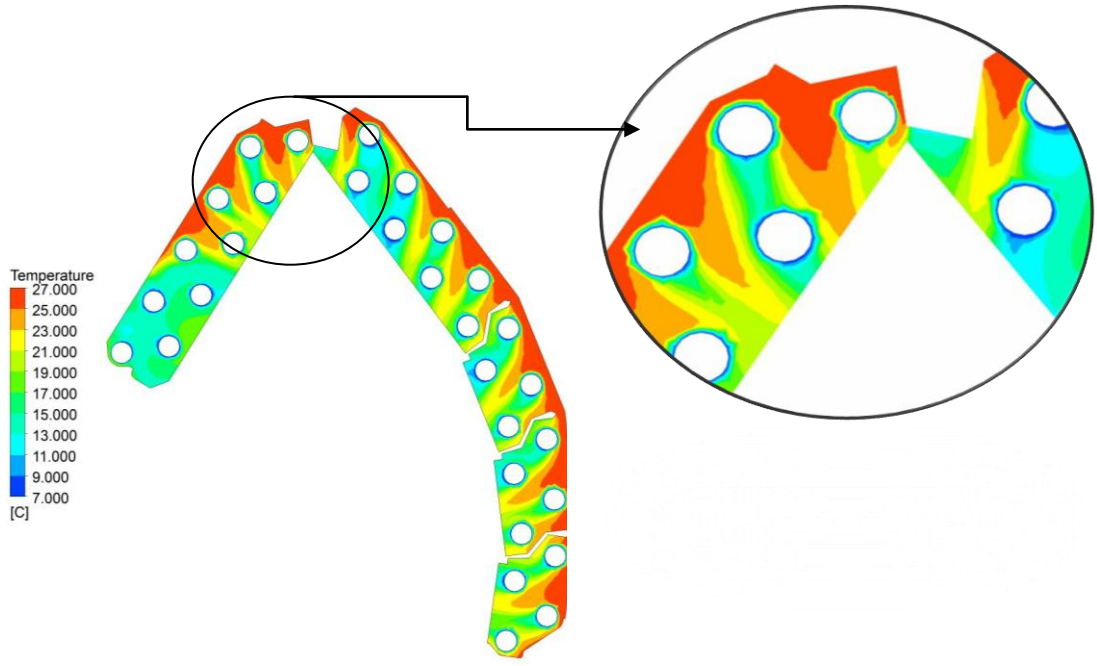


Figure 7.14 Temperature distributions through the air between fins

With the development of heat transfer and fluid flow analyses method at the commercial computational fluid dynamics package program, visualization of the whole evaporator model and also air conditioner indoor unit inside and outside is made available. In Figure 7.15, a temperature distribution visualization of the evaporator model with aluminum fins and air between fins was shown.

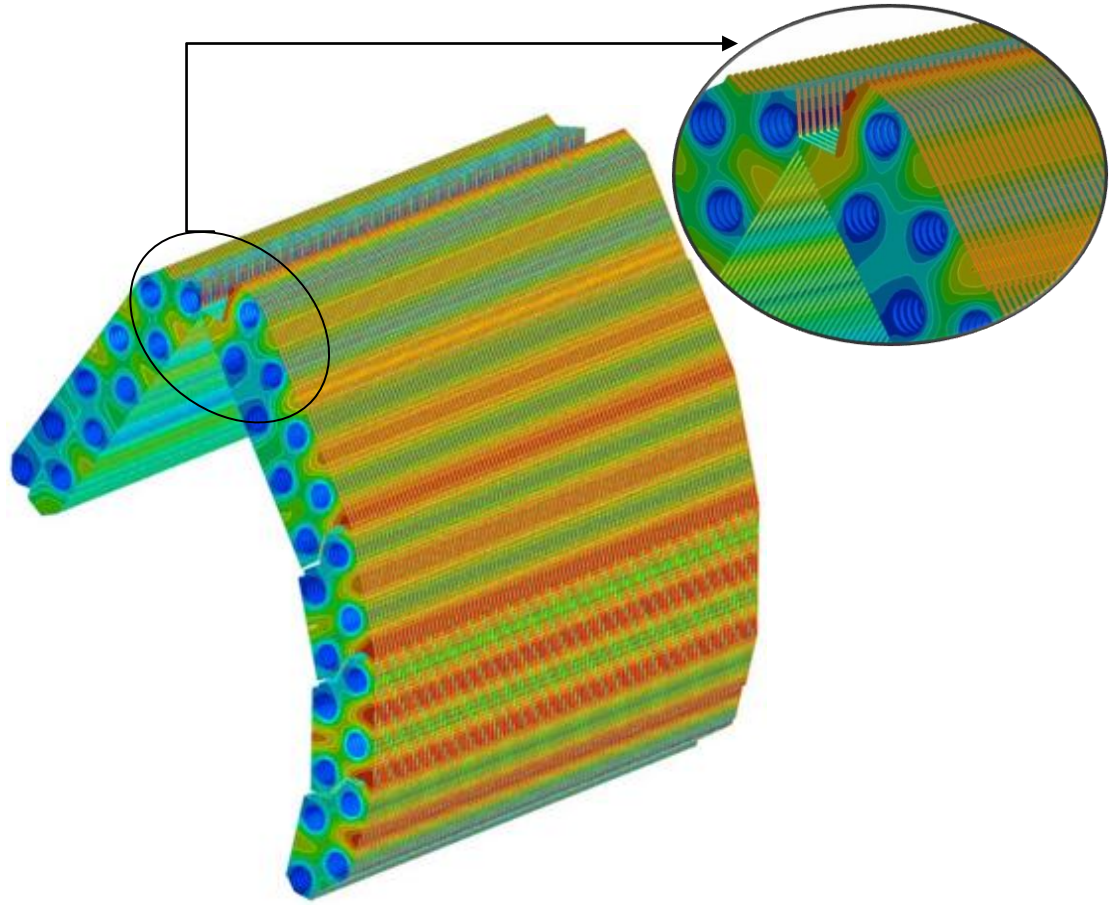


Figure 7.15 Air conditioner evaporator visualization

CHAPTER EIGHT
CONCLUSIONS

The aim of this thesis is to investigate the air side heat transfer and flow characteristics in split air conditioners' evaporator numerically. In literature researches, theoretical and numerical techniques for heat exchangers and also cross flow fans were examined. These researches showed that none of these studies involves heat transfer and fluid flow analyses together for complex air conditioner unit. To resolve this deficiency, a numerical method was developed.

At the beginning of this study, split type air-conditioning systems and heat exchangers theories were investigated. Numerical solution methodologies and finite volume techniques were examined and also a theoretical calculation was made in order to provide a base to our study.

For numerical study, three dimensional model of split air conditioner indoor unit section was prepared and Computational Fluid Dynamics and Heat Transfer (CFDHT) analyses were made. The air side heat transfer performance of the evaporator is analyzed with almost real model of the air conditioner inside unit with fan and ambient air. Results of the numerical study were compared with the measurements which were made from the outlet of the indoor unit. It is observed that theoretical, numerical and experimental results were all in coherence within acceptable limits. Capasity comparison between real life model and numerical model is in % 0.26 error percentages.

It must be indicated that, numerical studies were made for idealized situations and in virtual environment. Some unmodelled elements such as assembly components, filters, fin blastings and other structural losses cause this difference. Although, CFD result and experimental results not equal to each others, their relation is in linear consistency. In CFD results, because of the idealized conditions, the velocity magnitudes are higher than test measurements. Related to high velocity rates, mass flow average and temperature at outlet are higher than test results too. So, the

expectance from the numerical results should be just having an idea about the real life results with minimum error percentage.

The utility of this study by developing a numerical method for a split type air conditioner evaporator heat transfer calculations with a commercial computational fluid dynamic package program is to provide ease for performance and design process improvement studies in a fast and cheap way. Such as, for engineering research and development studies, numerical methods give opportunity to determine the design problems, to try different solution ideas and to improve the system in short times without high testing costs.

This thesis results discussion were made according to Vestel Air-conditioner Product Company test room results which were taken from the outlet region of the indoor unit with point measurements using probes or thermocouples. Despite it is adequate for outlet region results comparisons, for indoor unit optimization studies or air flow characteristics determination through the air-conditioner inside and outside, wide range of experimental data should be taken for absolute assessment with CFD visualization results.

This thesis is taking placement under 00343.STZ.2008-2 encoded SANTEZ project study and scope of this thesis is to provide and develop a numerical method for air-conditioner air side analyses.

REFERENCES

ANSYS CFD theory guide and user manuel (2009).

Anderson, J. D. (2001). *Fundamentals of aerodynamics* (3th ed.). McGraw-Hill.

ASHRAE (American Society of Heating, Refrigerating and Air-Conditioning Engineers) (2005). *Refrigeration handbook.*

Blazek, J. (2001). *Computational fluid dynamics: principles and applications*. Elsevier.

Borrajo-Palaez, R., Ortega-Casanova, J., & Cejudo-Lopez, J. M. (2010). A three-dimensional numerical study and comparison between the air side model and the air/water side model of a plain fin-and-tube heat exchanger. *Applied Thermal Engineering* (30), 1608-1615.

Central air-conditioner and refrigeration (n.d.). Retrieved June, 2010, from http://www.central-air-conditioner-and-refrigeration.com.

Chen, A., Li, S., & Huang, D. (2008). Numerical analysis of aerodynamic noise radiated from cross flow fan. *Higher Education Press And Springer.*

Coester, R. (1959). Theorestische und experimentelle untersuchungen an querstrom-geblasen. *Mitt Inst Fur Aerodyn, 28.*

Çengel, Y. (2008). *Fluid mechanics fundamentals and applications.*

Dang, T. Q., & Bushnell, P. R. (2009). Aerodynamics of cross-flow fans and their application to aircraft propulsion and flow control. (S. U. Department of Mechanical & Aerospace Engineering, Dü.) *Progress in Aerospace Sciences* (45), 1-29.

Eck, B. (1973). Fans. *Oxford: Pergamon Press.*

Evaporator coil for split indoor unit (2009). Retrieved May, 2010 from http://maxellgroup.tradeindia.com/Exporters_Suppliers/Exporter16275.247966/Evaporator-Coil-for-Split-Indoor-Unit.html.

Gabi, M., Dornstetter, S., & Klemm, T. (2003). Flow field and performance of cross flow fans experimental and theoretical investigations. *Journal Of Thermal Science 12 (3).*

Gemici, Z., Eğrican, A. N., & Koca, A. (2010). Theoretical and experimental examination of air conditioner heat exchangers. *Internatiol Communications in Heat And Mass Transfer*.

Heat pump and refrigeration cycle (n.d.). Retrieved June, 2010, from http://www.absoluteastronomy.com/topics/Heat_pump_and_refrigeration_cycle

How an air-conditioner works (n.d.). Retrieved June, 2010, from http://www.tech-faq.com/how-an-air-conditioner-works.html.

Incropera, F.P., DeWitt, D. P. (2000). *Fundamental of heat and mass transfer*.

Jang, J., & Chen, L. (1997). Numerical analysis of heat transfer and fluid flow in a three-dimensional wavy-fin and tube heat exchanger, Department of Mechanical Engineering. *International Journal Of Heat And Mass Transfer, 40 (16),* 3981-3990.

Kakaç, S., & Liu, H. (1998). *Heat exchangers selection rating and thermal design* (Second Edition b.).

Kim, T.A., Kim, D. W., Park, S. K., & Kim, Y. J. (2008). Performance of a cross-flow fan with various shapes of a rearguider and an exit duct. *Korea Journal of Mechanical Science and Technology* (22), 1876-1882.

Kim, Y., & Kim, Y. (2005). Heat transfer characteristics of flat plate finned-tube heat exchangers with large fin pitch. *International Journal Of Refrigeration* (28), 851-858.

Mendez, R. R., Sen, M., Yang, K. T., & McClain, R. (2003). Effect of fin spacing on convection in a plate fin and tube heat exchanger. *International Journal Of Heat And Mass Transfer* (43), 39-51.

Mortier, P. (1893). *Patent No. 507,445.* US Patent.

Murata, S., & Nisnihara, K. (1976). An experimental study of cross flow fan,. *Bulletin Of The Jsme , 19* (129).

Murata, S., & Tanaka, S. (1995). Scale effect in cross flow fans: Effect of fan dimensions on flow details and the universal representation of performances. *JSME International Journal , 38* (3), 388-397.

Noel, J.-Y., Farall, M., & Casarsa, L. (n.d.). Aero acoustics in a tangential blower:Validation of the CFD flow distribution using advanced PIV techniques.

Perrotin, T., & Clodic, D. (2004). Thermal-hydraulic cfd study in louvered fin-and-flat-tube heat exchangers. *International Journal Of Refrigeration* (27), 422-432.

Principles of home inspection: air conditioning and heat pumps (1992). Retrieved July, 2010, from http://www.recampus.com/documents/book02_c01.pdf

Pu, H., Ding, G., Ma, X., Hu, H., & Gao, Y. (2009). Long-term performance of air-side heat transfer and pressure drop for finned tube evaporators of air conditioners under ıntermittent operation conditions. *International Journal Of Refrigeration* .

Shah, R. K., & Sekulic, D. P. (2003). *Fundamentals of heat exchanger design.*

Shih, Y. C., Hou, H. C., & Chiang, H. (2008). On smilitude of the cross flow fan in a split-type air-conditioner. *Applied Thermal Engineering* (28), 1853-1864.

Şahin, H. M., Dal, A. R., & Baysal, E. (2007). 3-d numerical study on the correlation between variable ınclined fin angles and thermal behavior in plate fin-tube heat exchanger. *Applied Thermal Engineering* (27), 1806-1816.

Taler, D. (2004). Determination of heat transfer correlations for plate fin and tube heat exchangers. *Heat And Mass Transfer* (40), 809-822.

Tao, Y. B., He, Y. L., Huang, J., Wu, Z. G., & Tao, W. Q. (2007). Numerical study of local heat transfer coefficient and fin efficiency of wavy fin-and-tube heat exchangers. *International Journal Of Thermal Sciences* (46), 768-778.

Toffolo, A. (2004). An experimental investigation of the flow field pattern within the impeller of a cross-flow fan. *Experimental thermal and fluid science* (29), 53-64.

Toffolo, A. (2005). On the theoretical link between design parameters and performance ın cross-flow fans: a numerical and experimental study. *Computers and Fluids* (34), 49-66.

Tsai, G.-L., Tu, T.-H., Li, T.-C., & Wang, K.-H. (2006). Flow style investigation and noise reduction of a cross-flow fan with varied rotor-skew-angle rotor. *JSME International Journal , 49* (3).

Tuztas, M., & Egrican, A. N. (2002). Mathematical model of finned tube heat exchangers for thermal simulation software of air conditioner. *International Commitee Of Heat And Mass Transfer , 29* (4), 547-556.

Uskaner, Y. A., & Göksel, Ö. T. (1999) *Arka yönlendirme duvarının teğetsel fan performansına etkileri*. Gaziantep Üniversitesi Mühendislik Fakültesi Makina Mühendisliği Bölümü.

Wang, C. C. (2000). Recent progress on the air side performance of fin-and-tube heat exchangers. *International Journal Of Heat Exchangers, 1*, 49-76.

Wang, C. C., Lee, W. S., & Sheu, W. J. (2001). A comperative study of compact enhanced fin and tube heat exchangers. *International Journal of Heat and Mass Transfer* (44), 3565-3573.

Wikipedia (n.d.).Retrieved from http://en.wikipedia.org/wiki/Air_conditioner.

Xie, G., Wang, Q., & Sunden, B. (2009). Parametric study and multiple correlations on air-side heat transfer and friction characteristics of fin-and-tube heat exchangers with large number of large-diameter tube rows. *Applied Thermal Engineering* (29), 1-16.

Versteeg, H. K. & Malalasekera, W. (1995). *An Introduction to computational fluid dynamics: the finite volume method*, London: Prentice Hall.

Yan, W. M., Li, H. Y., Wu, Y. J., Lin, J. Y., & Chang, W. R. (2003). Performance of finned tube heat exchangers operating under frosting conditions. *International Journal Of Heat And Mass Transfer* (46), 871-877.

Yan, W., & Sheen, P. (2000). Heat transfer and friction characteristics of fin-and-tube heat exchangers. *International Journal Of Heat And Mass Transfer* (43), 1651-1659.

Younsi, M., Bakir, F., Kouidri, S., & Rey, R. (2007). Influence of impeller geometry on the unsteady flow in a centrifugal fan: Numerical and experimental analyses. *International Journal Of Rotating Machinery*.

Yun, J. Y., & Lee, K. S. (1999). Investigation of heat transfer characteristics on various kinds of fin and tube heat exchangers with interrupted surfaces. *International Journal Of Heat And Mass Transfer* (42), 2375-2385.